Supporting Information

Metallacycle-Cored Luminescent Ionic Liquid Crystals with Trigonal Symmetry

Long Chen,[a,c] Yu Cao,*[a] Haohui Huo,[a] Shuai Lu,[b] Yali Hou,[a] Tianyi Tan,[a] Xiaopeng Li,[b] Feng Liu [a] and Mingming Zhang*[a]

[a]Shaanxi International Research Center for Soft Matter, State Key Laboratory for Mechanical Behavior of Materials, Xi'an Jiaotong University, Xi'an 710049, P. R. China
[b]College of Chemistry and Environmental Engineering, Shenzhen University, Shenzhen 518055, P. R. China
[c]Key Laboratory of Catalytic Materials and Technology of Shaanxi Province, Kaili Catalyst & New Materials Co., Ltd, Xi'an 710201, P. R. China
*Corresponding authors. Email address: yu.cao@xjtu.edu.cn, mingming.zhang@xjtu.edu.cn

Contents

1. Gerneral materials and instrumentation

All reagents and deuterated solvents purchased as analytical grade and used without further purification. Column chromatography was performed using 300-400 mesh silica gel. Nuclear magnetic resonance spectra were afforded with Bruker Avance 400 MHz or 600 MHz pectrometer. ^{1}H and ^{13}C NMR chemical shifts are reported relative to residual solvent signals, and ^{31}P{^{1}H} NMR chemical shifts are referenced to an external unlocked sample of 85% H_3PO_4 (δ 0.0). Chemical shifts (ppm) were reported in parts per million (ppm). Coupling constants(*J*) were reported in Hertz. Multiplicity reported using the following abbreviations: s (singlet), d(doublet), t (triplet), q (quartet), m (multiplet), dd (doublet of doublet), dt (doublet of triplet). Mass spectra were recorded on a Micromass Quattro II triple-quadrupole mass spectrometer using electrospray ionization with a MassLynx operating system. The UV-vis experiments were conducted on Lambd 950 absorption spectrophotometer. The fluorescent experiments were conducted on a Hitachi F-7000 fluorescence spectrophotometer. Phase textures of all compounds were fully characterized by polarizing optical microscopy (Olympus BX51-P) in conjunction with a heating stage (Linkam LTS420E) and controller (T95-HS). Optical investigations were carried out under equilibrium conditions between two glass slides that were used without further treatment. Transition enthalpies were determined as obtained from differential scanning calorimetry (DSC) which were recorded on a TA DSC250 (heating and cooling rate: 10 K/min, peak temperatures).

Synchrotron X-ray diffraction and electron density reconstruction: High-resolution small-angle powder diffraction experiments were recorded on Beamline BL16B1 at Shanghai Synchrotron Radiation Facility, SSRF. Samples were held in evacuated 1 mm capillaries. A modified Linkam hot stage with a thermal stability within 0.2 ºC was used, with a hole for the capillary drilled through the silver heating block and mica windows attached to it on each side. A MarCCD detector was used. *q* calibration and linearization were verified using several orders of layer reflections from silver behemate and a series of *n*-alkanes. The measurement of the positions and intensities of the diffraction peaks is carried out using Galactic PeakSolve™ program, where experimental diffractograms are fitted using Gaussian shaped peaks. The diffraction peaks are indexed on the basis of their peak positions, and the lattice parameters and the space groups are subsequently determined. Once the diffraction intensities are measured and the corresponding space group determined, 3-d electron density maps can be reconstructed, on the basis of the general formula

$$E(xy) = \Sigma_{hk} F(hk) \exp[i2\pi(hx+ky)] \qquad \text{(Eqation S1)}$$

Here $F(hk)$ is the structure factor of a diffraction peak with index (hk). It is normally a complex number and the experimentally observed diffraction intensity.

$$I(hk) = K \cdot F(hk) \cdot F^*(hk) = K \cdot |F(hk)|^2 \qquad \text{(Eqation S2)}$$

Here K is a constant related to the sample volume, incident beam intensity etc. In this paper we are only interested in the relative electron densities, hence this constant is simply taken to be 1. Thus the electron density

$$E(xy) = \Sigma_{hk} \text{ sqrt}[I(hk)] \exp[i2\pi(hx+ky) + \phi_{hk}] \qquad \text{(Eqation S3)}$$

As the observed diffraction intensity $I(hk)$ is only related to the amplitude of the structure factor $|F(hk)|$, the information about the phase of $F(hk)$, ϕ_{hk}, can not be determined directly from experiment. However, the problem is much simplified when the structure of the ordered phase is centrosymmetric, and hence the structure factor $F(hk)$ is always real and ϕ_{hk} is either 0 or π.

This makes it possible for a trial-and-error approach, where candidate electron density maps are reconstructed for all possible phase combinations, and the "correct" phase combination is then selected on the merit of the maps, helped by prior physical and chemical knowledge of the system. This is especially useful for the study of nanostructures, where normally only a limited number of diffraction peaks are observed.

2. Synthetic Procedures and Characterization Data

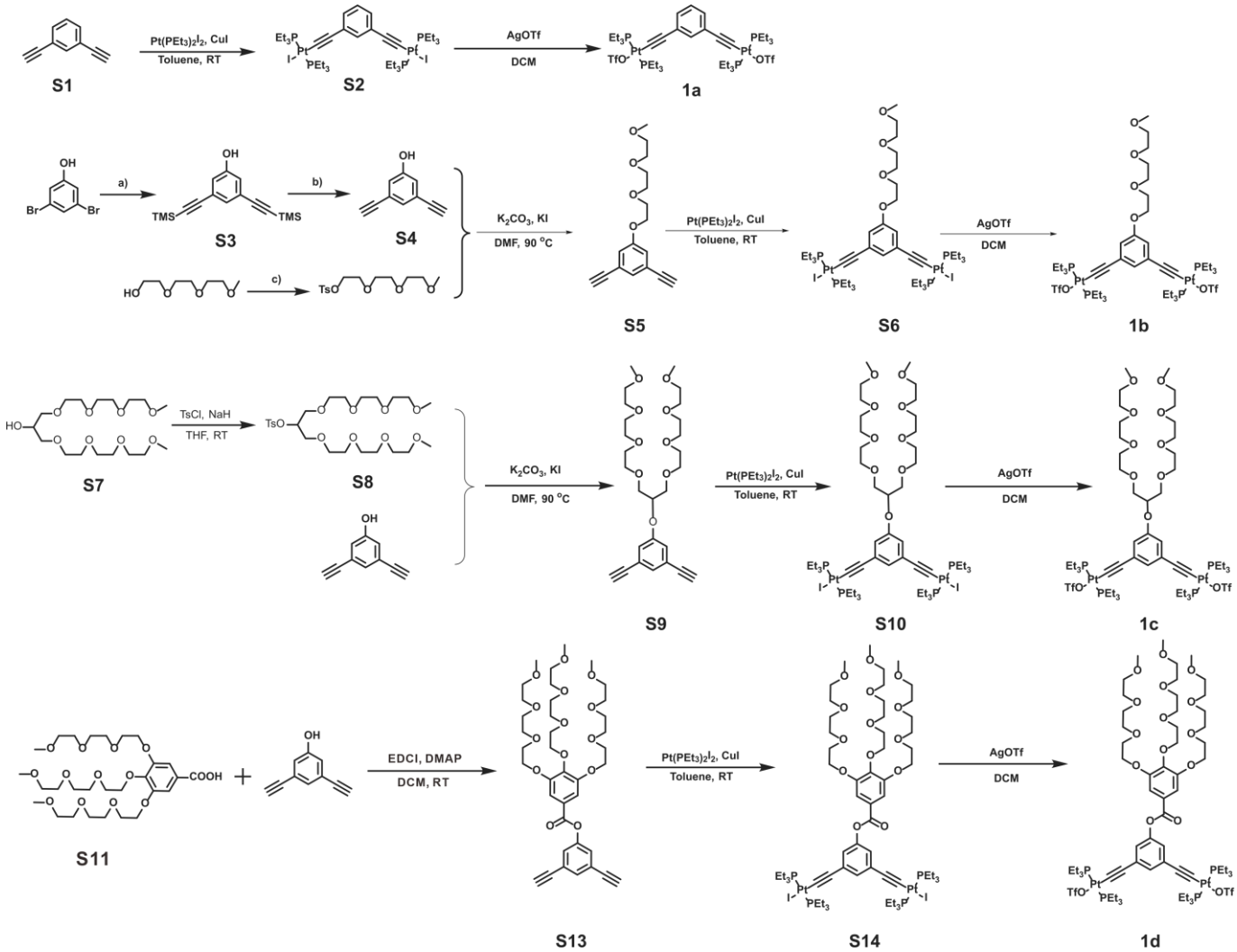

Scheme S1. Synthetic routes of Pt(II) acceptor and chemical structures of compounds used. Conditions: a) trimethylsiyl acetylene, $Pd(PPh_3)_4$, CuI, toluene; 82%; b) KF, MeOH/THF(1:1), rt; 90%; c) TsCl, NaOH, DCM; 95%.

2-(2-(2-Methoxyethoxy)ethoxy)ethyl tosylate [S1], compound **S2**[S2], **S3**[S3], **S4**[S3], **S5**[S4], **S6**[S4] **S7**[S5], **S8**[S5], **S9**[S4], **S10**[S4], **S11**[S1], **1a**[S2], **1b**[S4] and **1c**[S4] were synthesized according to the reported literature(In ref. *S1-S5*) and some of the reported spectra are not shown.

The synthesis of compound **3a-3d** uses conventional 3+3 reaction, whose quantitative yield is almost 100% as reported[S8-S9].

Synthesis of compound S2

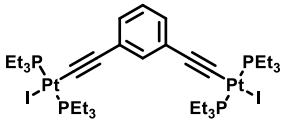

Compound **S1** (0.3 g, 2.38 mmol), $Pt(PEt_3)_2I_2$ (3.04 g, 4.22 mmol) were dissolved in dry toluene (60 mL) in a 100 mL Schlenk flask, CuI (20 mg, 0.20 mmol) and dry

diethylamine (10 mL) were added to the solution. Then the mixture was stirred at room temperature for 48 h under nitrogen. The product was concentrated to give a crude product which was purified by flash column chromatography with dichloromethane: ethyl acetate (50:1, v/v) as the eluent to afford compound **S2** as light yellow solid (1.83 g, 62%) .[S2] ^{1}H NMR (600 MHz, $CDCl_3$, 298K) δ 7.20 (s, 1H), 7.12 – 7.06 (m, 3H), 2.24 – 2.19(m, 24H), 1.30 – 1.08 (m, 36H). ^{31}P NMR (243 MHz, $CDCl_3$, 298K) δ 8.45 (s, ^{195}Pt satellites, $^{1}J_{Pt\text{-}P}$ = 2326.72 Hz).

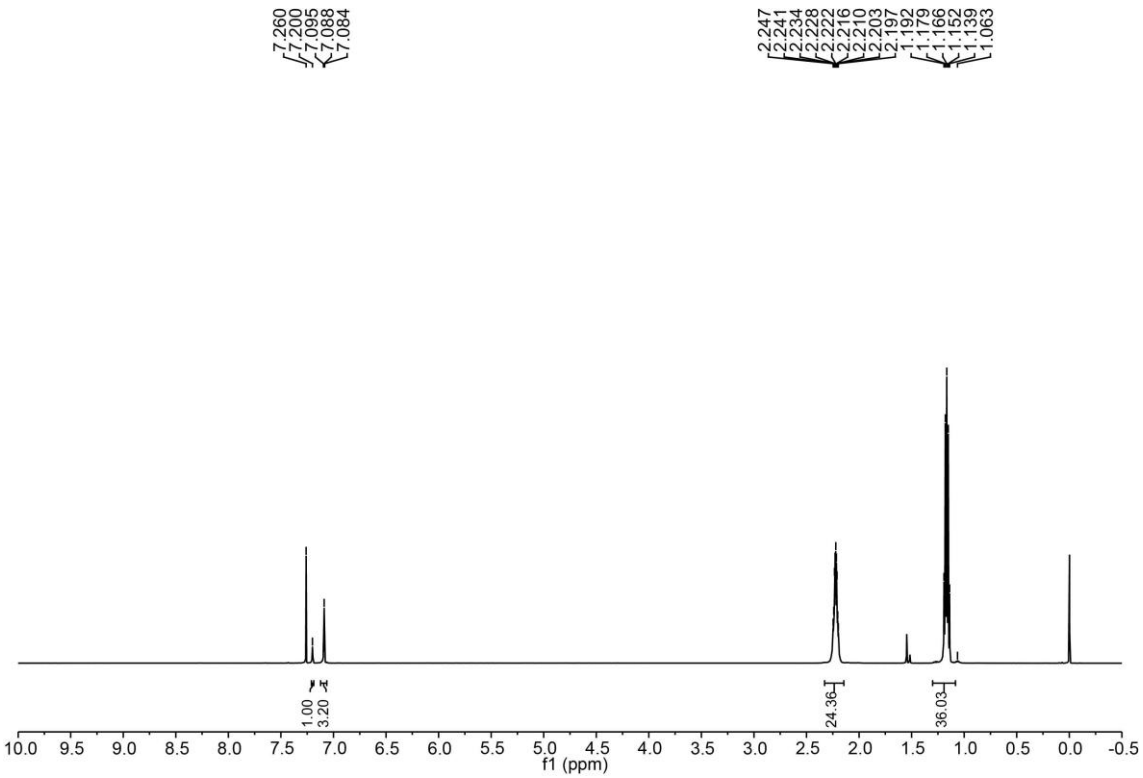

Fig. S1. ^{1}H NMR spectrum (600 MHz, $CDCl_3$, 298 K) recorded for **S2**.

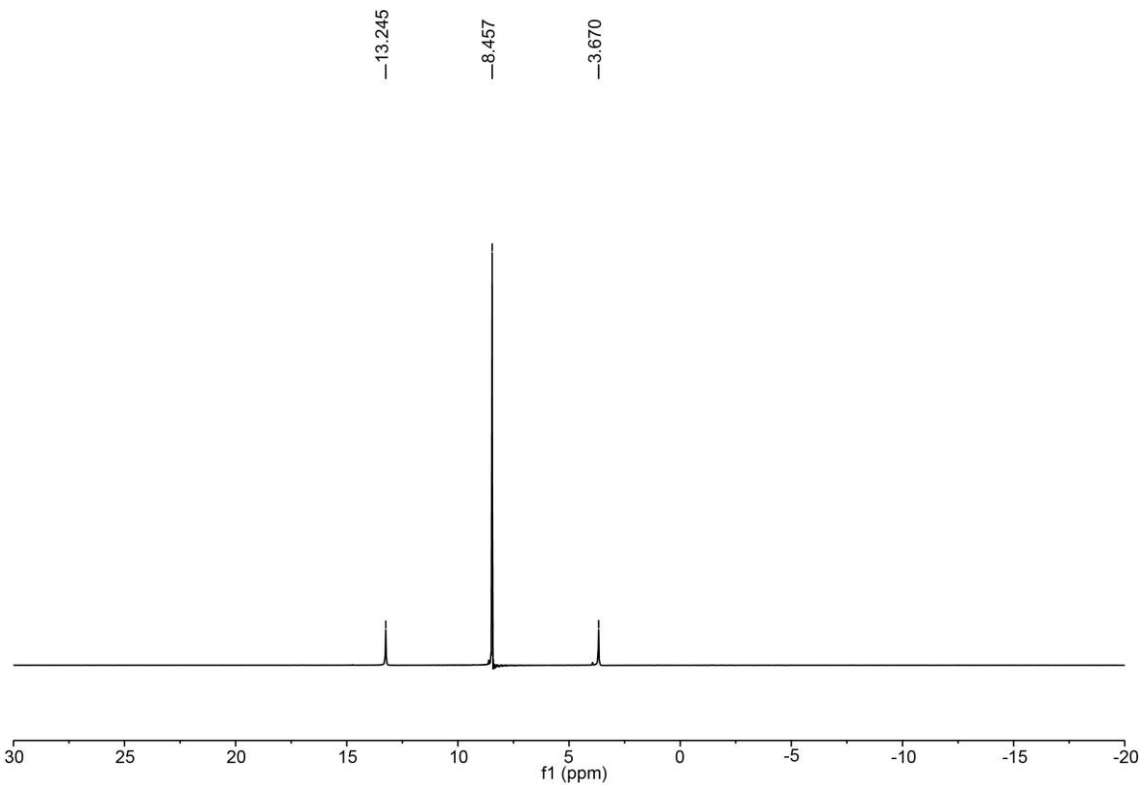

Fig. S2. $^{31}P\{^{1}H\}$ spectra (243 MHz, $CDCl_3$, 298 K) of **S2**.

Synthesis of compound 1a

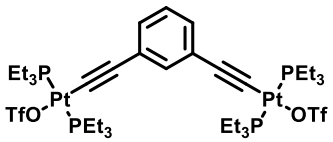

Compound **S2** (350 mg, 0.28 mmol), AgOTf (217 mg, 0.84 mmol) were added into a 40 mL brown vial, then freshly distilled CH_2Cl_2 (20 mL) was added. The resulting mixture was stirred in the dark at room temperature for 12 h. After filtering off the heavy creasy precipitate through a glass fiber filter, the suspension was obtianed. The solvent was removed under a flow of nitrogen to afford **1a** as a white solid (49 mg, 95%).[S2] ^{1}H NMR (600 MHz, CD_2Cl_2, 298K) δ 7.79 (s, 1H), 7.23 (s, 3H), 2.04 (s, 24H), 1.33 – 1.01 (m, 36H). ^{31}P NMR (243 MHz, CD_2Cl_2, 298K) δ 21.84 (s, ^{195}Pt satellites, $^{1}J_{Pt\text{-}P}$ = 2220.29 Hz).

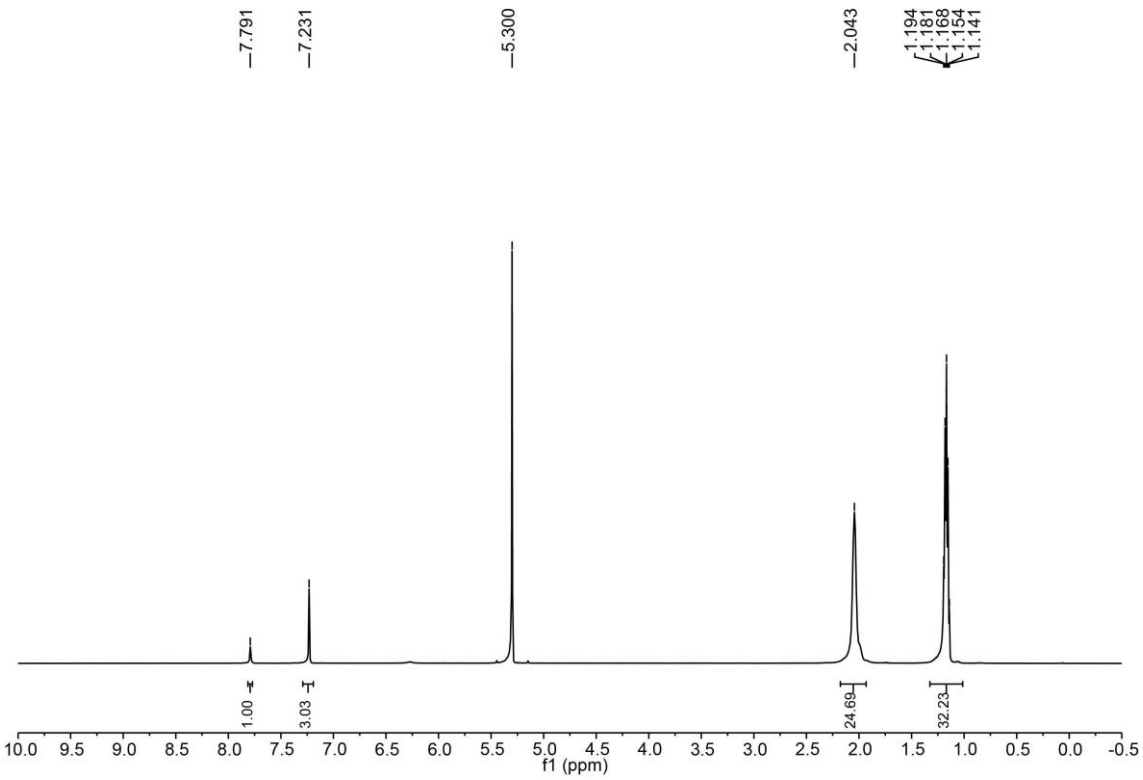

Fig. S3. ^{1}H NMR spectrum (600 MHz, CD_2Cl_2, 298 K) recorded for **1a**.

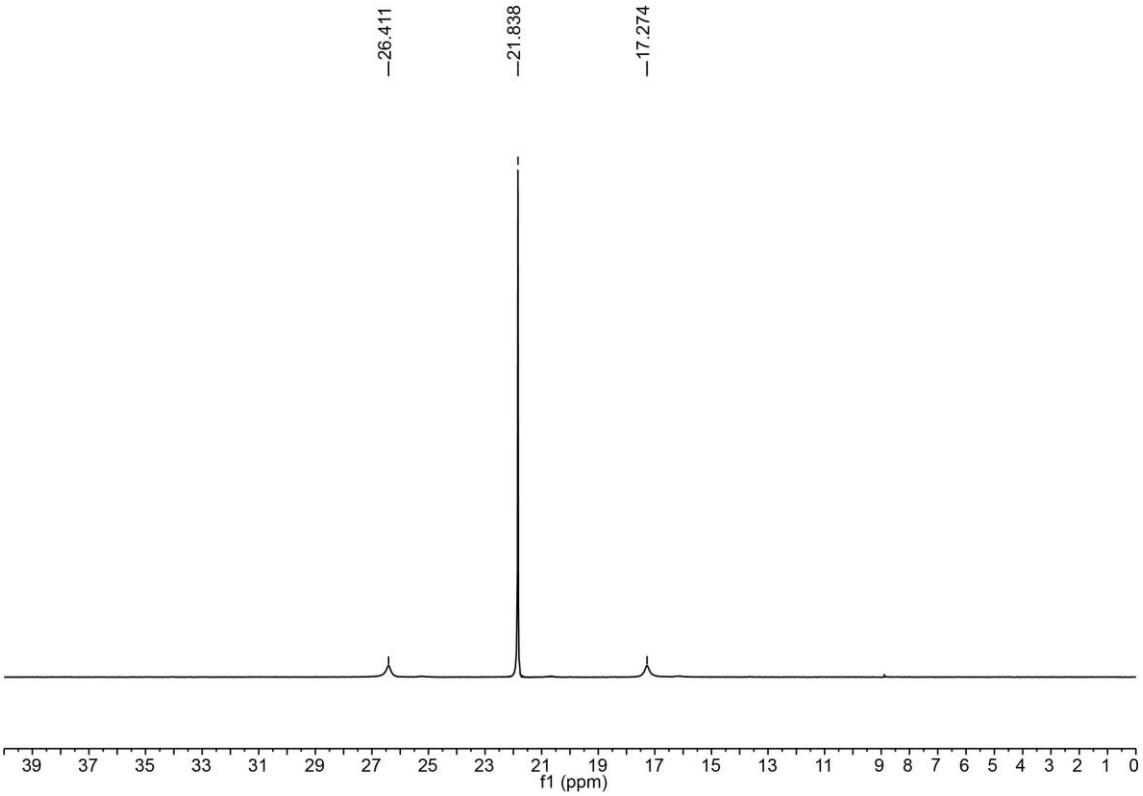

Fig. S4. ^{31}P{^{1}H} spectra (243 MHz, CD_2Cl_2, 298 K) of **1a**.

Synthesis of compound S3

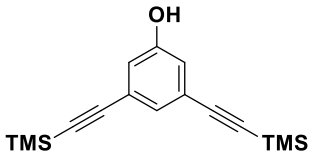

3,5-dibromophenol (5.0 g, 19.84 mmol), trimethylsiyl acetylene (12 mL, 79.40 mmol) were dissolved in dry tetrahydrofuran (60 mL) in a 100 mL Schlenk flask, $Pd(PPh_{3[})_4$ (2.29 g, 1.98 mmol), CuI (370 mg, 1.98 mmol) and dry triethylamine (10 mL) were added to the solution. Then the mixture was cooled by liquid nitrogen, degassed and purged with nitrogen for three times. The reaction mixture was stirred at 80℃ for 48 h under nitrogen. After cooling, the product was concentrated to give a crude product which was purified by flash column chromatography with dichloromethane: petroleum ether (1:1, v/v) as the eluent to afford compound **S3** (4.7 g, 82%) as a white solid.[S3] ^{1}H NMR (600 MHz, $CDCl_3$, 298K) δ 7.17 (t, J = 1.1 Hz, 1H), 6.88 (d, J = 1.2 Hz, 2H), 0.23 (s, 18H). ^{13}C NMR (151 MHz, $CDCl_3$, 298K) δ 154.97, 128.43, 124.46, 118.91, 103.67, 94.98, 77.71, 77.21, 77.00, 76.79, -0.15. ESI-HR-MS: *m/z* 325.0555 [**S3** + K]$^+$, calcd. for $[C_{16}H_{22}KOSi_2]^+$, 325.0841.

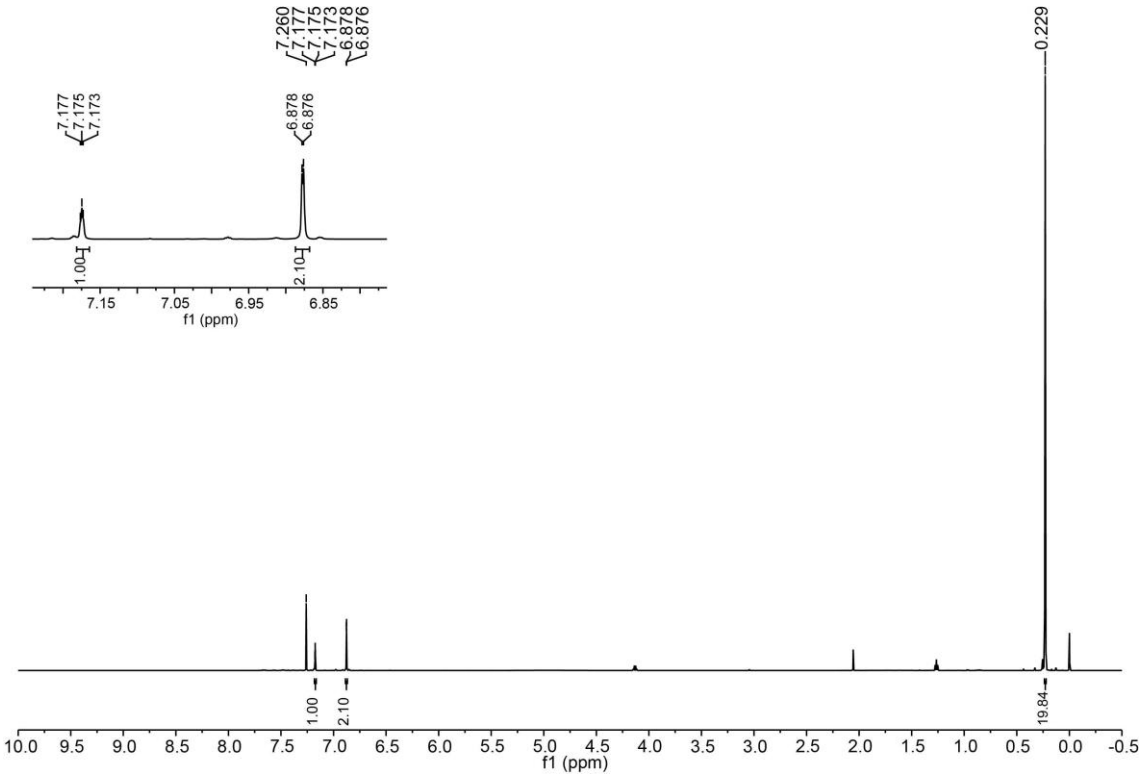

Fig. S5. ^{1}H NMR spectrum (600 MHz, $CDCl_3$, 298 K) recorded for **S3**.

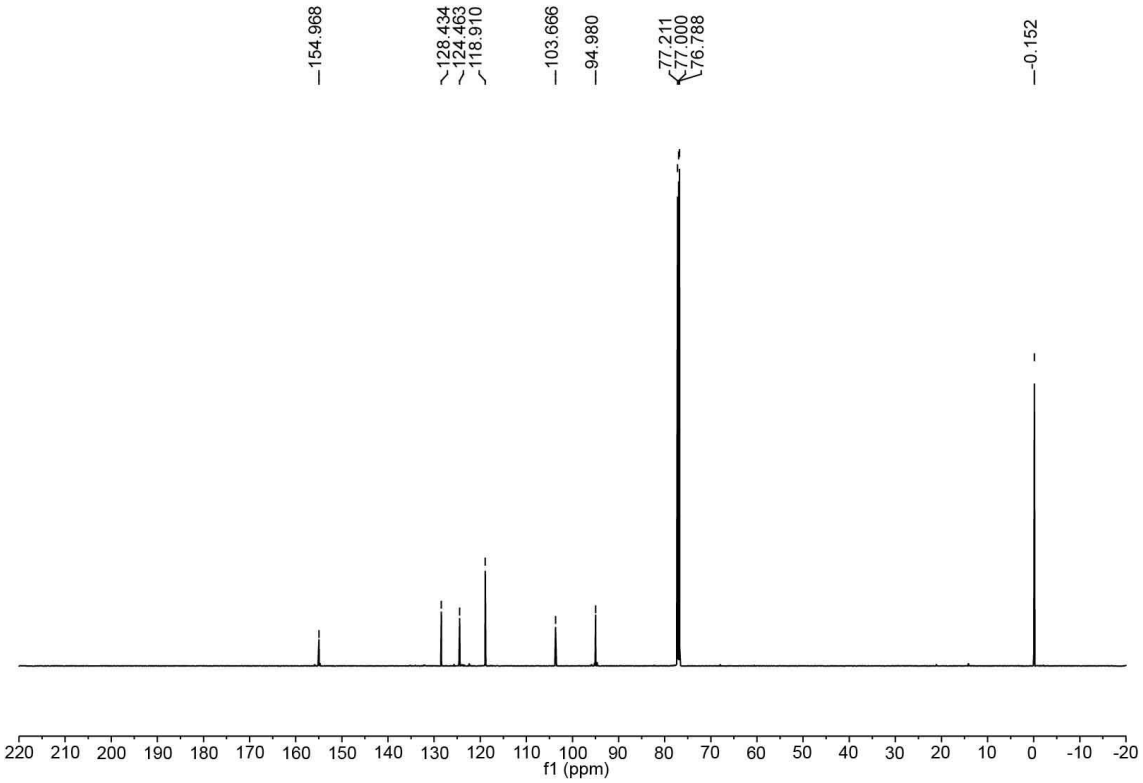

Fig. S6. ^{13}C NMR spectrum (151 MHz, $CDCl_3$, 298 K) recorded for **S3**.

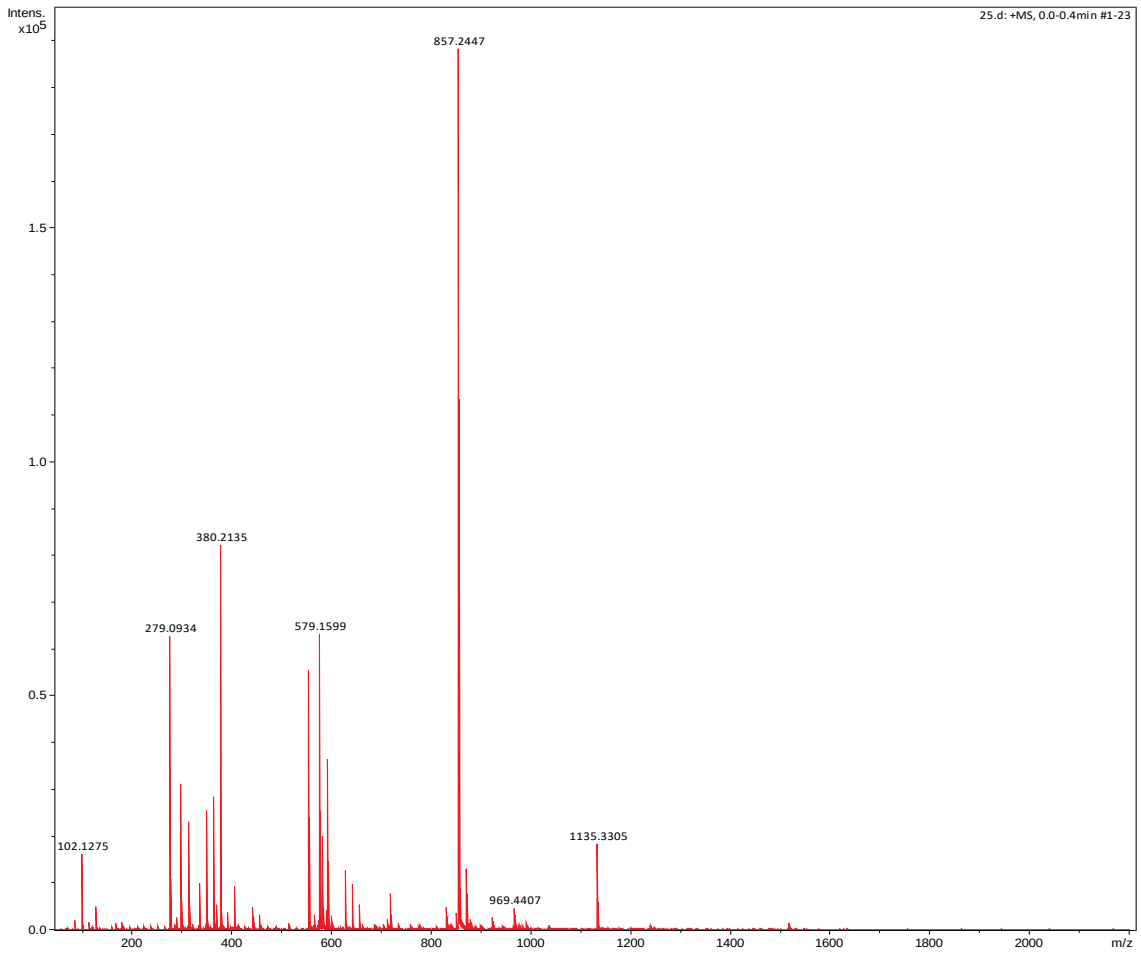

Fig. S7. ESI-HR-MS spectrum of **S3**.

Synthesis of compound S4

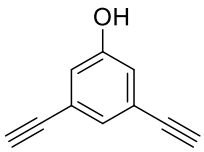

Compound **S3** (3.98 g, 13.89 mmol) and KF (2.42 g, 41.67 mmol) were dissolved in MeOH/THF (60 mL, v/v =1:1). The reaction mixture was allowed to stir at room temperature for 12 h, then filtered, the filtrate was collected, and the solvent was removed under reduced pressure. The residue was purified by flash column chromatography with dichloromethane: petroleum ether (1:2, v/v) as the eluent to afford compound **S4** (1.78 g, 90%) as a white solid.[S3] ^{1}H NMR (600 MHz, $CDCl_3$, $CDCl_3$, 298 K) δ 7.21 (d, *J* = 1.0 Hz, 1H), 6.95 (s, 2H), 3.07 (s, 2H). ^{13}C NMR (151 MHz, $CDCl_3$, 298 K) δ 155.06, 128.56, 123.63, 119.55, 82.20, 77.94. ESI-HR-MS: *m/z* 143.0736 [**S4** + H]$^+$, calcd. for $[C_{10}H_7O]^+$, 143.0491.

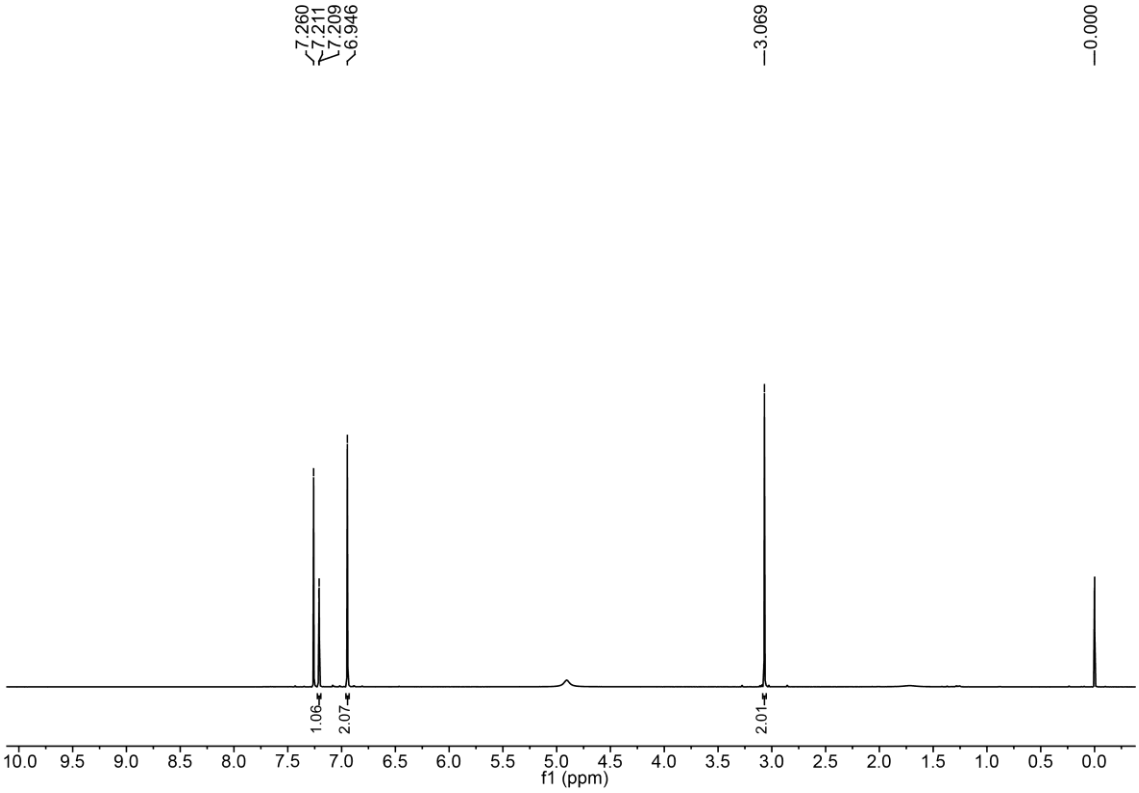

Fig. S8. ^{1}H NMR spectrum (600 MHz, $CDCl_3$, 298 K) recorded for **S4**.

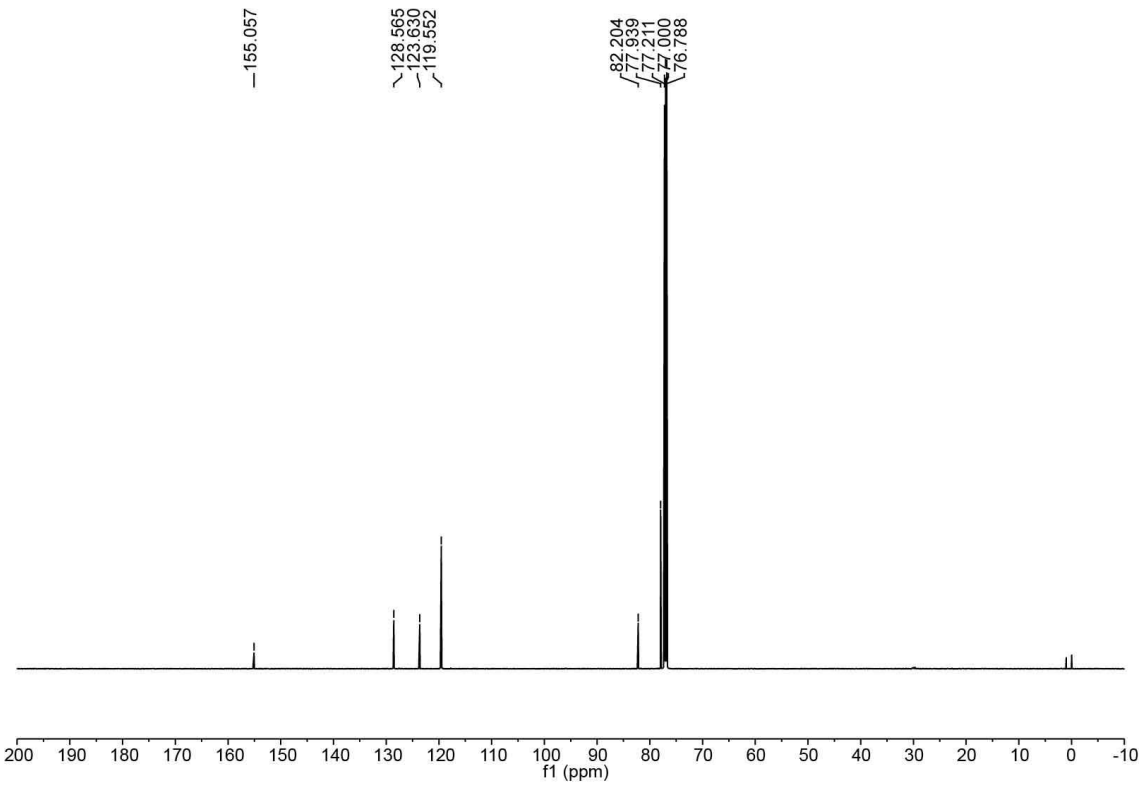

Fig. S9. ^{13}C NMR spectrum (151 MHz, $CDCl_3$, 298 K) recorded for **S4**.

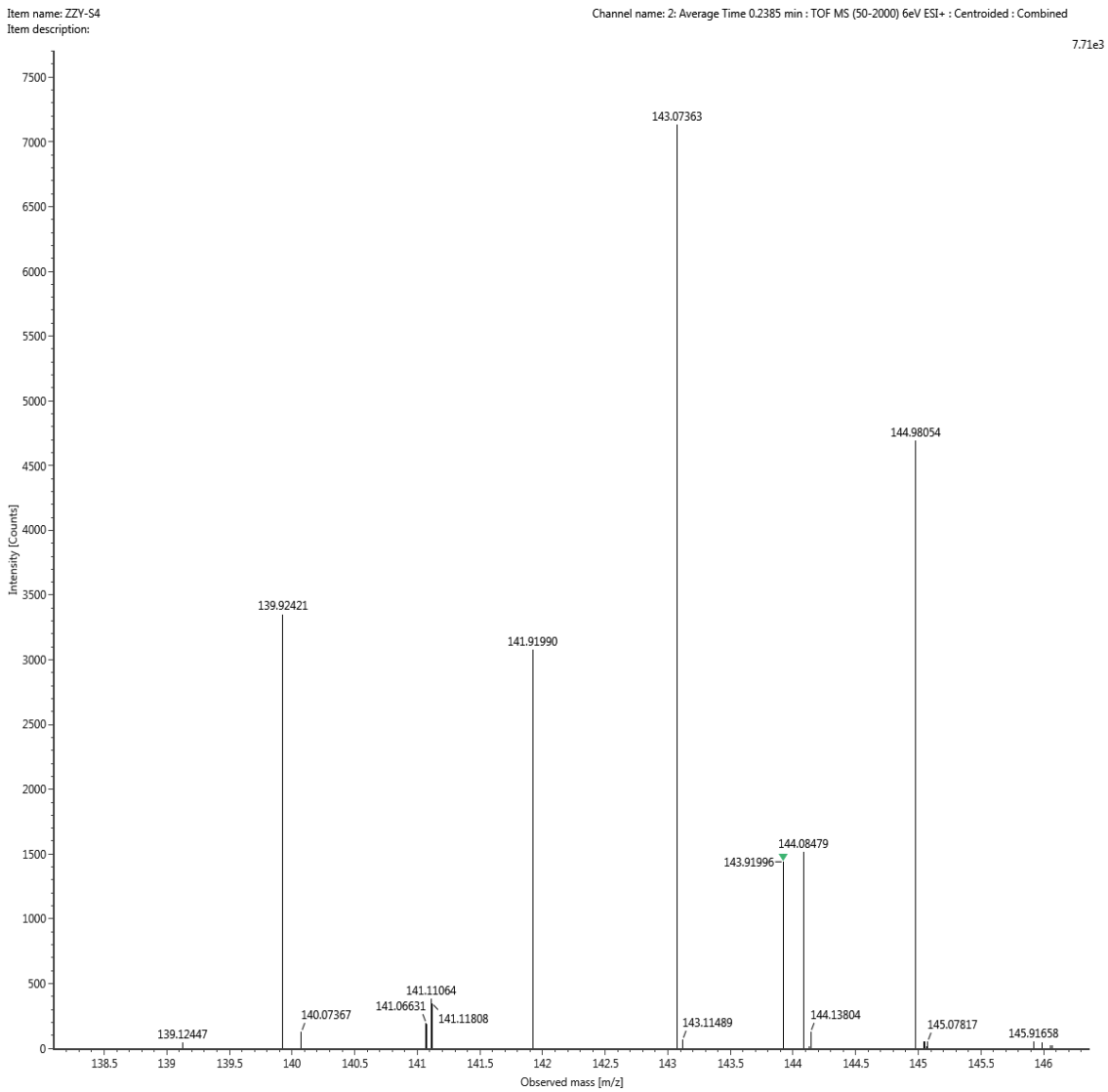

Fig. S10. ESI-HR-MS spectrum of **S4**.

Synthesis of compound S5

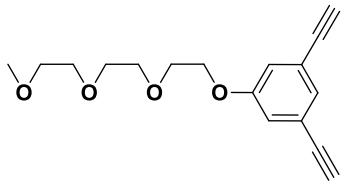

Compound **S4** (1.0 g, 7.03 mmol), 2-(2-(2-Methoxyethoxy)ethoxy)ethyl tosylate (2.56 g, 8.44 mmol) and K_2CO_3 (2.9 g, 21.1 mmol) were dissolved in DMF (40 mL). After the reaction mixture was allowed to stir at 90 ^{o}C for 18 h, most of the reaction solvent was removed under reduced pressure. The residue was purified by flash column chromatography with petroleum ether: ethyl acetate (3:1, v/v) as the eluent to afford compound **S5** (2.06 g, 85%) as a colorless oil.[S4] ^{1}H NMR (600 MHz, $CDCl_3$, 298K) δ 7.20 (s, 1H), 7.01 (d, *J* = 1.1 Hz, 2H), 4.12 – 4.08 (m, 2H), 3.85 – 3.81 (m, 2H), 3.71 (dd, *J* = 6.0, 3.5 Hz, 2H), 3.68 – 3.63 (m, 5H), 3.54 (dd, *J* = 5.5, 3.8 Hz, 2H), 3.37 (d, *J* = 4.6 Hz, 3H), 3.06 (s, 2H). ^{13}C NMR (151 MHz, $CDCl_3$, 298K) δ 158.20, 128.22, 123.21, 118.79, 82.38, 77.71, 71.76, 70.72, 70.49, 70.43, 69.37, 67.57, 58.87. ESI-HR-MS: *m/z* 311.1260 [**S5** + Na]$^{+}$, calcd. for [$C_{17}H_{20}NaO_4$]$^{+}$, 311.1254.

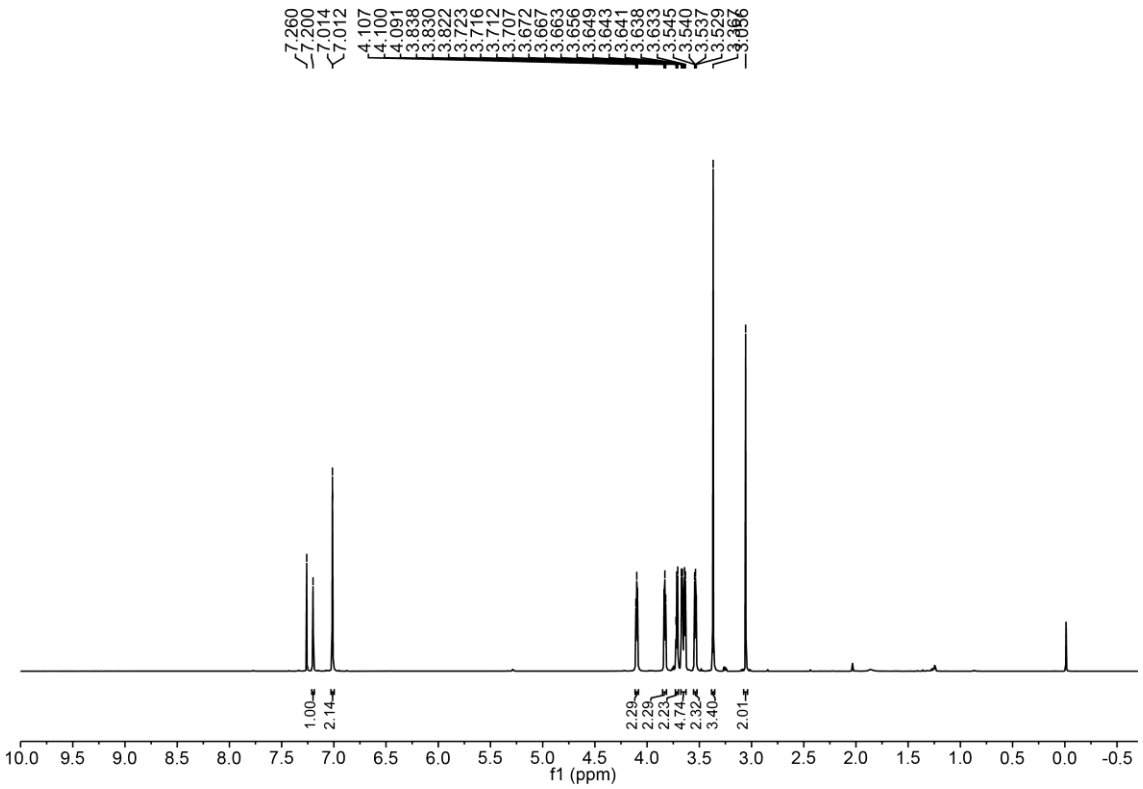

Fig. S11. ^{1}H NMR spectrum (600 MHz, $CDCl_3$, 298 K) recorded for **S5**.

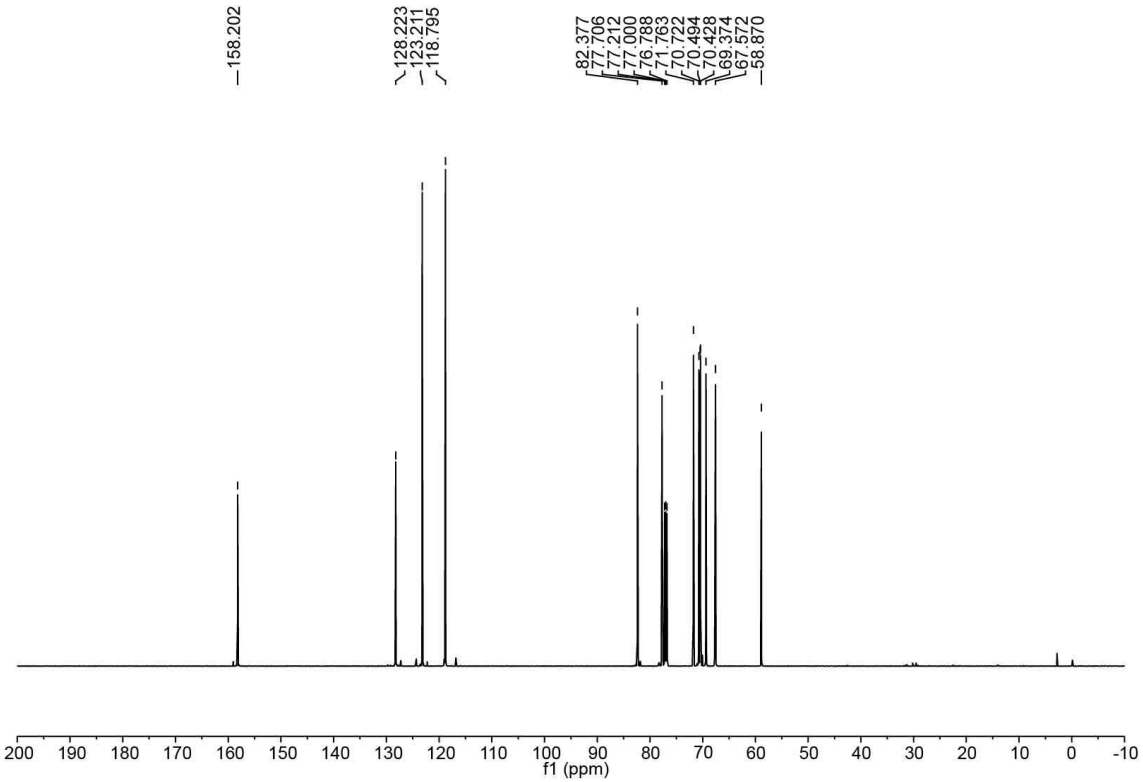

Fig. S12. ^{13}C NMR spectrum (151 MHz, $CDCl_3$, 298 K) recorded for **S5**.

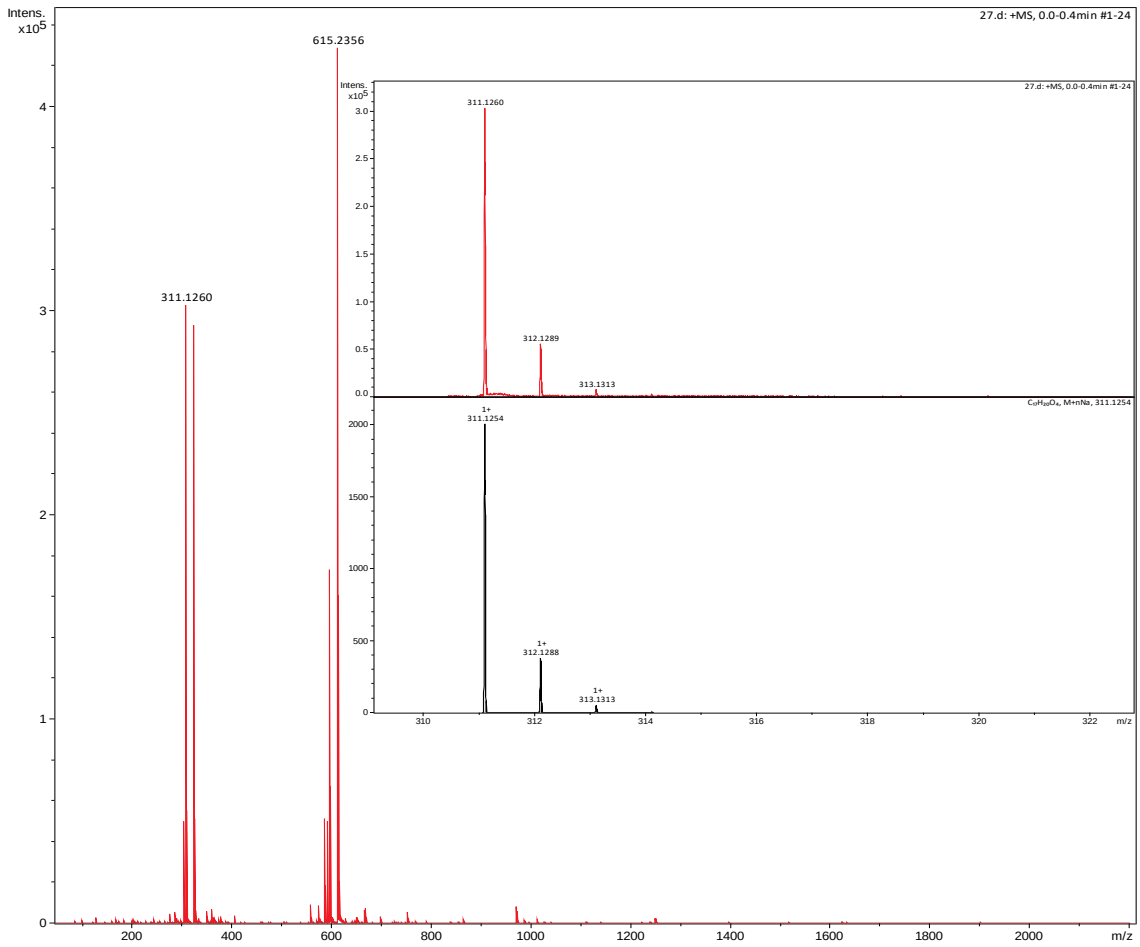

Fig. S13. ESI-HR-MS spectrum of **S5**.

Synthesis of compound S6

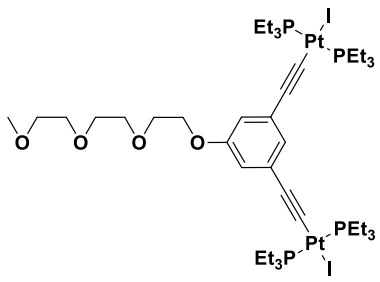

Compound **S5** (0.17 g, 0.61 mmol), $Pt(PEt_3)_2I_2$ (1.68 g, 2.45 mmol) were dissolved in dry toluene (60 mL) in a 100 mL Schlenk flask, CuI (23 mg, 0.12 mmol) and dry diethylamine (5 mL) were added to the solution. Then the mixture was stirred at room temperature for 48 h under nitrogen. Then, the product was concentrated to give a crude product which was purified by flash column chromatography with dichloromethane: ethyl acetate (30:1, v/v) as the eluent to afford compound **S6**.[S4] ^{1}H NMR (600 MHz, $CDCl_3$, 298K) δ 6.82 (s, 1H), 6.67 (s, 2H), 4.10 – 4.06 (m, 2H), 3.86 – 3.82 (m, 2H), 3.75 – 3.71 (m, 2H), 3.71 – 3.67 (m, 2H), 3.67 – 3.63 (m, 2H), 3.58 – 3.54 (m, 2H), 3.38 (s, 3H), 2.28 – 2.14 (m, 24H), 1.22 – 1.10 (m, 36H). ^{31}P NMR (243 MHz, $CDCl_3$, 298K) δ 8.51 (s, ^{195}Pt satellites, $^1J_{Pt\text{-}P}$ = 2325.02 Hz). ESI-HR-MS: *m/z* 1425.2100 [**S6** + Na]$^+$, calcd. for $[C_{41}H_{78}I_2NaO_4P_4Pt_2]^+$, 1425.2128.

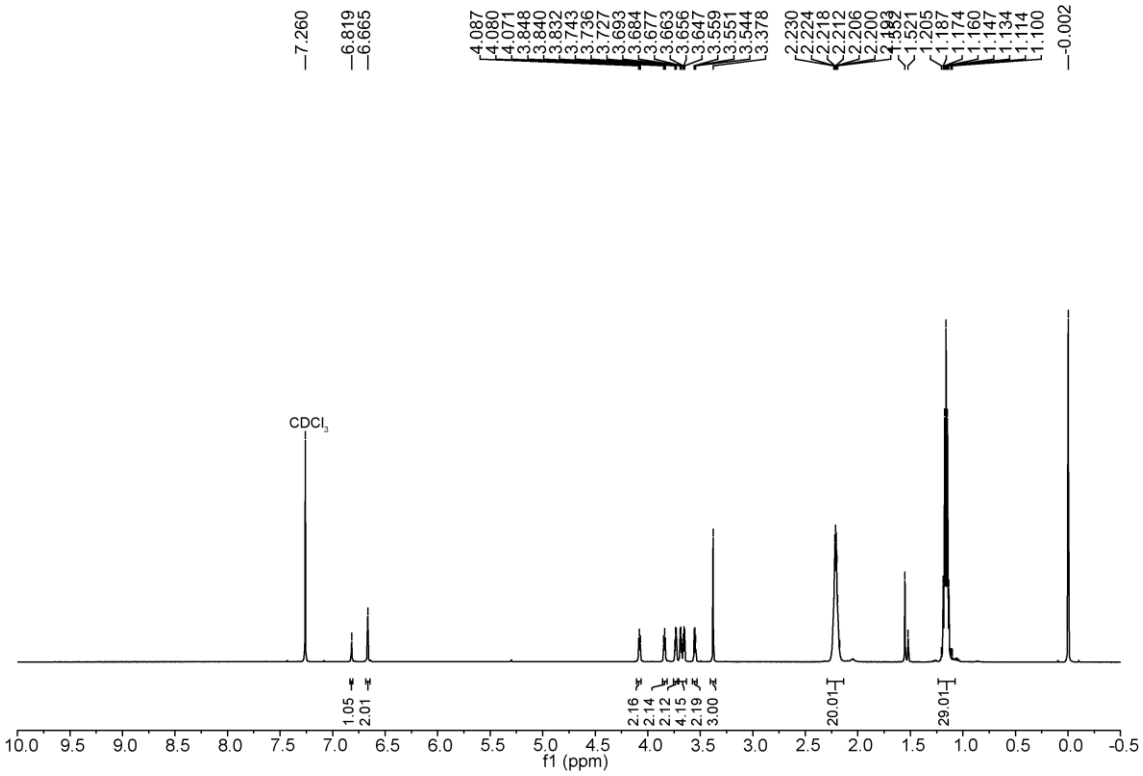

Fig. S14. ^{1}H NMR spectrum (600 MHz, $CDCl_3$, 298 K) recorded for **S6**.

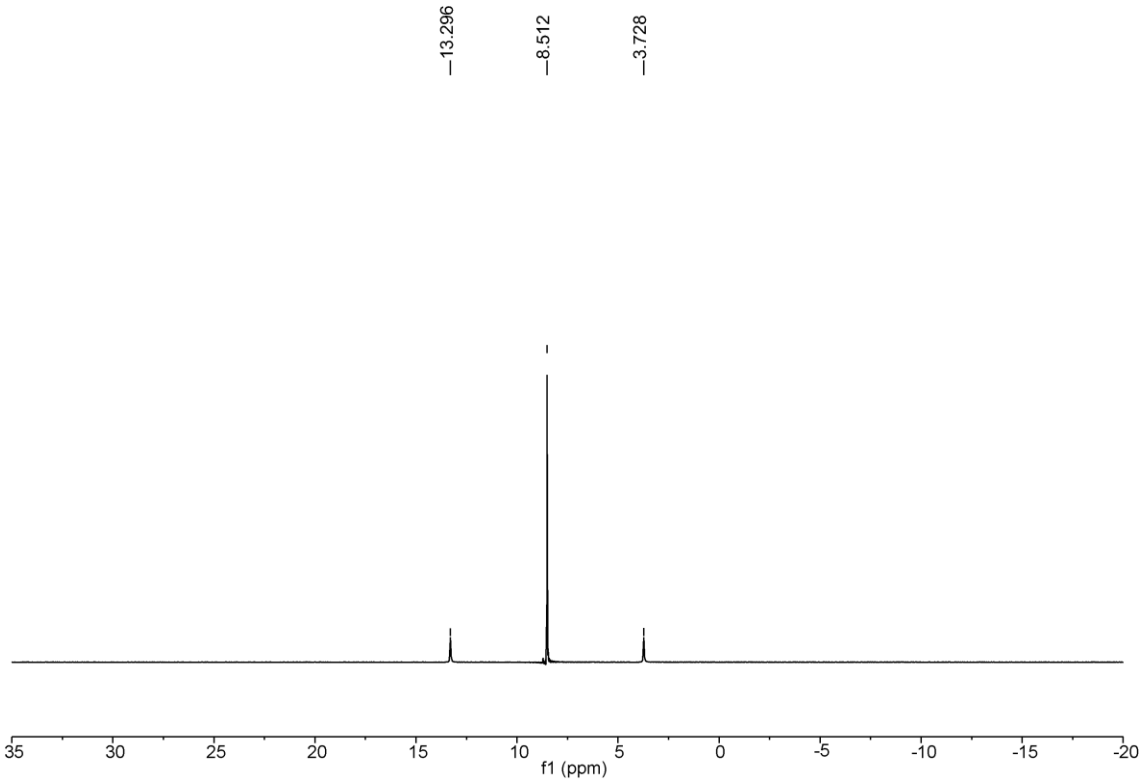

Fig. S15. ^{31}P{^{1}H} spectra (243 MHz, $CDCl_3$, 298 K) of **S6**.

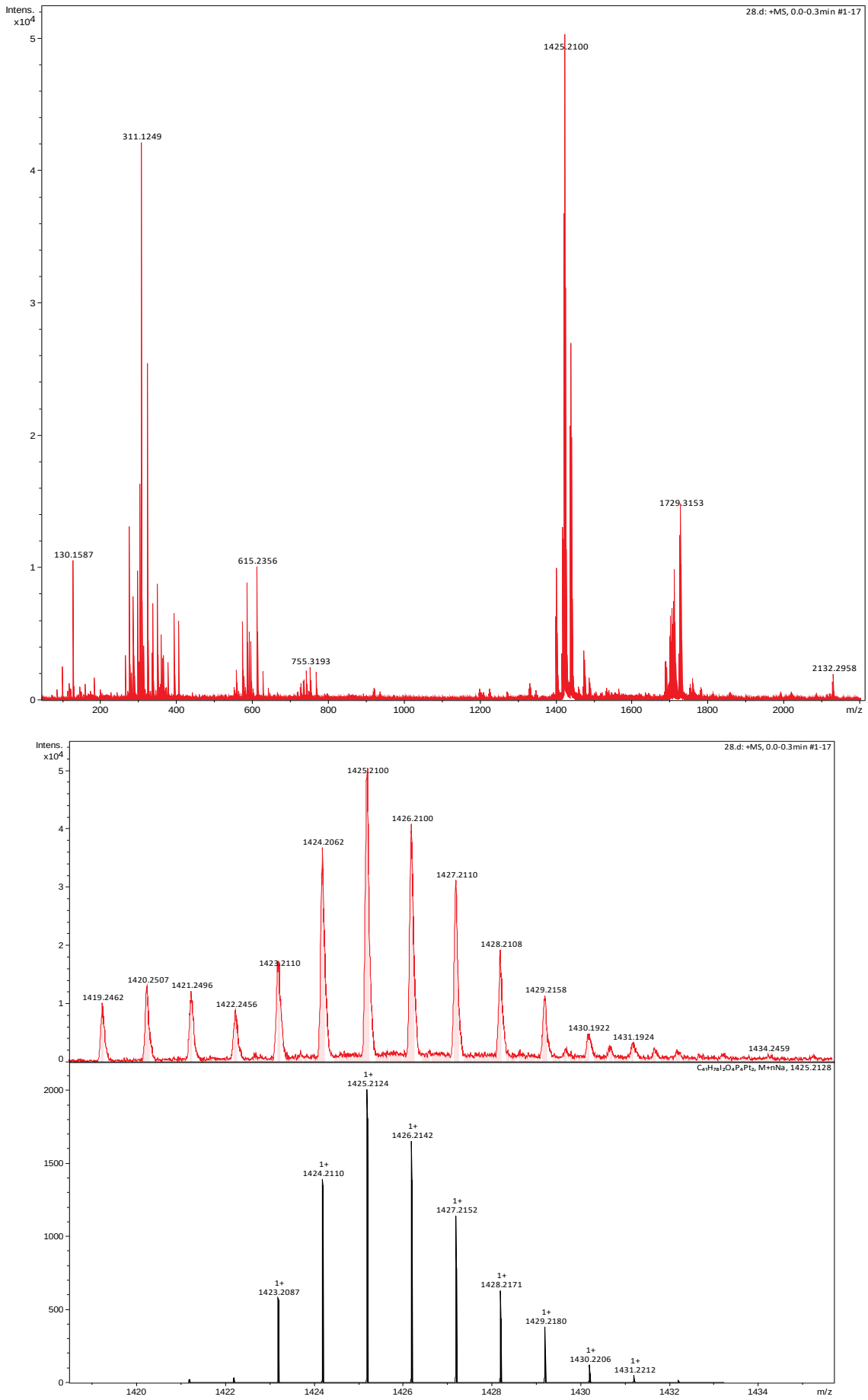

Fig. S16. ESI-HR-MS spectrum of **S6**.

*Synthesis of compound **1b***

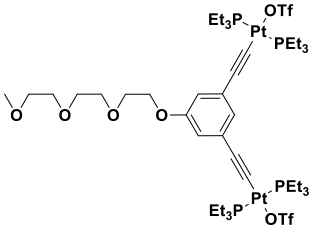

Compound **S6** (50 mg, 0.035 mmol), AgOTf(27 mg, 0.106 mmol) were were added into a 10 mL brown vial, then freshly distilled CH_2Cl_2 (8 mL) was added. The resulting mixture was stirred in the dark at room temperature for 12 h. After filtering off the heavy creasy precipitate through a glass fiber filter, the suspension was obtianed. The solvent was removed under a flow of nitrogen to afford **1b** as a white solid (49 mg, 95%).[S4] ^{1}H NMR (600 MHz, $CDCl_3$, 298K) δ 7.34 (s, 1H), 6.88 (s, 2H), 4.22 – 4.16 (m, 2H), 3.91 (d, *J* = 4.7 Hz, 2H), 3.78 (d, *J* = 4.6 Hz, 2H), 3.72 (s, 2H), 3.69 (s, 2H), 3.63 – 3.58 (m, 2H), 3.44 (s, 3H), 2.13 – 2.02 (m, 24H), 1.25 – 1.12 (m, 36H). ^{31}P NMR (243 MHz, $CDCl_3$,, 298K) δ 21.84 (s, ^{195}Pt satellites, $^1J_{Pt\text{-}P}$ = 2204.25 Hz). ESI-HR-MS: *m/z* 1148.4183 [**1b** – 2OTf]$^+$, calcd. for $[C_{41}H_{78}O_4P_4Pt_2]^+$, 1148.4146.

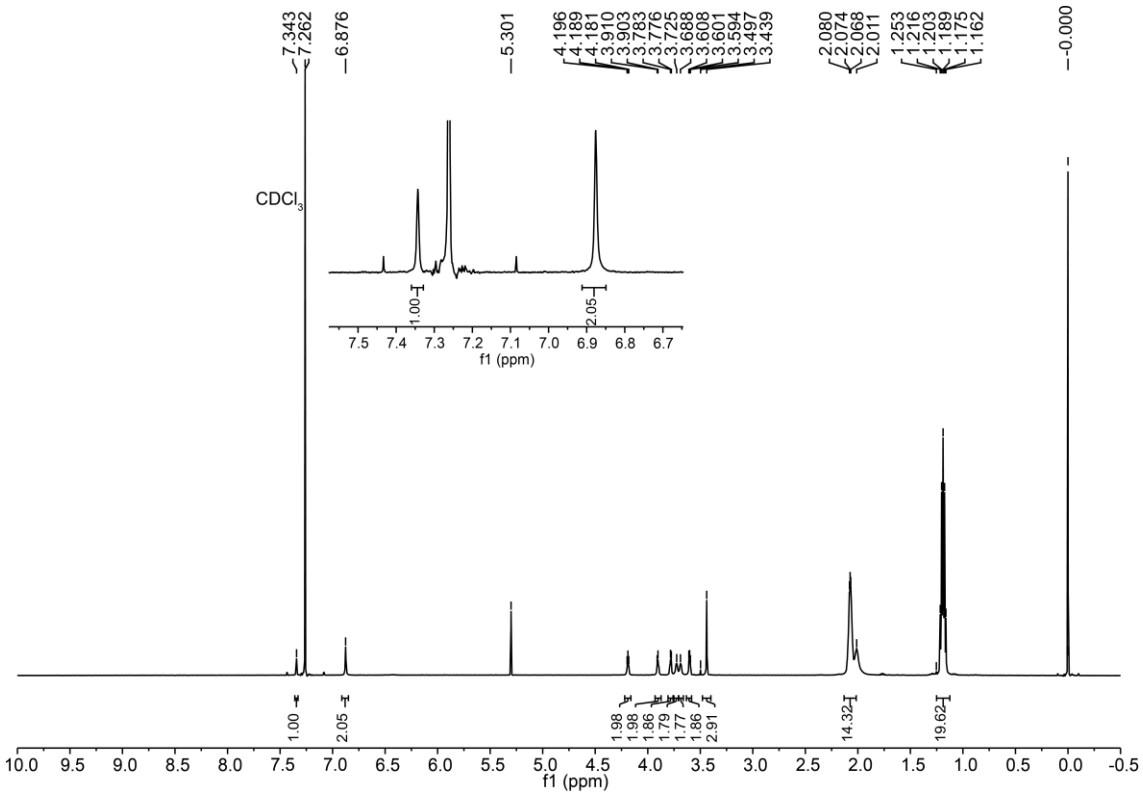

Fig. S17. ^{1}H NMR spectrum (600 MHz, $CDCl_3$, 298 K) recorded for **1b**.

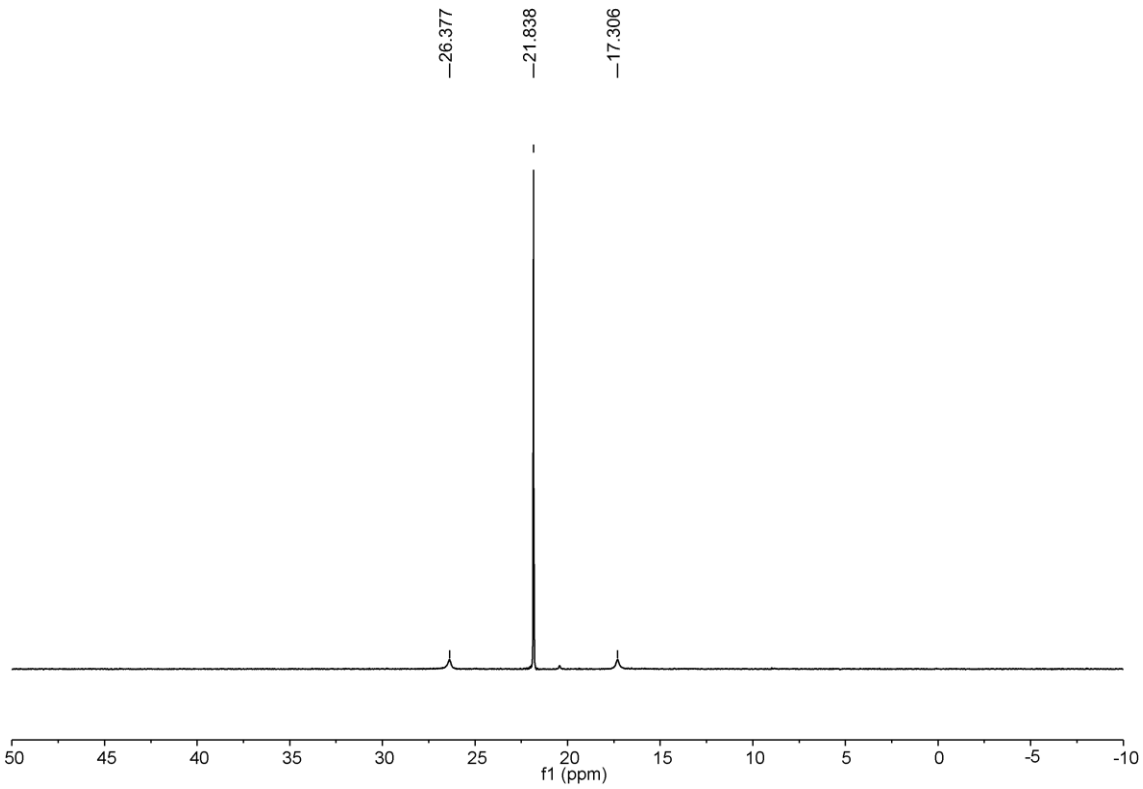

Fig. S18. $^{31}P\{^{1}H\}$ spectra (243 MHz, CD_2Cl_2, 298 K) of **1b**.

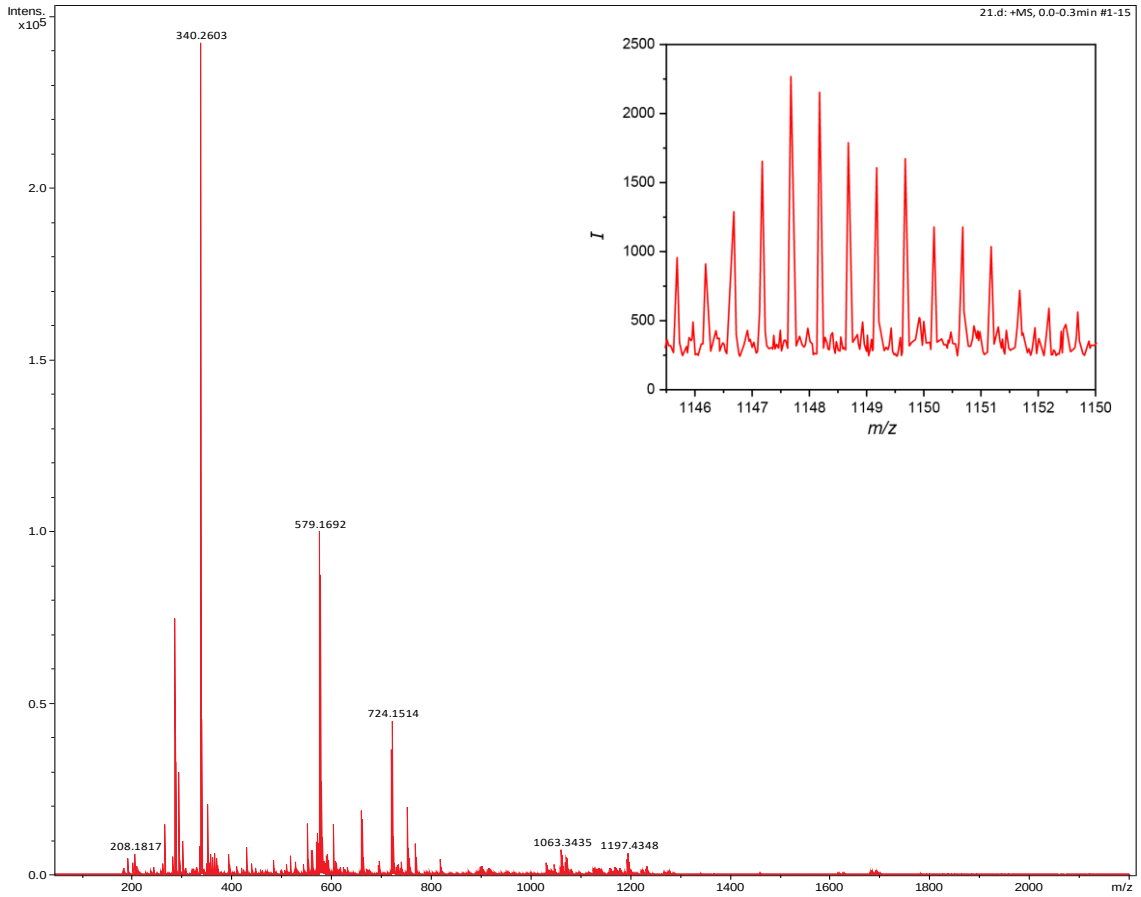

Fig. S19. ESI-HR-MS spectrum of **1b**.

Synthesis of compound S7

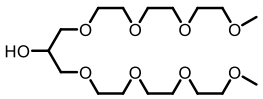

Methoxytriethylene glycol (5.0 g, 0.03 mol) was added to a dry 50 mL Schlenk flask. Then, Na metal (190 mg) was added slowly and stirred under N_2 atmosphere at 100 °C for 1 hour. After the solution was cooled to 65 °C, and epichlorohydrin (0.63 mL, 0.005 mol) was added drop-wise. Upon complete addition of epichlorohydrin, reaction mixture was heated to 100 °C, and allowed to react for 3 days. After completion of the reaction, NH_4Cl (1.06 g, 0.02 mol) was added and reacted at 100 °C for 1 h. The product was concentrated to give a crude product which was purified by flash column chromatography with ethyl acetate: methanol (9:1, v/v) as the eluent to afford compound **S7** as a light yellowish oil(3.2g, 28%).[S5] ^{1}H NMR (600 MHz, $CDCl_3$, 298K) δ 3.97 – 3.95 (m, 1H), 3.68 – 3.60 (m, 22H), 3.57 – 3.47 (m, 6H), 3.37 (s, 6H).

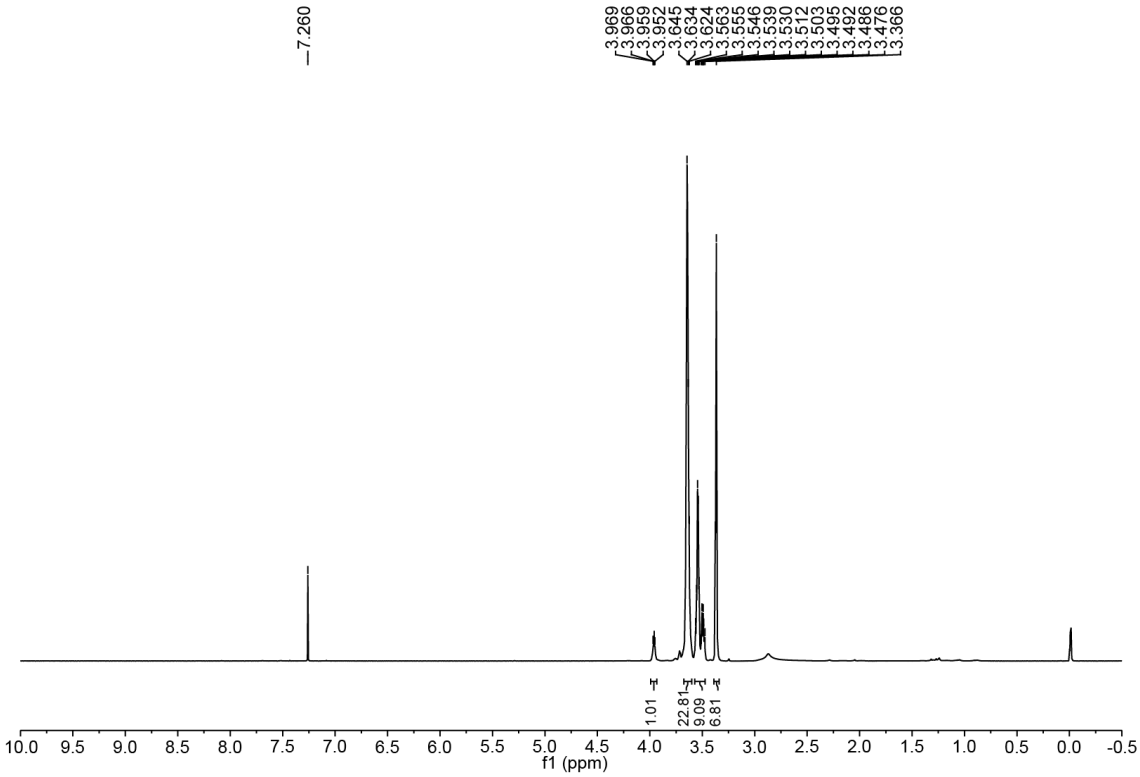

Fig. S20. ^{1}H NMR spectrum (600 MHz, $CDCl_3$, 298 K) recorded for **S7**.

Synthesis of compound S8

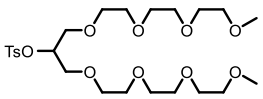

Compound **S7** (1.24 g, 2.62 mmol), NaH (80 mg, 3.15 mmol) were dissolved in dry tetrahydrofuran (40 mL) at ice bath conditions and stired for 15 minutes . TsCl (0.75 g, 3.94 mmol) was added to the solution. The reaction mixture was stirred at room temperature for 8 h under nitrogen.Then the product was concentrated to give a crude product which was purified by flash column chromatography with dichloromethane: methanol (80:1, v/v) as the eluent to afford compound **S8** (2.93 g, 80%) as a colorless oil.[S5] ^{1}H NMR (600 MHz, $CDCl_3$, 298K) δ 7.80 (d, J = 8.2 Hz, 2H), 7.31 (d, J = 8.2 Hz,

2H), 4.71 – 4.65 (m, 1H), 3.67 – 3.47 (m, 26H), 3.40 – 3.32 (m, 6H), 2.43 (s, 3H). ^{13}C NMR (151 MHz, $CDCl_3$, 298K) δ 144.49, 133.99, 129.57, 127.99, 79.61, 71.87, 70.85, 70.54, 70.46, 70.31, 69.62, 58.99, 21.60. ESI-HR-MS: *m/z* 561.2340 [**S8** + Na]$^+$, calcd. for $[C_{24}H_{42}NaO_{11}S]^+$, 561.2391.

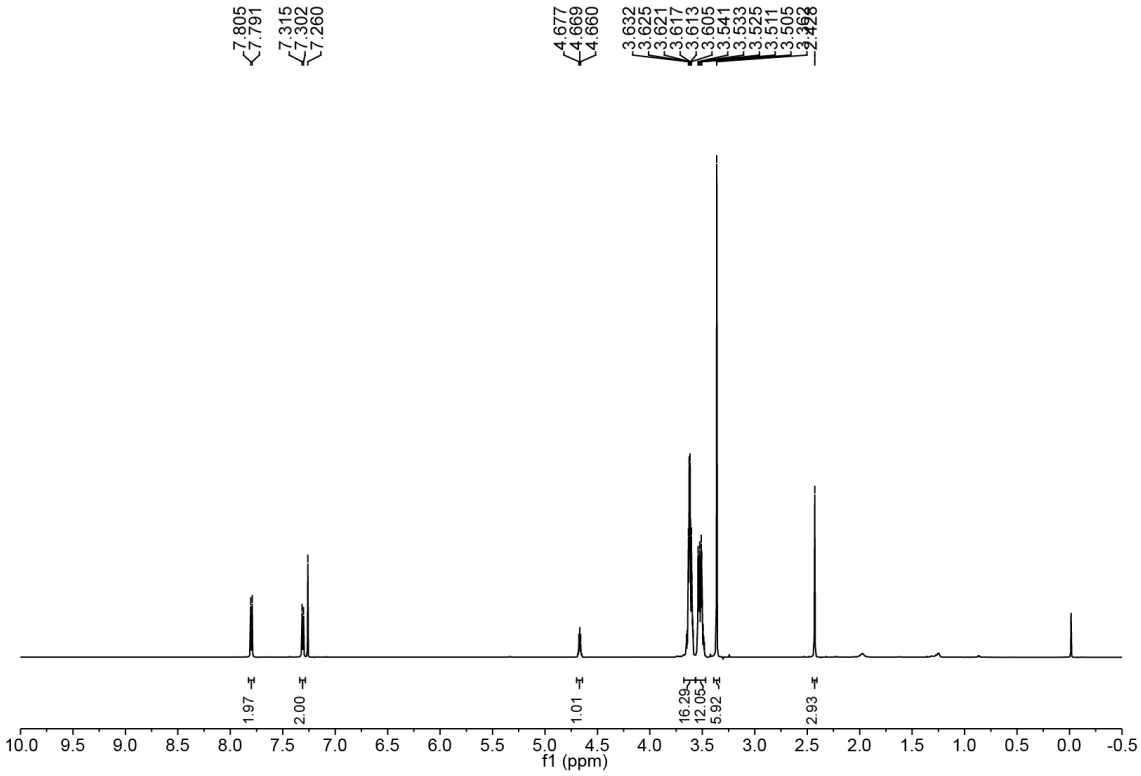

Fig. S21. ^{1}H NMR spectrum (600 MHz, $CDCl_3$, 298 K) recorded for **S8**.

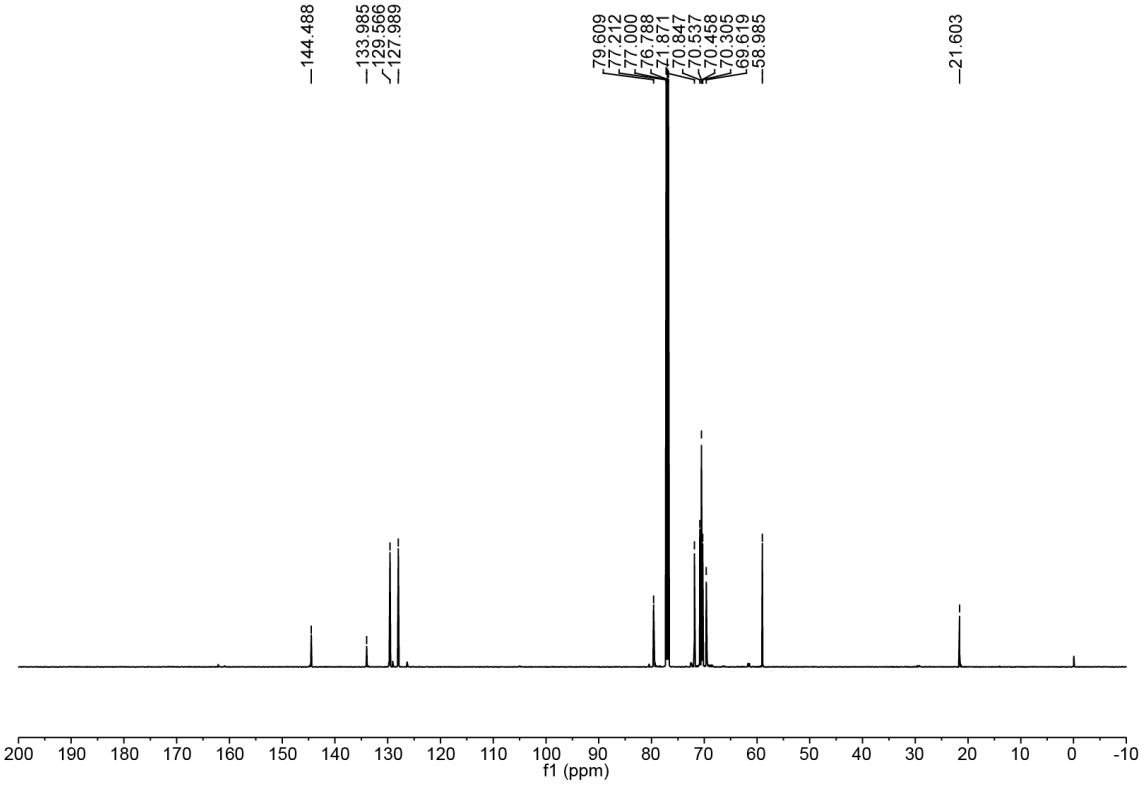

Fig. S22. ^{13}C NMR spectrum (151 MHz, $CDCl_3$, 298 K) recorded for **S8**.

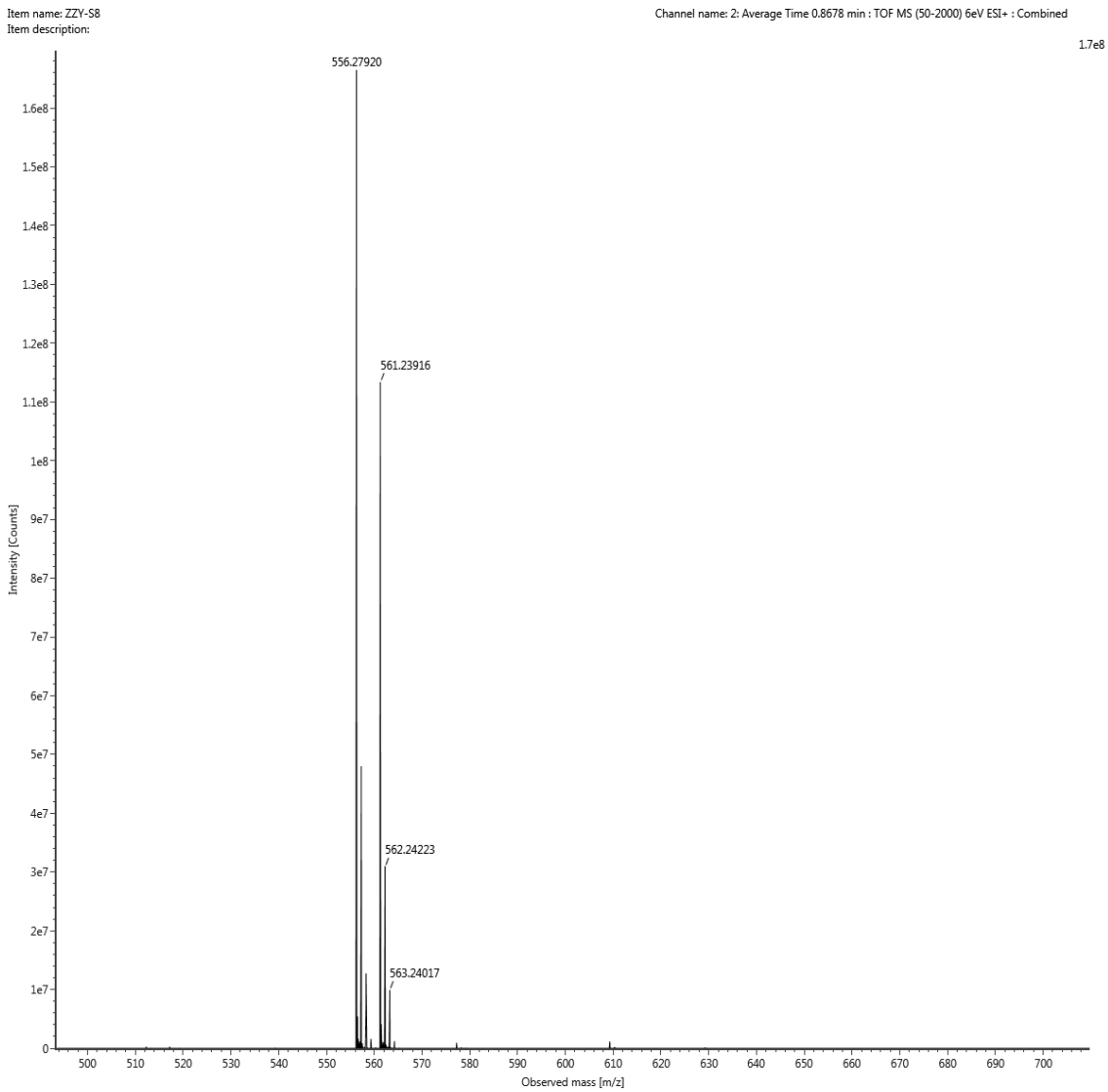

Fig. S23. ESI-HR-MS spectrum of **S8**.

Synthesis of compound S9

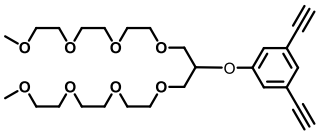

Compound **S8** (1.07 g, 1.98 mmol) and **S4** (235 mg, 1.65 mmol) were dissolved in dry CH_3CN (20mL). K_2CO_3 (0.64 g, 4.95 mmol) and KI (83 mg, KI) were added to the solution. The reaction mixture was stirred at 90 °C for 12 h under nitrogen atmosphere. Precipitated salts were removed by filtration and the crude product was purified by flash column chromatography with dichloromethane: methanol (40:1, v/v) as the eluent to afford compound **S9** (0.84 g, 84%) as a colorless oil.[S4] ^{1}H NMR (600 MHz, $CDCl_3$, 298K) δ 7.20 (s, 1H), 7.10 (s, 2H), 4.52 (s, 1H), 3.68 – 3.59 (m, 24H), 3.55 – 3.52 (m, 4H), 3.37 (s, 6H), 3.05 (s, 2H); ^{13}C NMR (151 MHz, $CDCl_3$, 298K) δ 157.96, 128.70, 123.34, 120.66, 82.47, 77.70, 77.45, 71.89, 71.10, 70.62, 70.59, 70.52, 70.48, 70.45, 59.01. ESI-HR-MS: *m/z* 531.2566 [**S9** + Na]$^+$, calcd. for $[C_{27}H_{40}NaO_9]^+$, 531.2565.

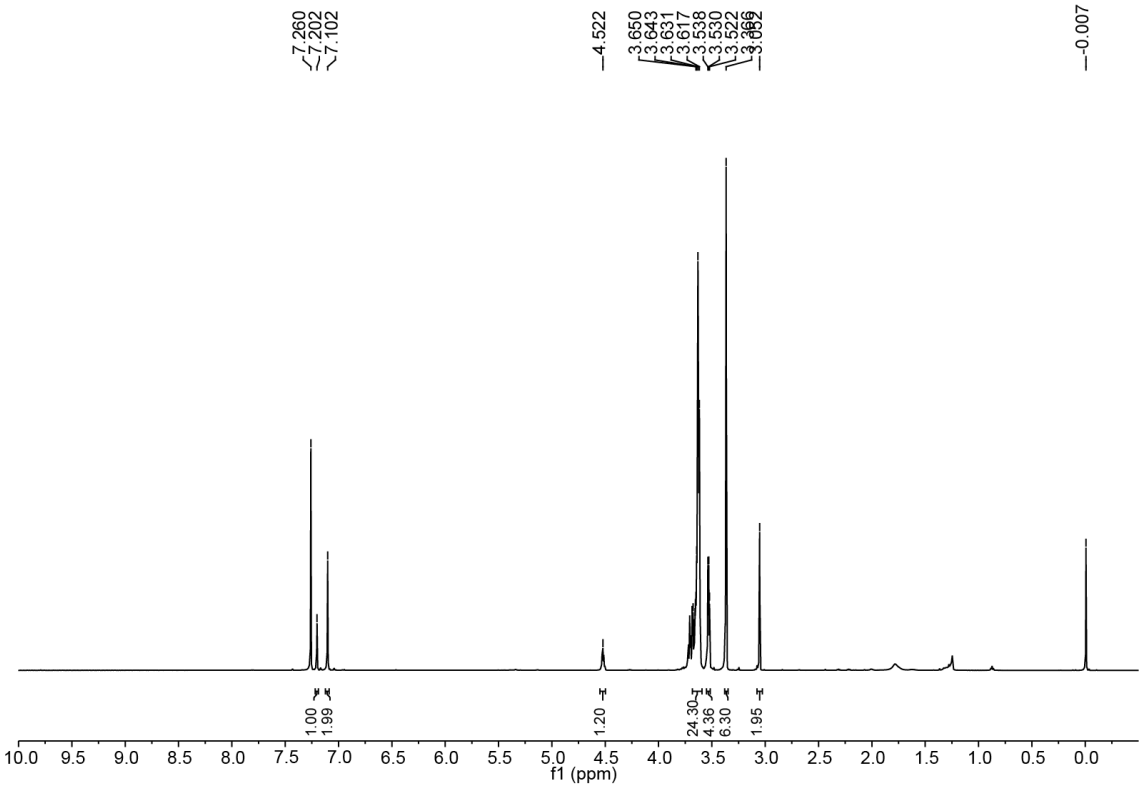

Fig. S24. ^{1}H NMR spectrum (600 MHz, $CDCl_3$, 298 K) recorded for **S9**.

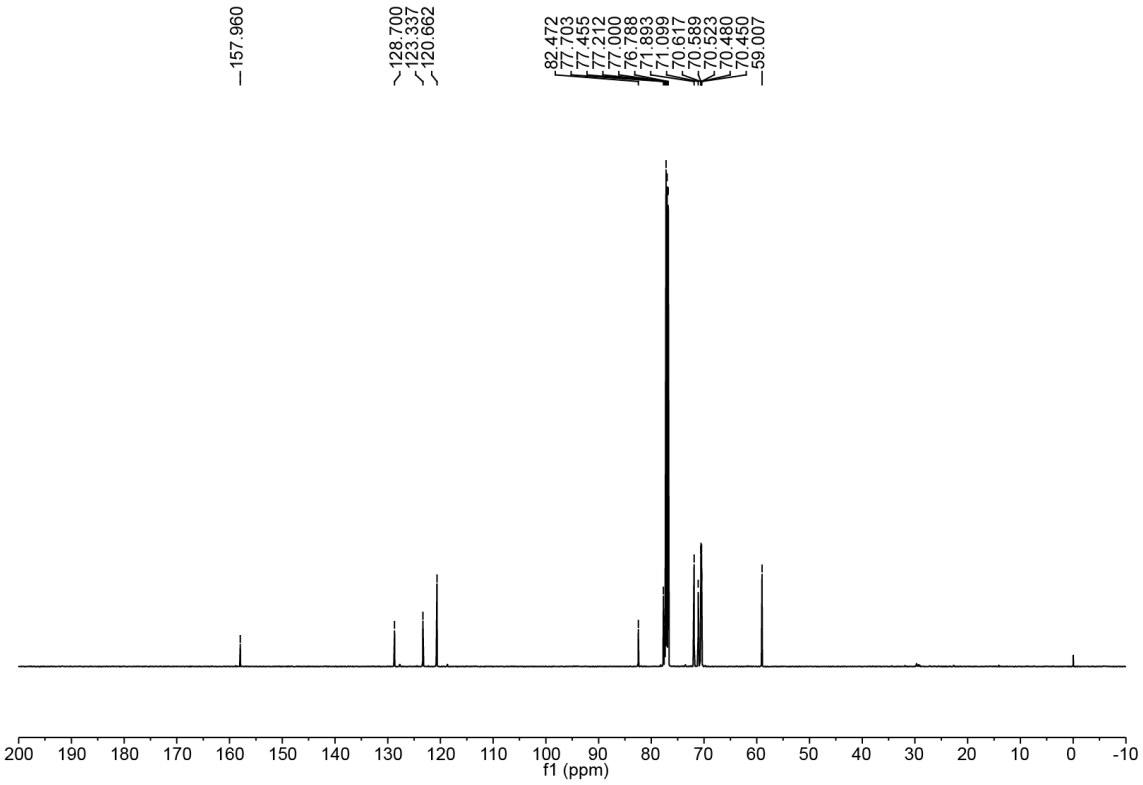

Fig. S25. ^{13}C NMR spectrum (600 MHz, $CDCl_3$, 298 K) recorded for **S9**.

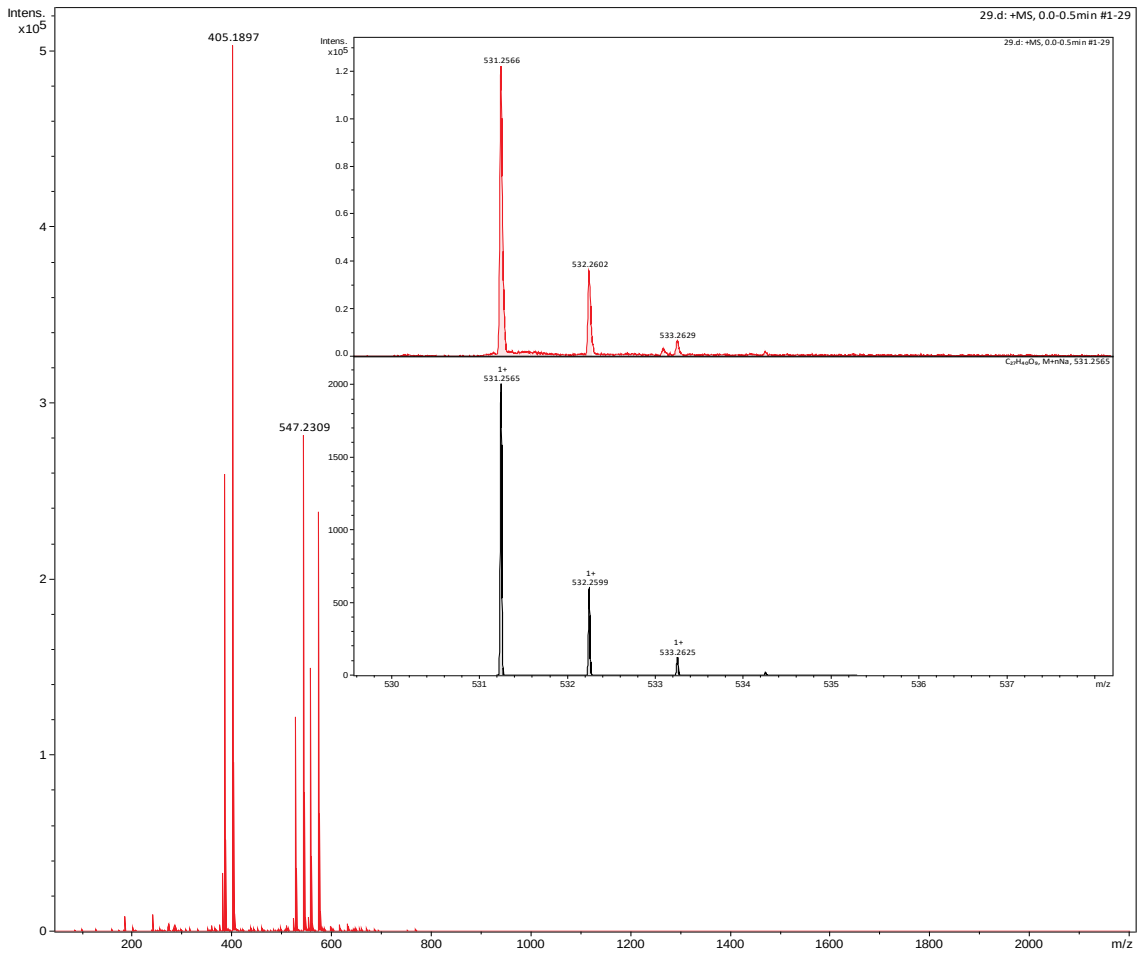

Fig. S26. ESI-HR-MS spectrum of **S9**.

Synthesis of compound S10

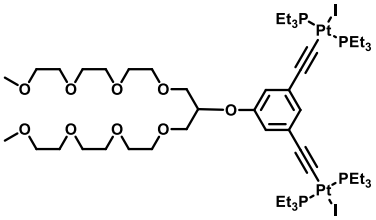

Compound **S9** (0.282 g, 0.55 mmol), $Pt(PEt_3)_2I_2$ (1.52 g, 2.21 mmol) were dissolved in dry toluene (50 mL) in a 100 mL Schlenk flask, CuI (10 mg, 0.10 mmol) and dry diethylamine (10 mL) were added to the solution. Then the mixture was stirred at room temperature for 48 h under nitrogen. The product was concentrated to give a crude product which was purified by flash column chromatography with dichloromethane: methanol (50:1, v/v) as the eluent to afford compound **S10** as a colorless oil.[S4] ^{1}H NMR (600 MHz, $CDCl_3$, 298K) δ 6.82 (s, 1H), 6.70 (s, 2H), 4.52 – 4.45 (m, 1H), 3.75 – 3.51 (m, 24H), 3.37 (s, 6H), 2.31 – 2.14 (m, 20H), 1.17 (dd, J = 16.0, 8.0 Hz, 29H). ^{31}P NMR (243 MHz, $CDCl_3$, 298K) δ 8.52 (s, ^{195}Pt satellites, $^1J_{Pt\text{-}P}$ = 2323.80 Hz). ESI-HR-MS: *m/z* 1645.3436 [**S10** + Na]$^+$, calcd. for $[C_{51}H_{98}I_2NaO_9P_4Pt_2]^+$, 1645.3438.

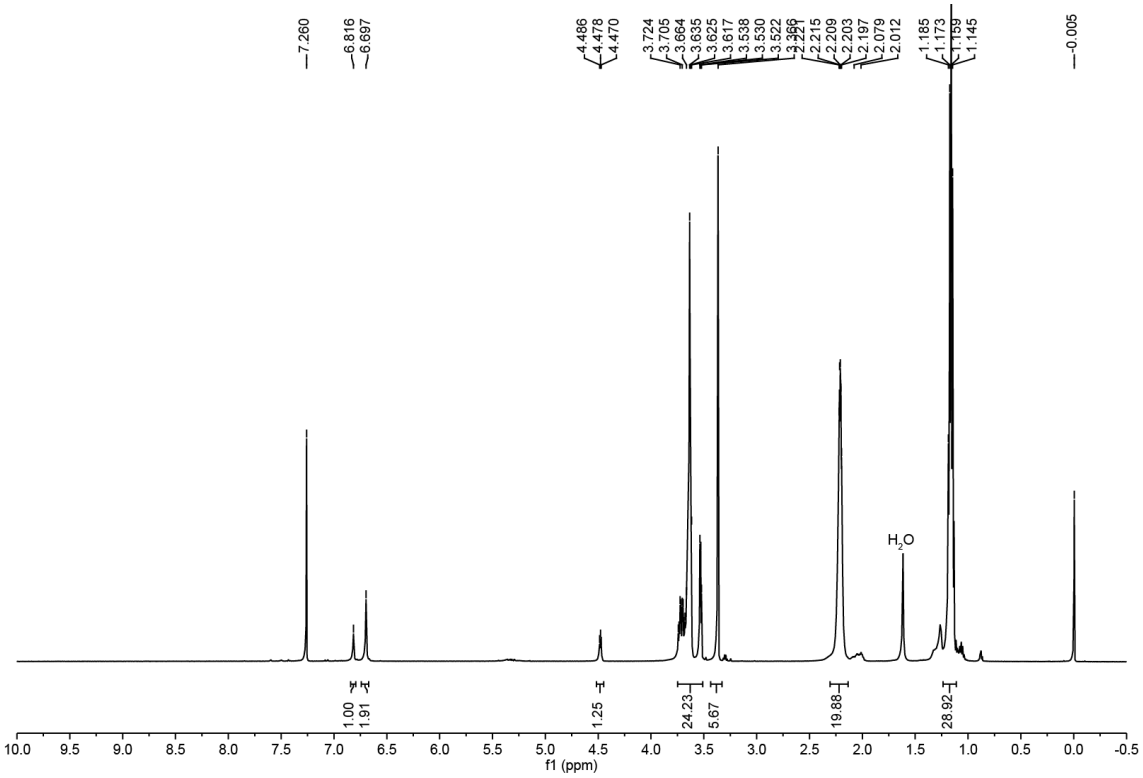

Fig. S27. ^{1}H NMR spectrum (600 MHz, $CDCl_3$, 298 K) recorded for **S10**.

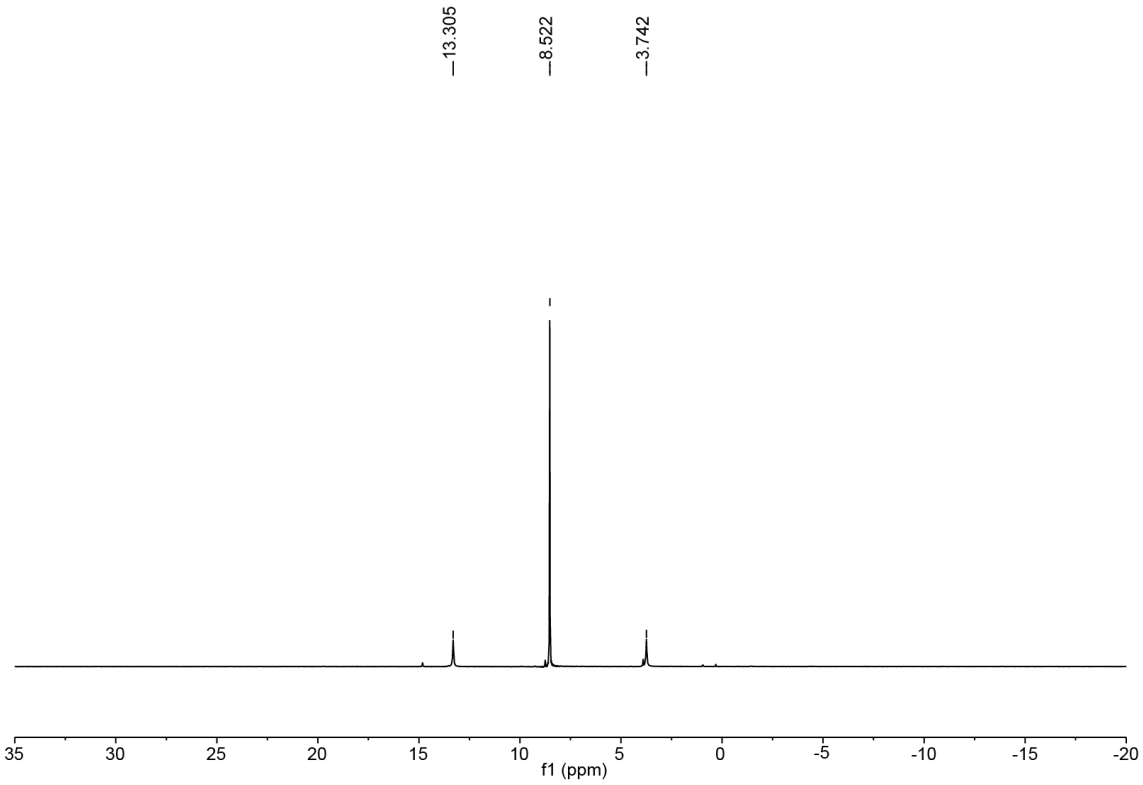

Fig. S28. ^{31}P{^{1}H} NMR spectrum (243 MHz, $CDCl_3$, 298 K) recorded for **S10**.

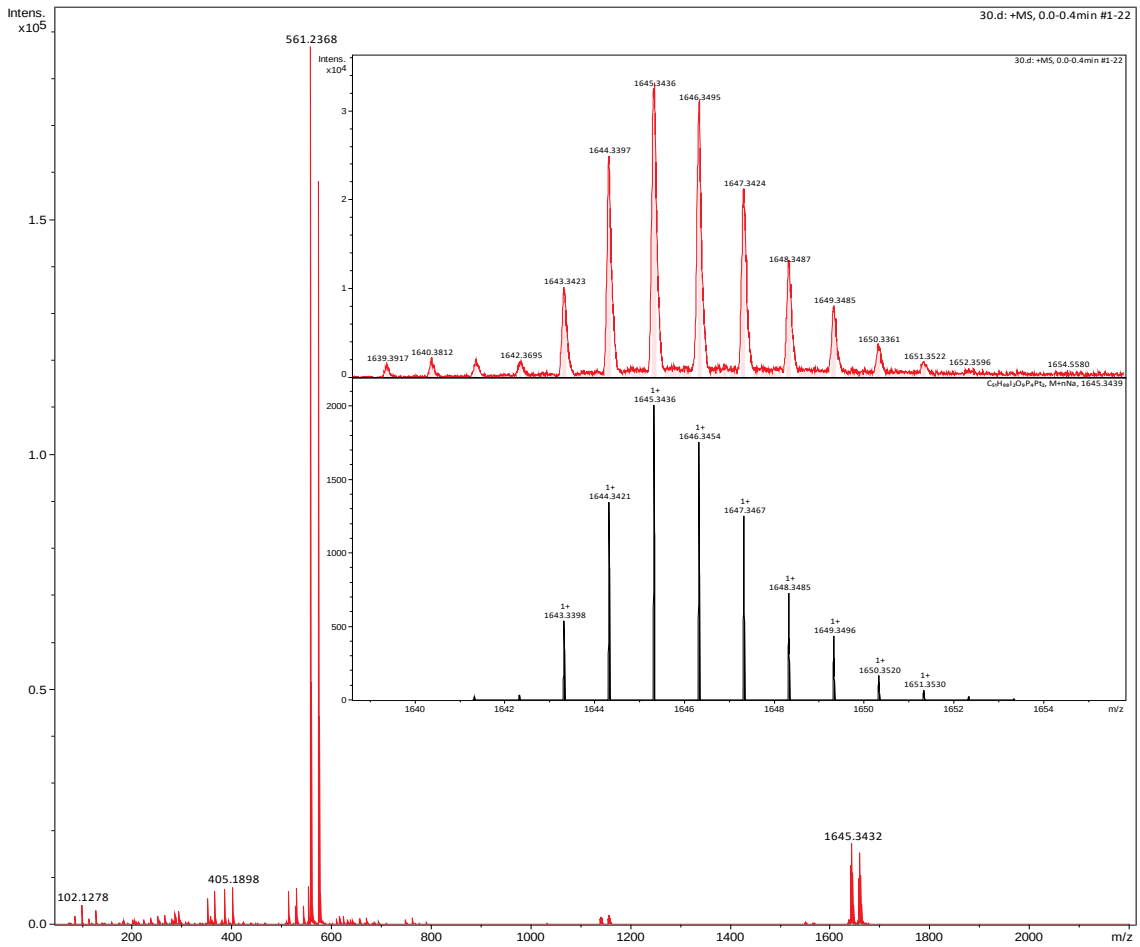

Fig. S29. ESI-HR-MS spectrum of **S10**.

Synthesis of compound 1c

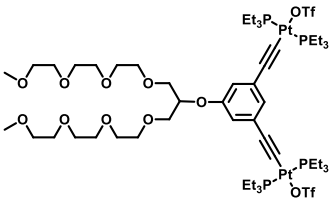

Compound **S10** (342 mg, 0.21 mmol) and AgOTf (632 mg, 0.63 mmol) were added into a 40 mL brown vial, then freshly distilled CH_2Cl_2 (30 mL) was added. The resulting mixture was stirred in the dark at room temperature for 16 h. After filtering off the heavy creasy precipitate through a glass fiber filter, the suspension was obtained. The solvent was removed under a flow of nitrogen to afford **1c** as a white solid (332 mg, 95%).[S4] ^{1}H NMR (600 MHz, CD_2Cl_2, 298K) δ 7.27 (s, 2H), 6.98 (s, 1H), 4.98 (s, 2H), 3.79 (t, J = 77.4 Hz, 28H), 3.44 (d, J = 6.9 Hz, 7H), 2.09 (s, 24H), 1.20 (dd, J = 16.0, 7.9 Hz, 34H). ^{31}P NMR (243 MHz, CD_2Cl_2, 298K) δ 21.84 (s, ^{195}Pt satellites, $^1J_{Pt\text{-}P}$ = 2216.40 Hz). ESI-HR-MS: *m/z* 1667.4568 [**1c** + H]$^+$, calcd. for [$C_{53}H_{99}F_6O_{15}P_4Pt_2S_2$]$^+$, 1667.4570.

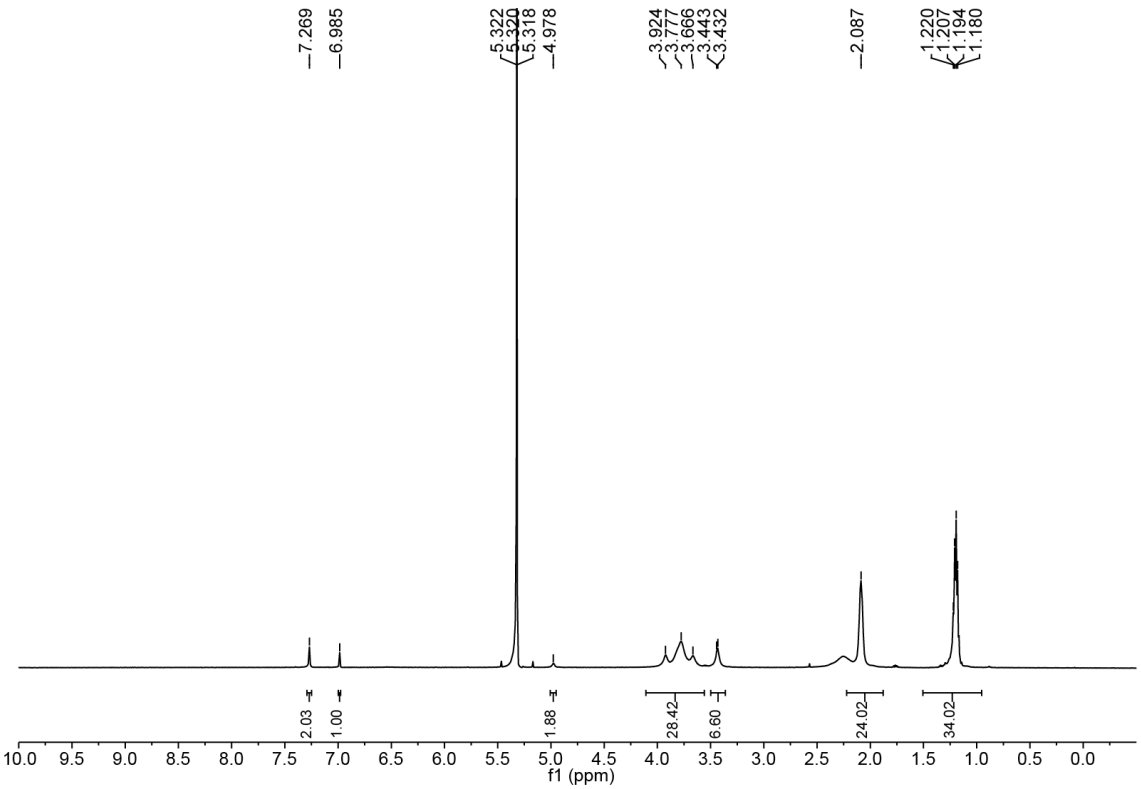

Fig. S30. ^{1}H NMR spectrum (600 MHz, $CDCl_3$, 298 K) recorded for **1c**.

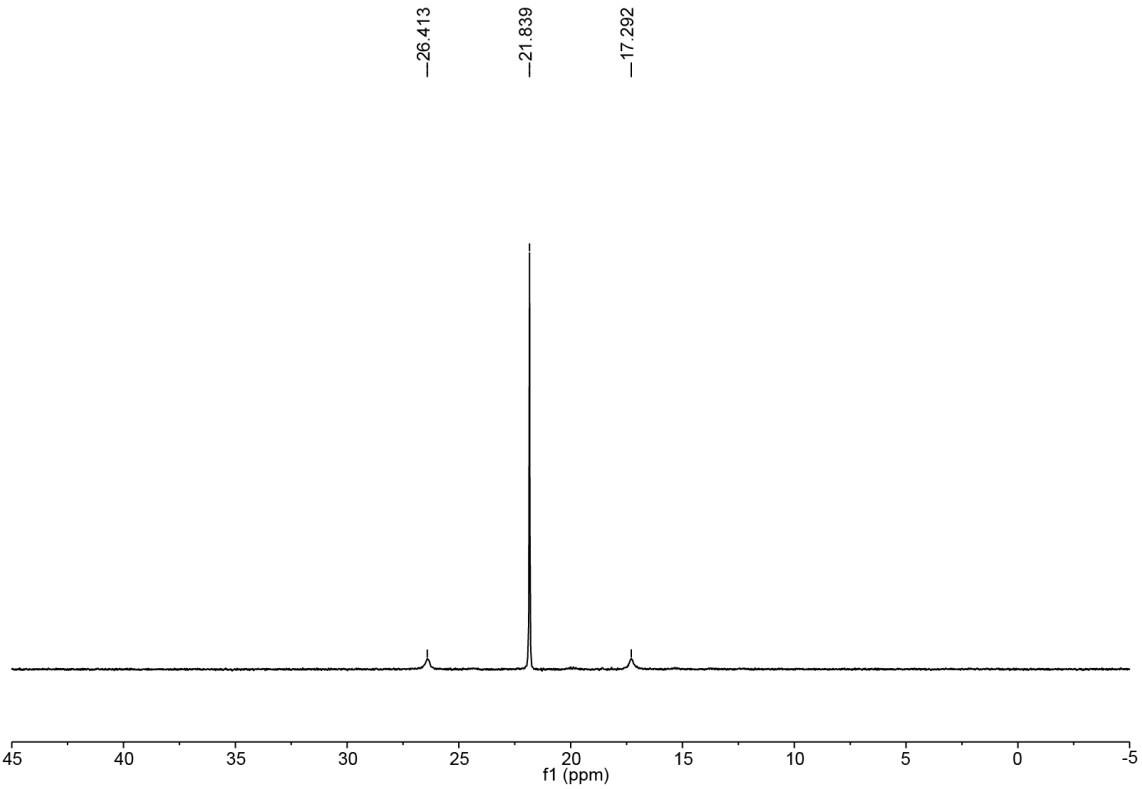

Fig. S31. ^{31}P{^{1}H} NMR spectrum (243 MHz, $CDCl_3$, 298 K) recorded for **1c**.

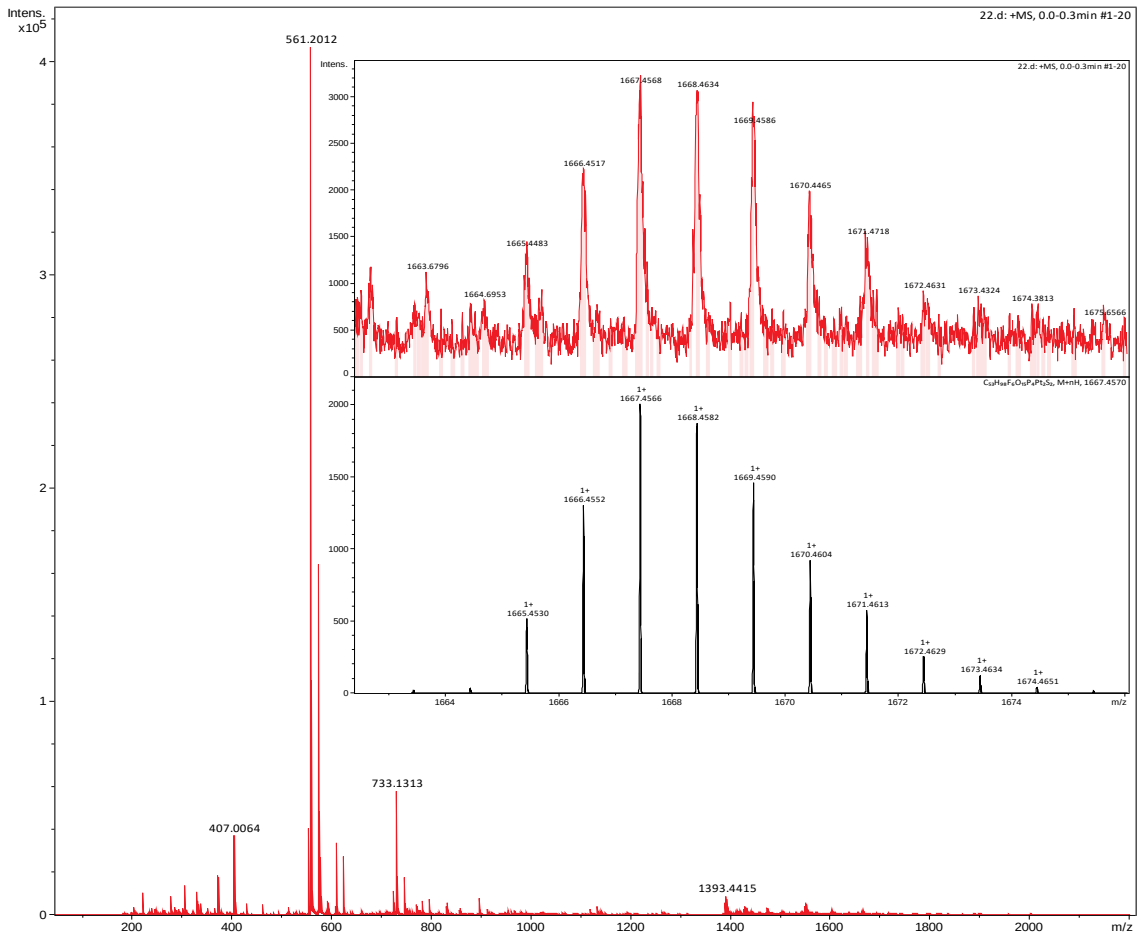

Fig. S32. ESI-HR-MS spectrum of **1c**.

Synthesis of compound S11

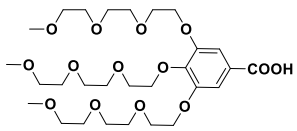

Compound **S11** was synthesized according to the above procedure [S1]. ^{1}H NMR (600 MHz, $CDCl_3$, 298K) δ 7.35 (s, 2H), 4.27 – 4.17 (m, 6H), 3.89 – 3.78 (m, 6H), 3.76 – 3.70 (m, 6H), 3.69 – 3.61 (m, 12H), 3.57 – 3.52 (m, 6H), 3.37 (s, 9H); ^{13}C NMR (151 MHz, $CDCl_3$, 298K) δ 170.05, 152.11, 142.86, 124.19, 109.28, 72.26, 71.74, 70.64, 70.50, 70.42, 70.36, 70.32, 69.46, 68.67, 58.83. ESI-HR-MS: *m/z* 631.2936 [**S11** + Na]$^{+}$, calcd. for $[C_{28}H_{48}NaO_{14}]^{+}$, 631.2938.

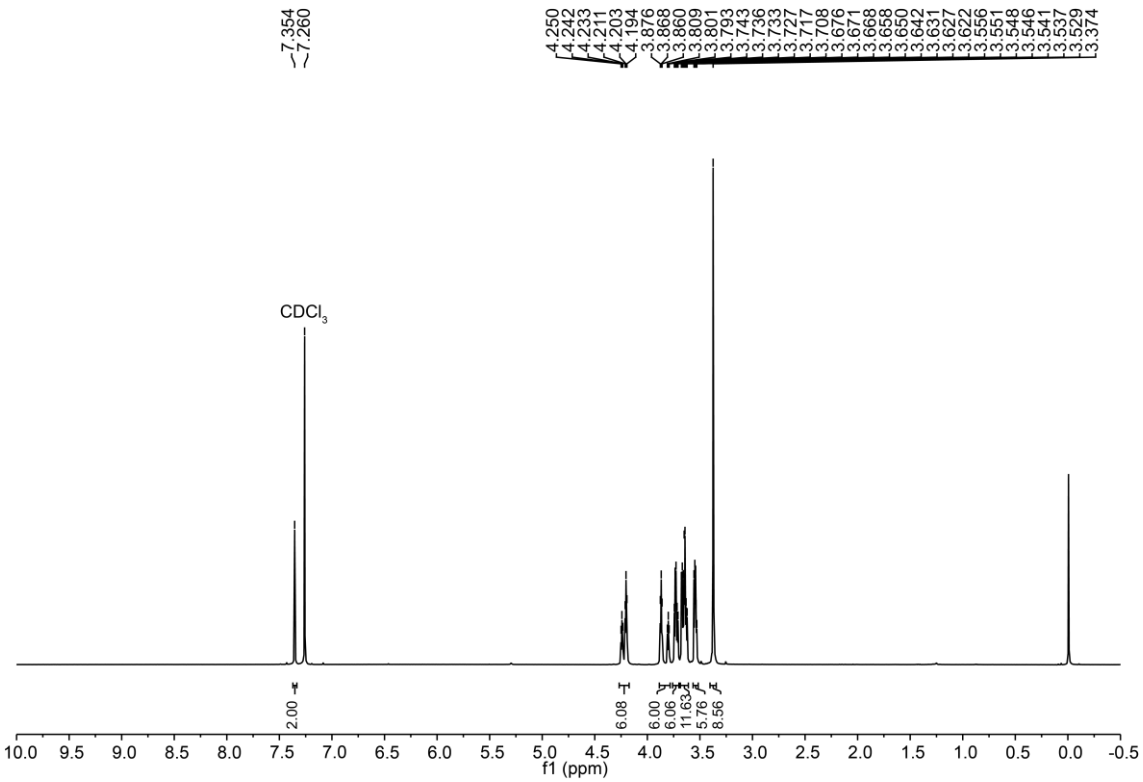

Fig. S33. ^{1}H NMR spectrum (600 MHz, $CDCl_3$, 298 K) recorded for **S11**.

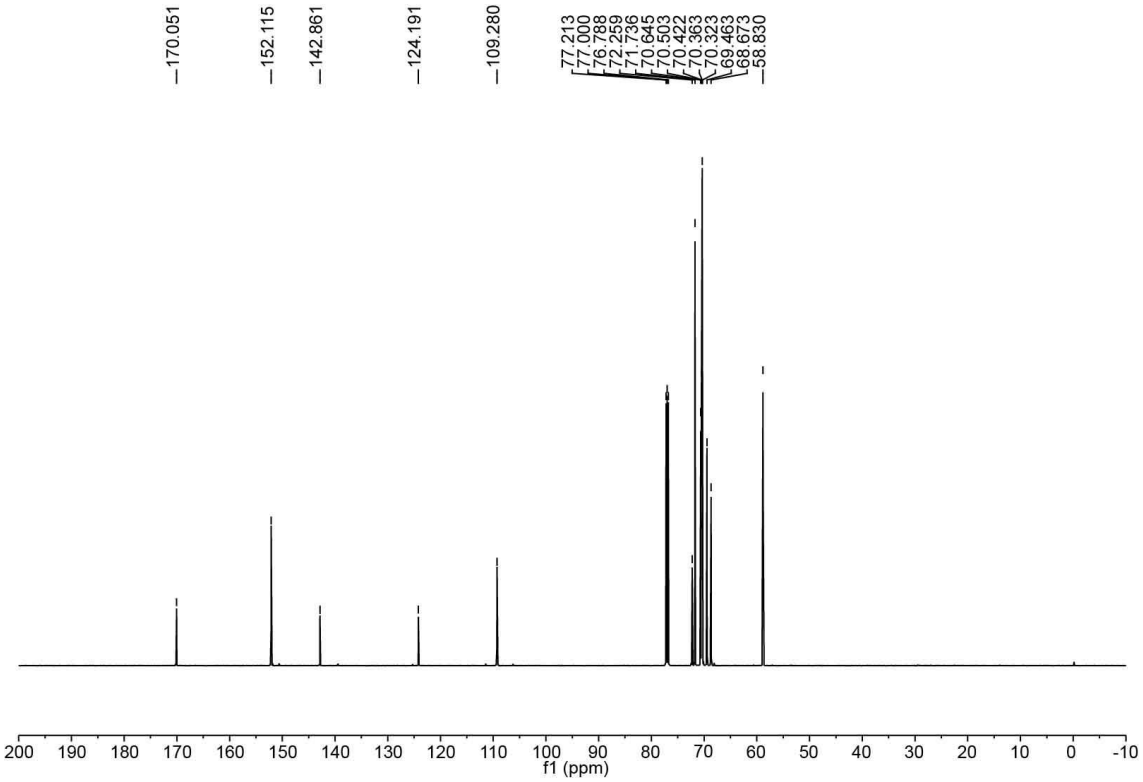

Fig. S34. ^{13}C NMR spectrum (151 MHz, $CDCl_3$, 298 K) recorded for **S11**.

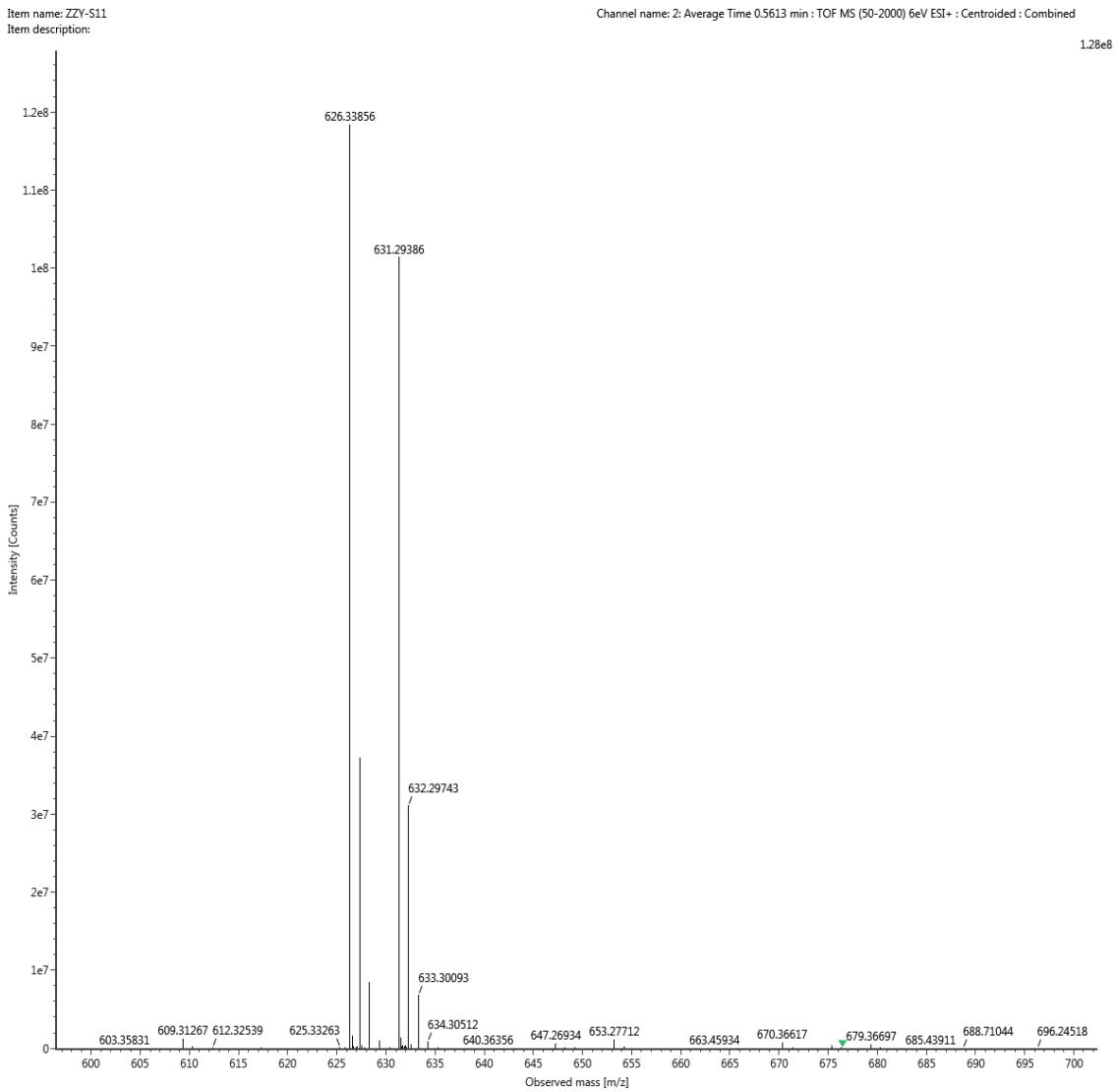

Fig. S35. ESI-HR-MS spectrum of **S11**.

Synthesis of compound S13

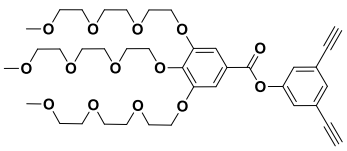

Compound **S4**(0.5 g, 3.52 mmol) and **S11** (2.56 g, 4.22 mmol) were dissolved in dry dichloromethane (40 mL) . EDCl (0.81 g, 4.22 mmol) and DMAP (85.9 mg, 0.71 mmol) were added to the solution. The reaction mixture was stirred at room temperature for 16 h under nitrogen.Then the product was concentrated to give a crude product which was purified by flash column chromatography with dichloromethane: methanol (50:1, v/v) as the eluent to afford compound **S13** (2.1 g, 85%) as a colorless oil. ^{1}H NMR (600 MHz, $CDCl_3$, 298K) δ 7.49 (d, *J* = 1.1 Hz, 1H), 7.41 (s, 2H), 7.30 (s, 2H), 4.27 – 4.19 (m, 6H), 3.88 – 3.79 (m, 6H), 3.74 – 3.70 (m, 6H), 3.67 – 3.60 (m, 12H), 3.55 – 3.50 (m, 6H), 3.36 (s, 9H), 3.12 (s, 2H). ^{13}C NMR (151 MHz, $CDCl_3$, 298K) δ 164.02, 152.36, 150.38, 143.41, 133.03, 125.87, 123.64, 123.34, 109.58, 81.53, 78.81, 72.38, 71.80, 71.78, 70.71, 70.56, 70.47, 70.44, 70.41, 69.49, 68.87, 58.89.ESI-HR-MS: *m/z* 755.3292 [**S13** + Na]$^{+}$, calcd. for $[C_{38}H_{52}NaO_{14}]^{+}$, 755.3249.

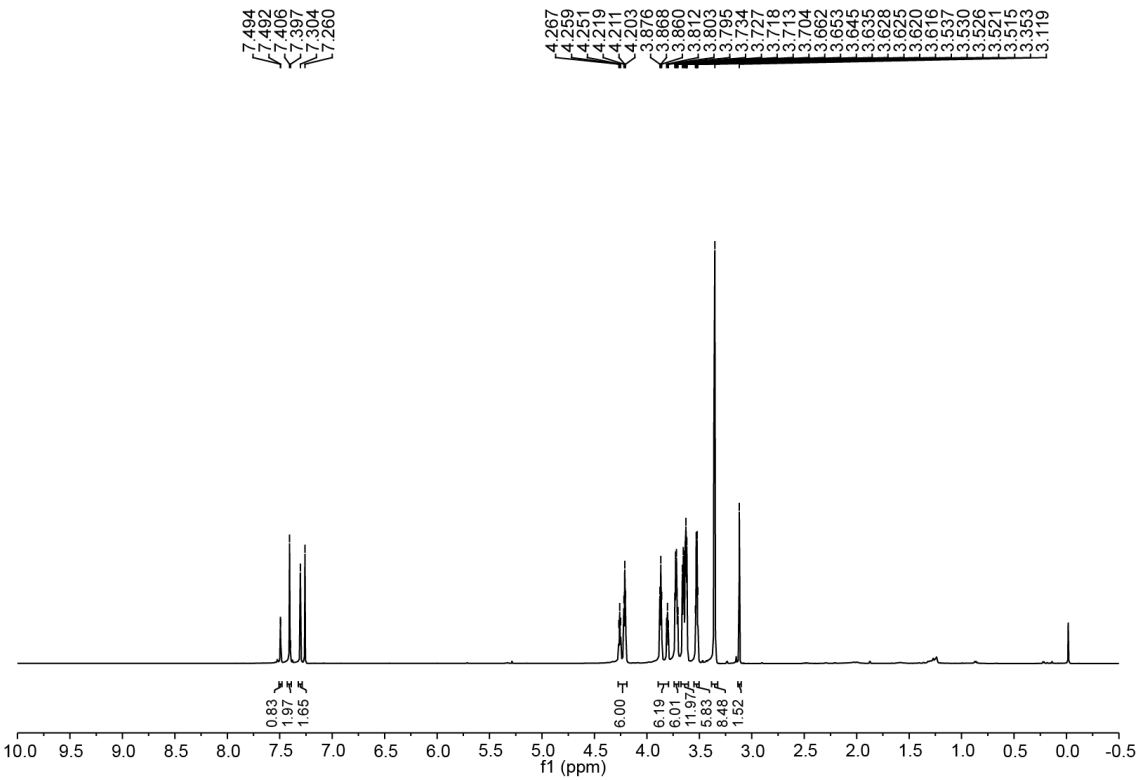

Fig. S36. ^{1}H NMR spectrum (600 MHz, $CDCl_3$, 298 K) recorded for **S13**.

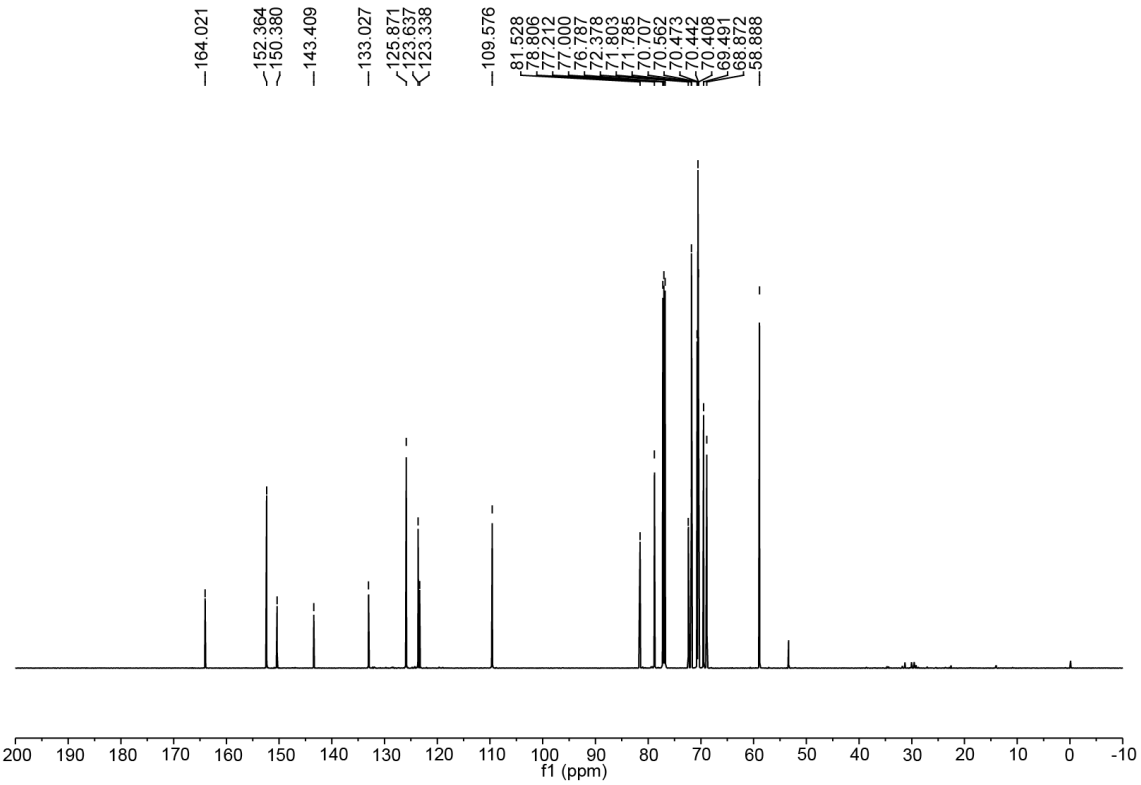

Fig. S37. ^{13}C NMR spectrum (151 MHz, $CDCl_3$, 298 K) recorded for **S13**.

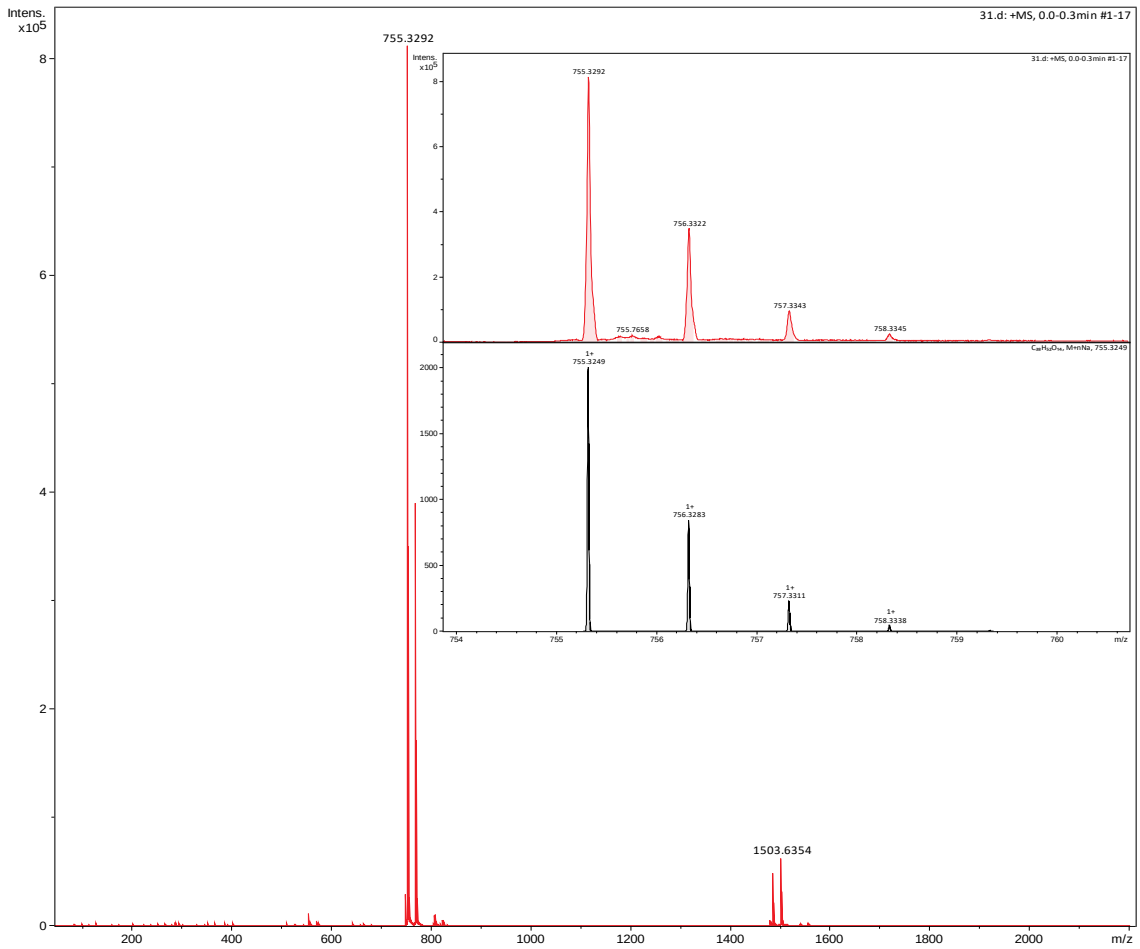

Fig. S38. ESI-HR-MS spectrum of **S13**.

Synthesis of compound S14

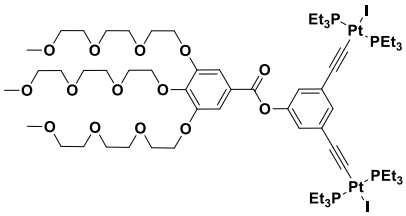

Compound S**13** (0.53 g, 0.73 mmol), $Pt(PEt_3)_2I_2$ (2.0 g, 2.91 mmol) were dissolved in dry toluene (60 mL) in a 100 mL Schlenk flask, CuI (23 mg, 0.12 mmol) and dry diethylamine (5 mL) were added to the solution. Then the mixture was stirred at room temperature for 48 h under nitrogen. The product was concentrated to give a crude product which was purified by flash column chromatography with dichloromethane: methanol (60:1, v/v) as the eluent to afford compound **S14** as a colorless oil. ^{1}H NMR (600 MHz, $CDCl_3$, 298K) δ 7.43 (s, 2H), 7.08 (s, 1H), 6.86 (s, 2H), 4.27 – 4.21 (m, 6H), 3.90 – 3.80 (m, 9H), 3.76 – 3.71 (m, 7H), 3.69 – 3.60 (m, 12H), 3.54 (dd, J = 9.6, 4.9 Hz, 6H), 3.37 (d, J = 6.6 Hz, 9H), 2.26 – 2.18 (m, 24H), 1.21 – 1.13 (m, 36H). ^{31}P NMR (243 MHz, $CDCl_3$, 298K) δ 8.59 (s, ^{195}Pt satellites, $^1J_{Pt\text{-}P}$ = 2321.14 Hz). ESI-HR-MS: *m/z* 1869.4122 [**S14** + Na]$^+$, calcd. for $[C_{62}H_{110}I_2NaO_{14}P_4Pt_2]^+$, 1869.4122.

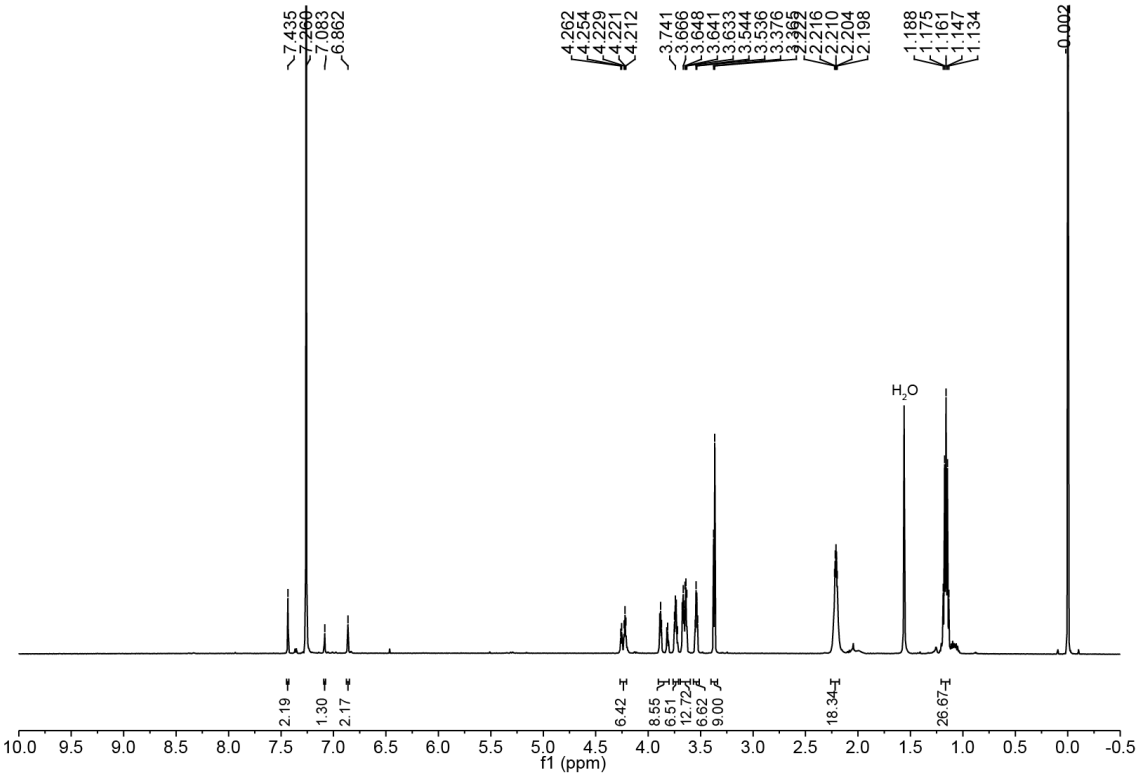

Fig. S39. ^{1}H NMR spectrum (600 MHz, $CDCl_3$, 298 K) recorded for **S14**.

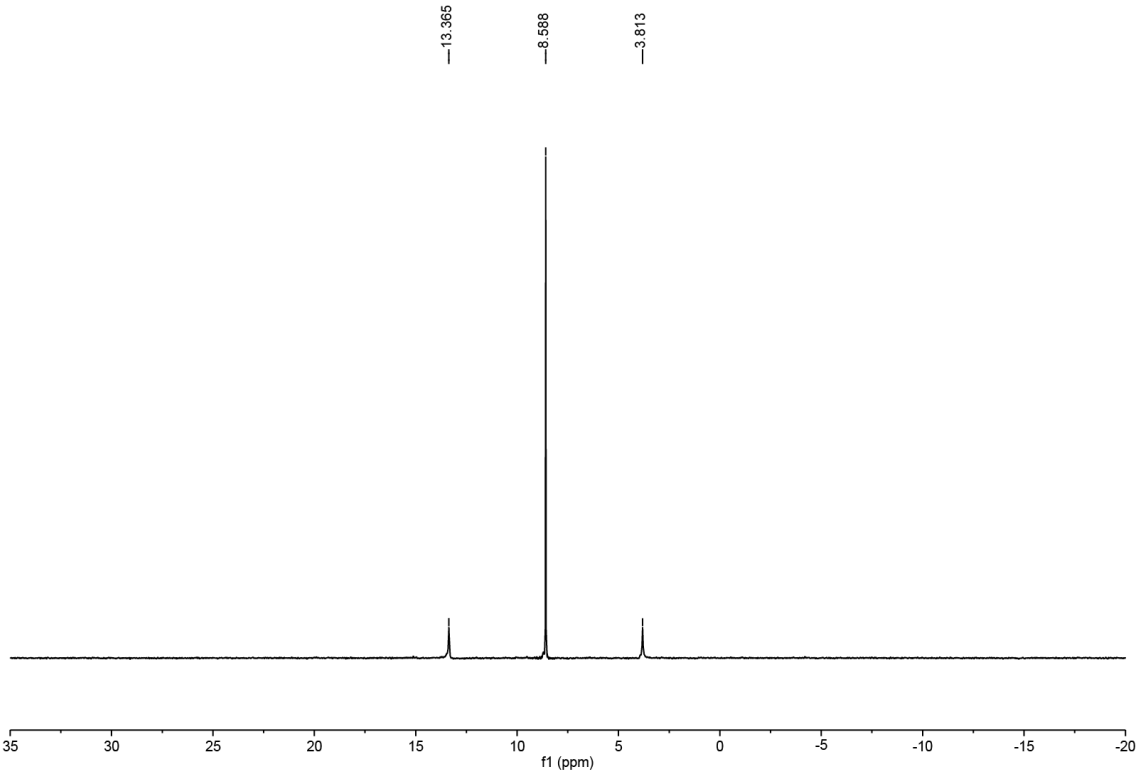

Fig. S40. ^{31}P{^{1}H} NMR spectrum (243 MHz, $CDCl_3$, 298 K) recorded for **S14**.

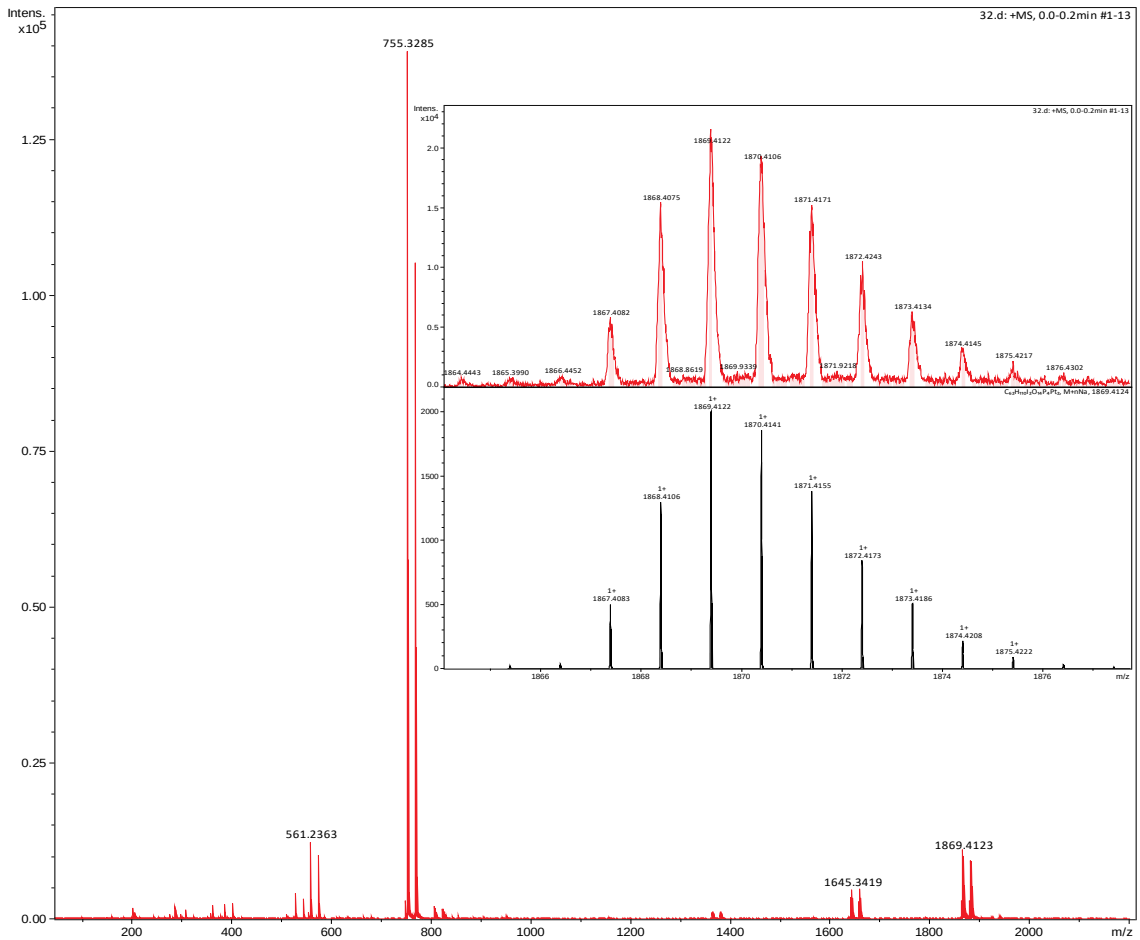

Fig. S41. ESI-HR-MS spectrum of **S14**.

Synthesis of compound 1d

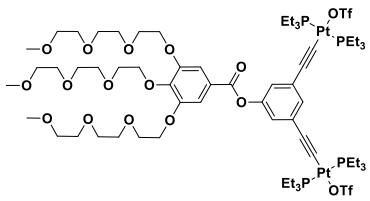

Compound **5** (300 mg, 0.162 mmol) and AgOTf (166 mg, 0.649 mmol) were added into a 40 mL brown vial, then freshly distilled CH_2Cl_2 (30 mL) was added. The resulting mixture was stirred in the dark at room temperature for 16 h. After filtering off the heavy creasy precipitate through a glass fiber filter, the suspension was obtained. The solvent was removed under a flow of nitrogen to afford **1d** as a white solid (285 mg, 93%). ^{1}H NMR (600 MHz, $CDCl_3$) δ 7.73 (s, 1H), 7.50 (s, 2H), 7.05 (s, 2H), 4.42 (s, 6H), 4.15 – 3.53 (m, 30H), 3.43 (s, 9H), 2.07 (s, 24H), 1.24 – 1.13 (m, 36H). ^{31}P NMR (243 MHz, CD_2Cl_2) δ 21.95 (s, ^{195}Pt satellites, $^1J_{Pt\text{-}P}$ = 2208.14 Hz). ESI-HR-MS: *m/z* 1913.5911 [**1d** + Na]$^+$, calcd. for $[C_{64}H_{110}F_6NaO_{20}P_4Pt_2S_2]^+$, 1913.5074.

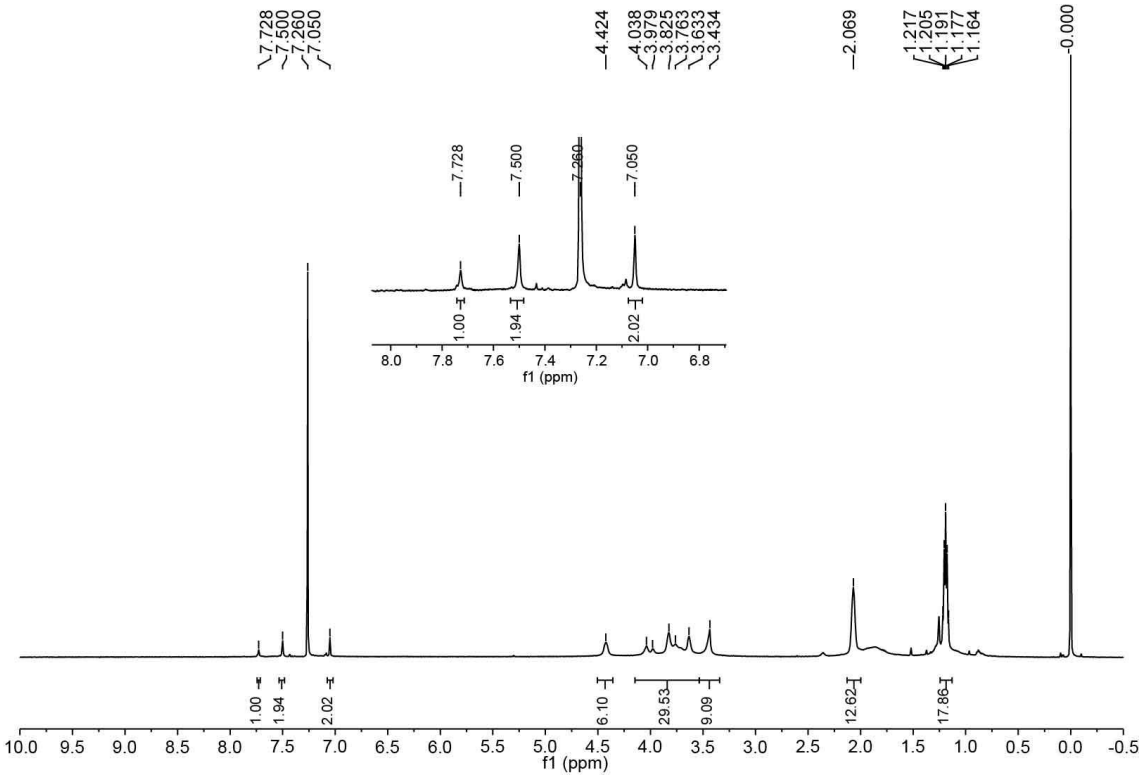

Fig. S42. ^{1}H NMR spectrum (600 MHz, $CDCl_3$, 298 K) recorded for **1d**.

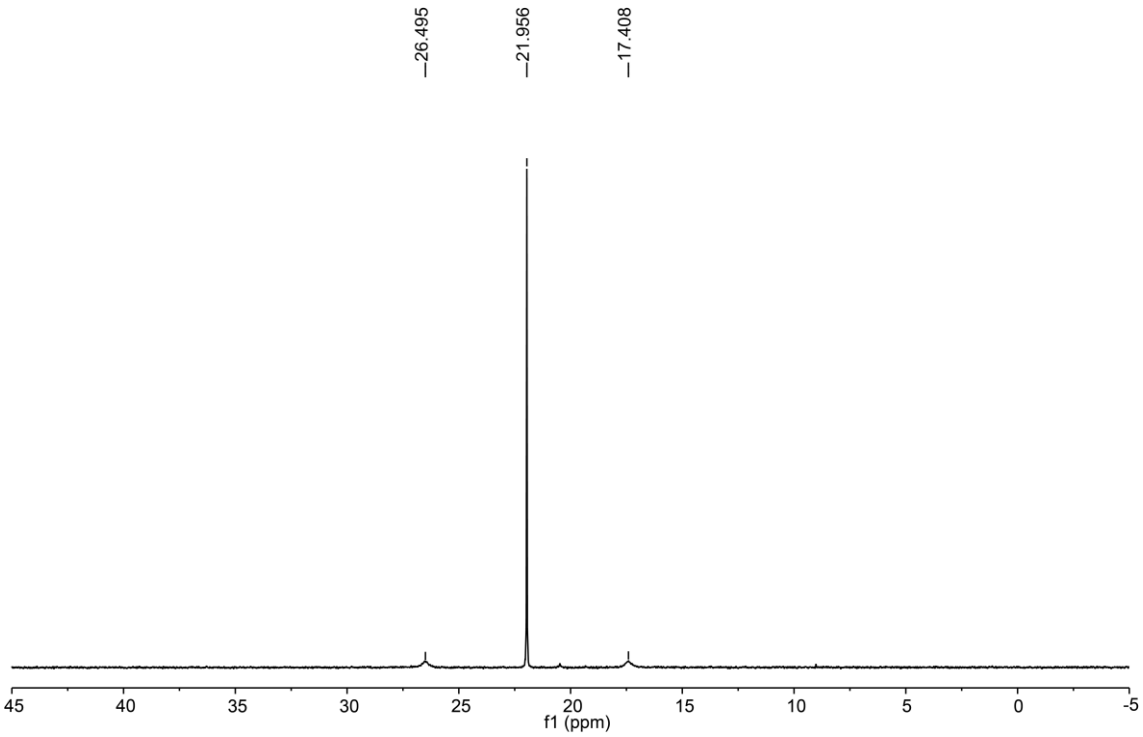

Fig. S43. ^{31}P{^{1}H} NMR spectrum (243 MHz, CD_2Cl_2, 298 K) recorded for **1d**.

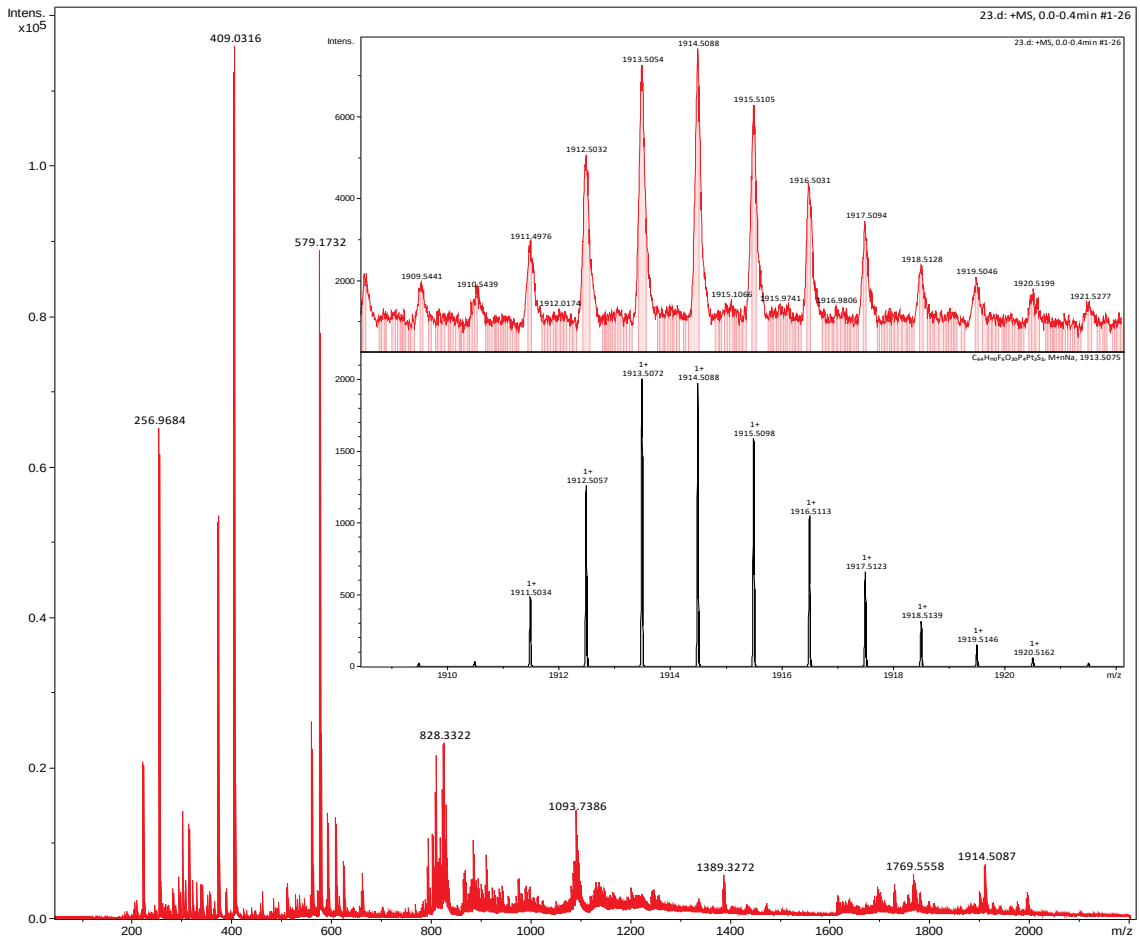

Fig. S44. ESI-HR-MS spectrum of **1d**.

Synthesis of 3a

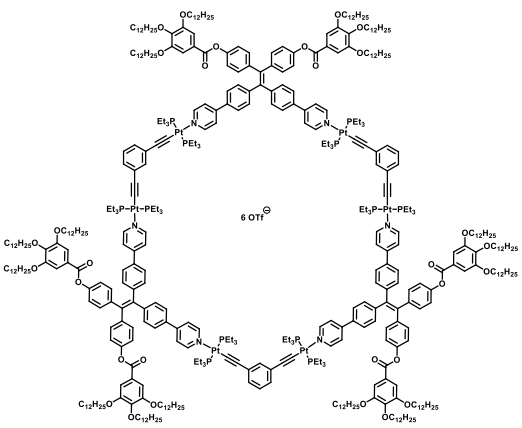

A solution of dipyridyl donor ligand (278.4 mg, 0.152 mmol) in anhydrous dichloromethane (20 mL) was added dropwise to a solution of compound **1a** (195.2 mg, 0.159 mmol) in anhydrous dichloromethane (20 mL) under continuous stirring. The reaction mixture was stirred at room temperature for 16 h. The solvent was removed under nitrogen flow to afford hexagon **3a** (quantitative yield). ^{1}H NMR (600 MHz, CD_2Cl_2, 298K) δ 8.80 – 8.71 (m, 12H), 7.95 (s, 12H), 7.81 (s, 3H), 7.71 (d, *J* = 7.2 Hz, 12H), 7.61 (s, 6H), 7.34 (d, *J* = 18.8 Hz, 24H), 7.26 (s, 3H), 7.21 (d, *J* = 8.3 Hz, 12H), 7.06 (d, *J* = 7.7 Hz, 12H), 4.09 – 3.93 (m, 36H), 1.97 – 1.64 (m, 108H), 1.53 – 1.21 (m, 324H), 1.20 – 1.16 (m, 108H), 0.88 – 0.86 (m, 54H). ^{13}C NMR (151 MHz, $CDCl_3$, 298K) δ 164.95, 152.94, 152.37, 150.82, 150.13, 146.36, 143.06, 140.14, 139.04, 132.84, 132.47, 127.13, 125.12, 123.96, 123.67, 122.91, 121.84, 121.45, 119.71, 117.59, 108.47, 73.57, 69.22, 31.91, 31.90, 30.33, 29.72, 29.71, 29.68, 29.64, 29.61, 29.55, 29.38, 29.34, 29.28, 26.08, 26.03, 22.67, 14.10, 7.85. ^{31}P NMR (243 MHz, CD_2Cl_2, 298K) δ 15.28 (s, ^{195}Pt satellites, $^{1}J_{Pt\text{-}P}$

= 2245.32 Hz). ESI-TOF-MS: *m/z* 1410.0023 [**3a** – 6OTf]$^{6+}$, 1721.6698 [**3a** – 5OTf]$^{5+}$, 2189.3977 [**3a** – 4OTf]$^{4+}$, 2968.9067 [**3a** – 3OTf]$^{3+}$.

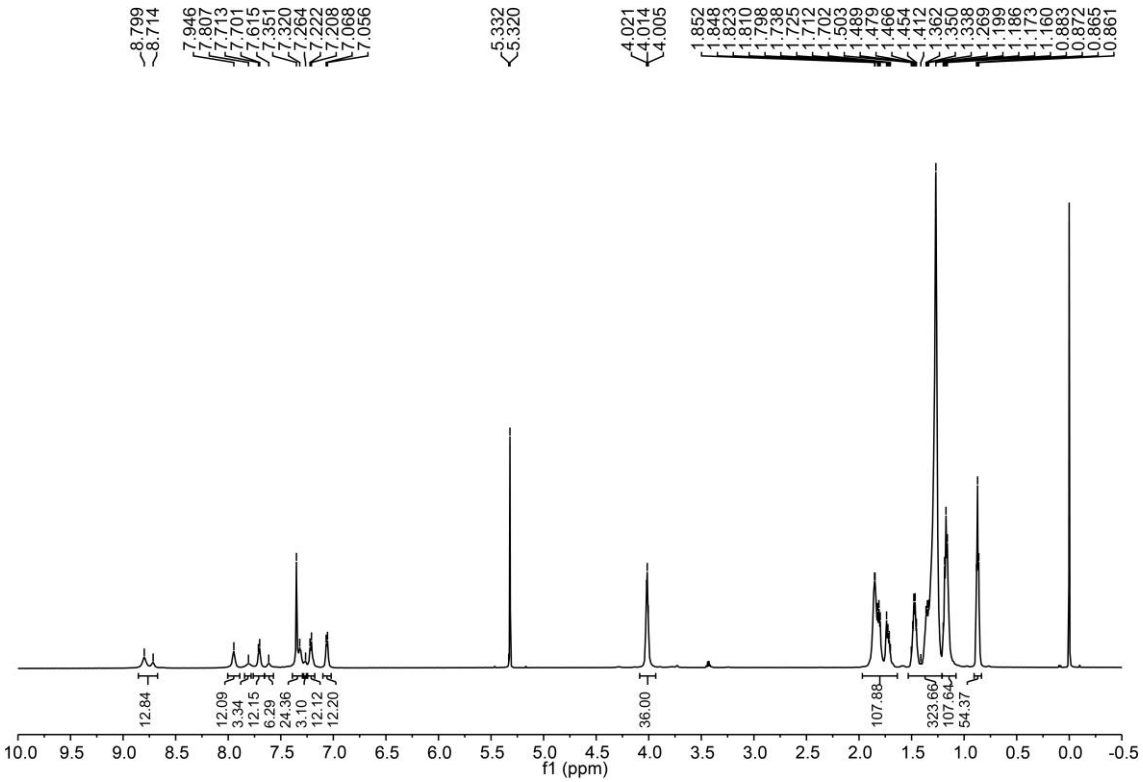

Fig. S45. ^{1}H NMR spectrum (600 MHz, CD_2Cl_2, 298 K) recorded for **3a**.

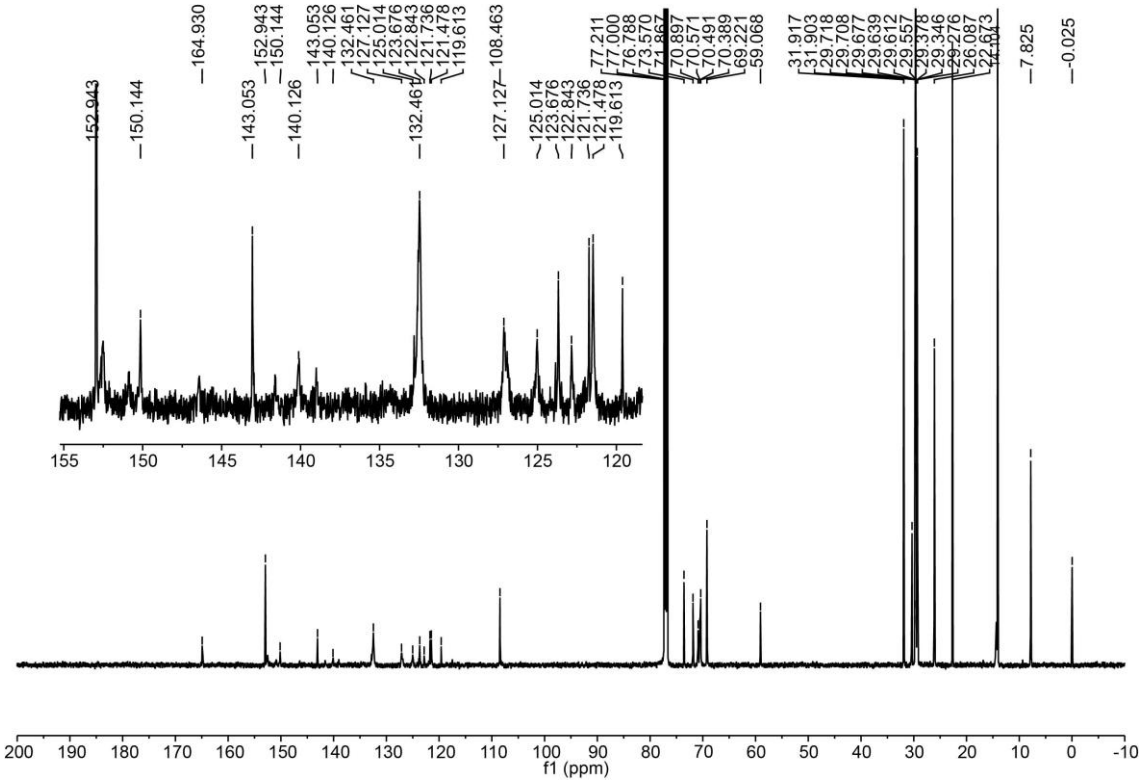

Fig. S46. ^{13}C NMR spectrum (151 MHz, $CDCl_3$, 298 K) recorded for **3a**.

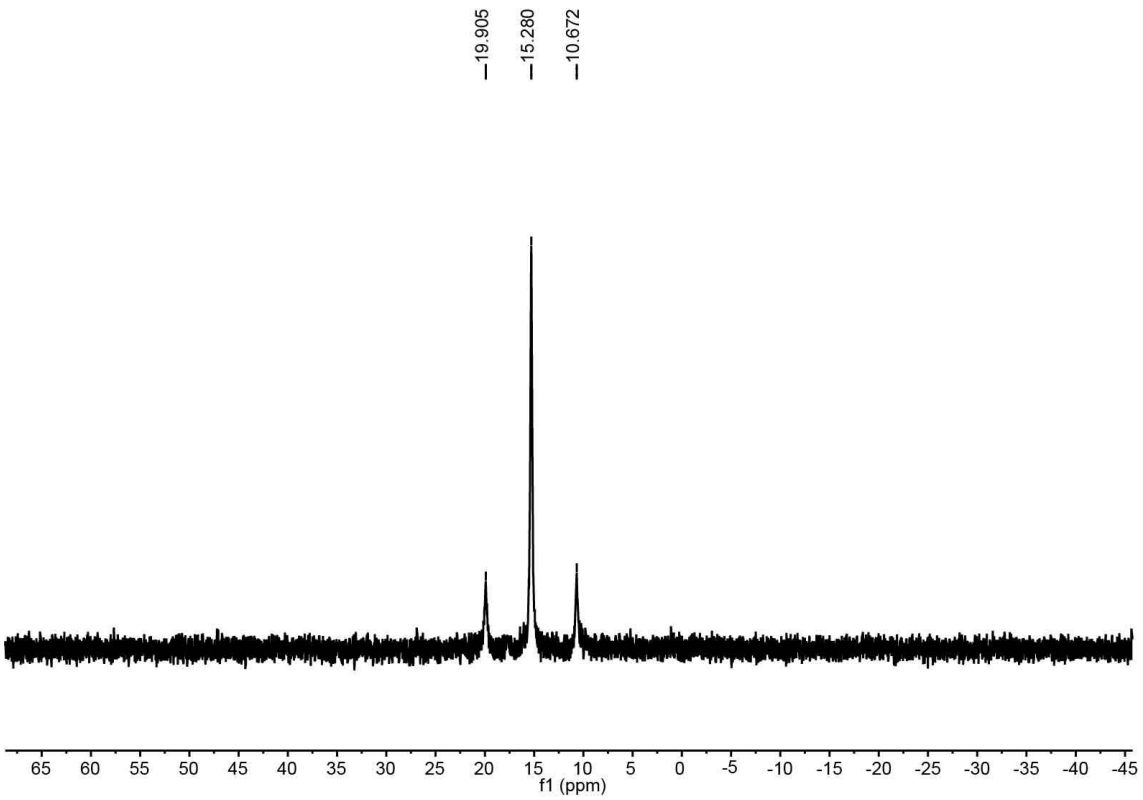

Fig. S47. $^{31}P\{^{1}H\}$ NMR spectrum (243 MHz, CD_2Cl_2, 298 K) recorded for **3a**.

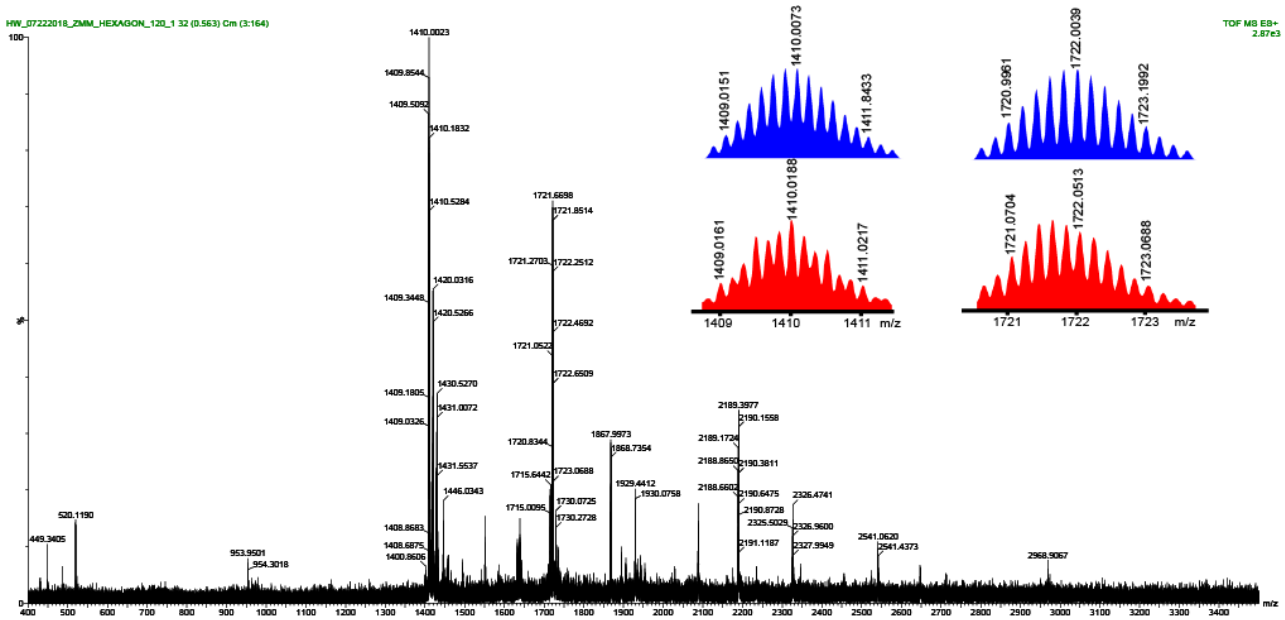

Fig. S48. ESI-TOF-MS spectrum of **3a**

Synthesis of 3b

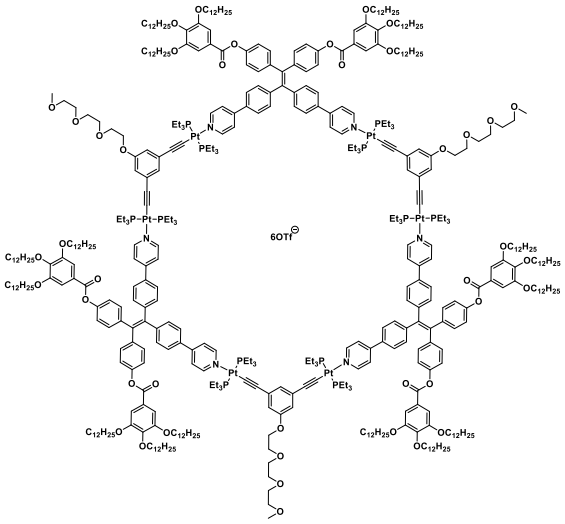

A solution of dipyridyl donor ligand (331.8 mg, 0.229 mmol) in anhydrous dichloromethane (15 mL) was added dropwise to a solution of compound **3** (420 mg, 0.229 mmol) in anhydrous dichloromethane (15 mL) under continuous stirring. The reaction mixture was stirred at room temperature for 16 h. The solvent was removed under nitrogen flow to afford hexagon **3b** (quantitative yield). ^{1}H NMR (600 MHz, CD_2Cl_2, 298K) δ 8.71 – 8.65 (m, 12H), 7.94 (s, 12H), 7.72 (d, *J* = 7.7 Hz, 12H), 7.63 (s, 3H), 7.35 (s, 12H), 7.32 (s, 12H), 7.21 (dd, *J* = 13.0, 7.5 Hz, 12H), 7.06 (d, *J* = 7.0 Hz, 12H), 6.77 (s, 6H), 4.11 (s, 6H), 4.07 – 3.95 (m, 36H), 3.81 (s, 6H), 3.66 (s, 6H), 3.63 (s, 6H), 3.59 (d, *J* = 4.3 Hz, 6H), 3.50 (s, 7H), 3.33 (d, *J* = 2.2 Hz, 6H), 1.89 – 1.68 (m, 108H), 1.51 – 1.21 (m, 324H), 1.22 – 1.12 (m, 108H), 0.91 – 0.82 (m, 54H). ^{13}C NMR (151 MHz, $CDCl_3$, 298K) δ 164.95, 152.94, 150.12, 143.12, 143.06, 140.11, 132.44, 127.00, 124.85, 123.52, 121.40, 119.28, 108.46, 73.57, 69.21, 31.90, 31.89, 30.32, 29.70, 29.66, 29.62, 29.60, 29.54, 29.36, 29.33, 29.26, 26.07, 26.02, 22.65, 14.08, 7.61. ^{31}P NMR (243 MHz, CD_2Cl_2, 298K) δ 15.79 (s, ^{195}Pt satellites, $^{1}J_{Pt\text{-}P}$ = 2330.12 Hz). ESI-TOF-MS: *m/z* 1490.8842 [**3b** – 6OTf]$^{6+}$, 1818.8544 [**3b** – 5OTf]$^{5+}$.

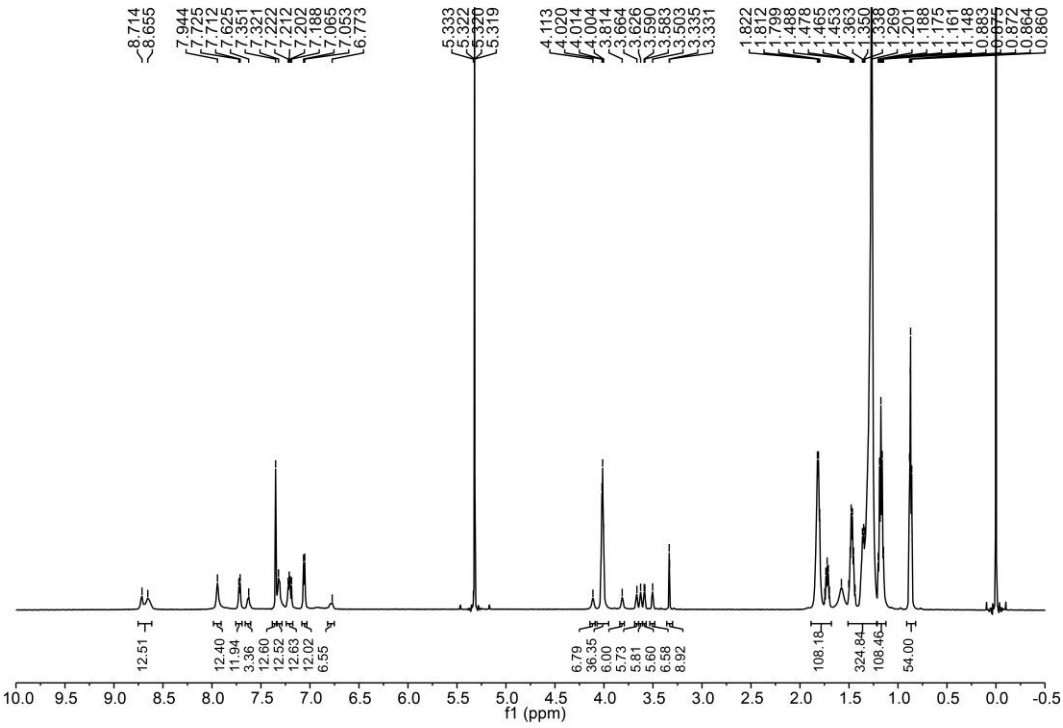

Fig. S49. ^{1}H NMR spectrum (600 MHz, CD_2Cl_2, 298K) recorded for **3b**.

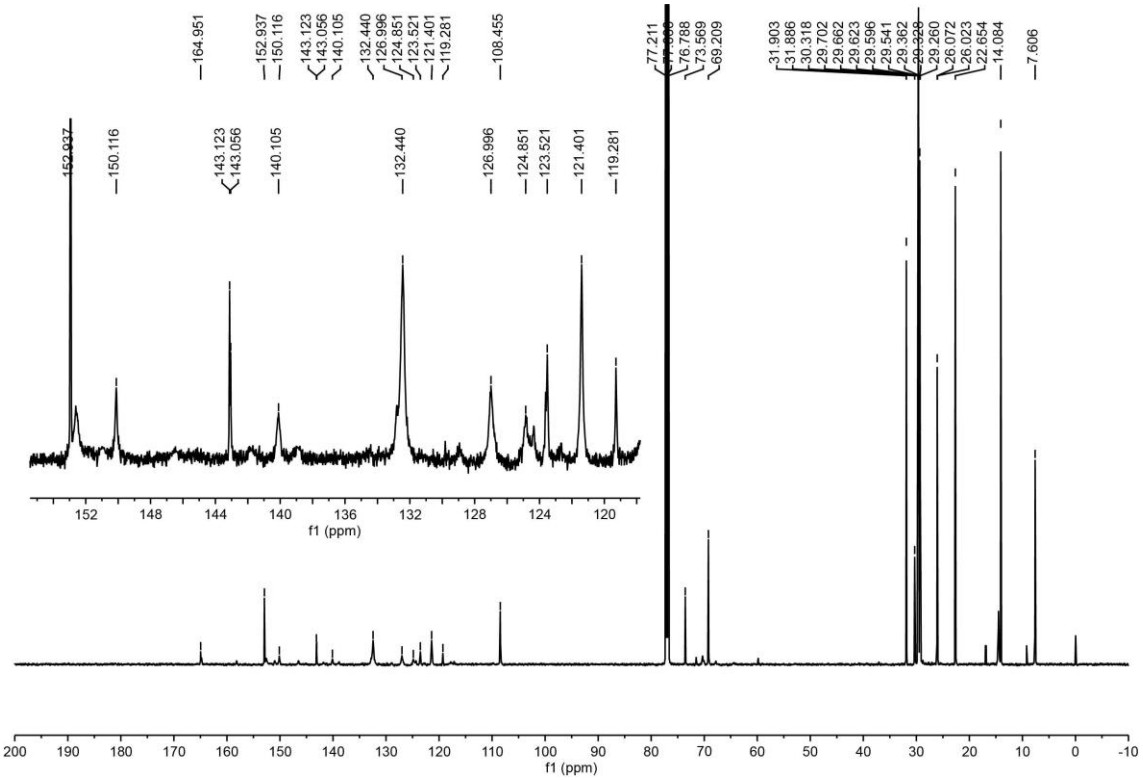

Fig. S50. ^{13}C NMR spectrum (151 MHz, $CDCl_3$, 298 K) recorded for **3b**.

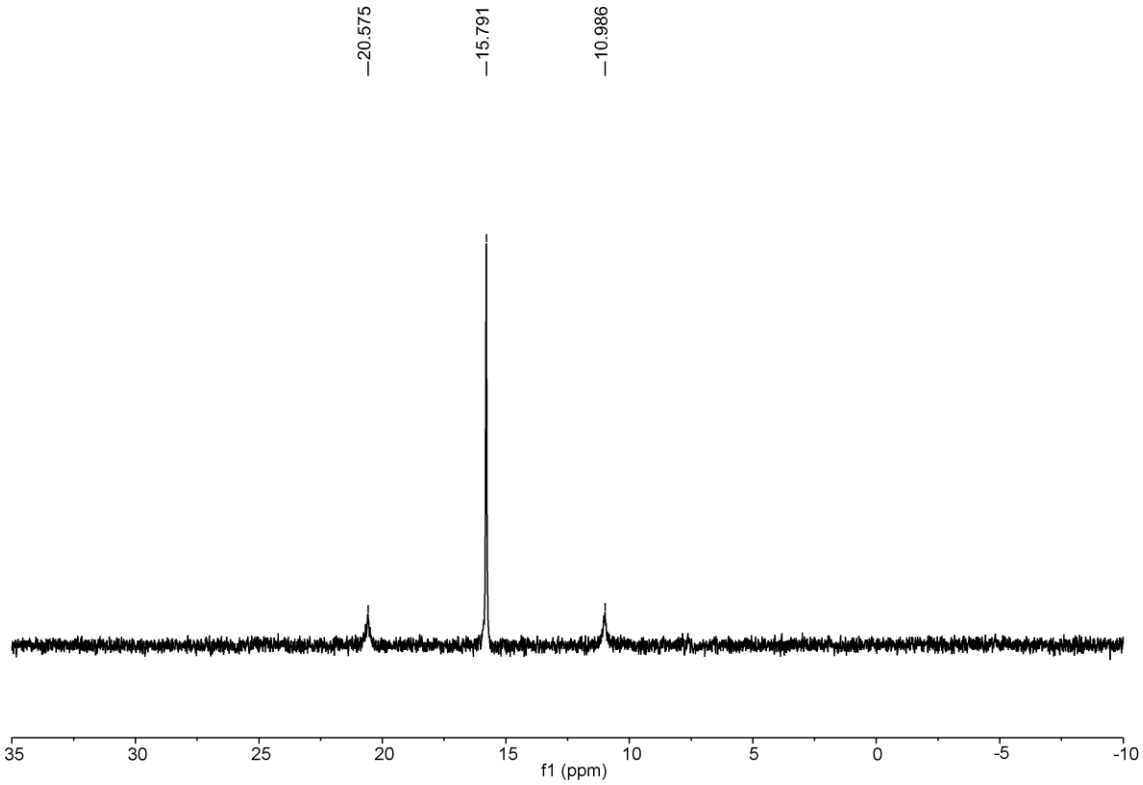

Fig. S51. $^{31}P\{^1H\}$ NMR spectrum (243 MHz, CD_2Cl_2, 298 K) recorded for **3b**.

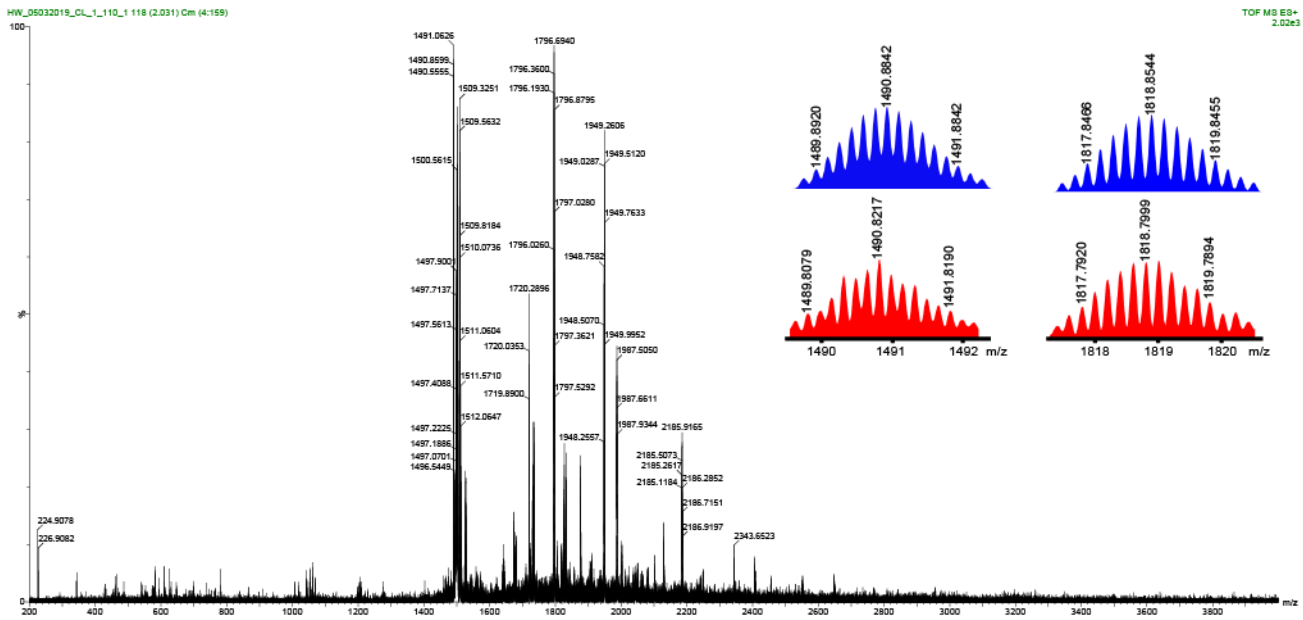

Fig. S52. ESI-TOF-MS spectrum of **3b**.

Synthesis of 3c

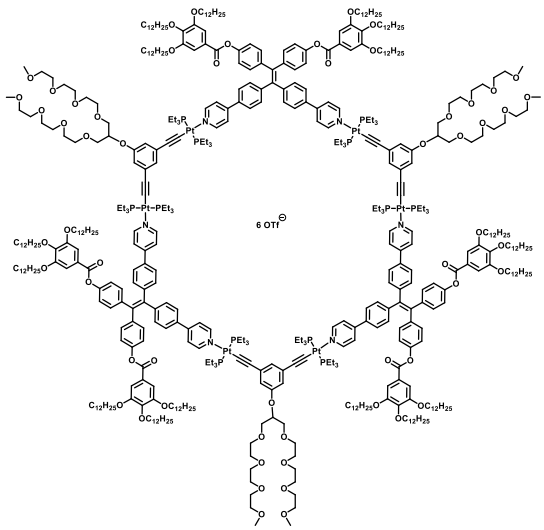

A solution of dipyridyl donor ligand (315.2 mg, 0.166 mmol) in anhydrous dichloromethane (15 mL) was added dropwise to a solution of compound **6** (305.2 mg, 0.166 mmol) in anhydrous dichloromethane (15 mL) under continuous stirring. The reaction mixture was stirred at room temperature for 16 h. The solvent was removed under nitrogen flow to afford hexagon **2**(quantitative yield). ^{1}H NMR (600 MHz, CD_2Cl_2, 298K) δ 8.78 – 8.56 (m, 12H), 7.98 – 7.89 (m, 12H), 7.80 – 7.68 (m, 12H), 7.59 (s, 3H), 7.35 (s, 12H), 7.32 – 7.26 (s, 12H), 7.22 (s, 12H), 7.06 (d, *J* = 6.8 Hz, 12H), 6.78 (s, 6H), 4.55 (s, 3H), 4.02 (s, 36H), 3.92 – 3.50 (m, 84H), 3.32 (s, 18H), 1.87 – 1.67 (m, 108H), 1.52 – 1.22 (m, 324H), 1.22 – 1.11 (m, 108H), 0.88 – 0.87 (m, 54H). ^{13}C NMR (151 MHz, $CDCl_3$, 298K) δ 164.93, 152.94, 150.14, 143.05, 140.13, 132.46, 127.13, 125.01, 123.68, 122.84, 121.74, 121.48, 119.61, 108.46, 77.21, 77.00, 76.79, 73.57, 70.49, 70.39, 69.22, 59.07, 31.92, 31.90, 30.33, 29.80, 29.72, 29.71, 29.68, 29.64, 29.61, 29.56, 29.51, 29.38, 29.35, 29.28, 26.09, 26.04, 22.67, 14.10, 7.82. ^{31}P NMR (243 MHz, CD_2Cl_2, 298K) δ 15.53 (s, ^{195}Pt satellites, $^{1}J_{Pt\text{-}P}$ = 2317.73 Hz). ESI-TOF-MS: *m/z* 1600.9518 [**3c** – 6OTf]$^{6+}$, 1950.9319 [**3c** – 5OTf]$^{5+}$, 2475.8995 [**3c** – 4OTf]$^{4+}$, 3350.8533 [**3c** – 3OTf]$^{3+}$

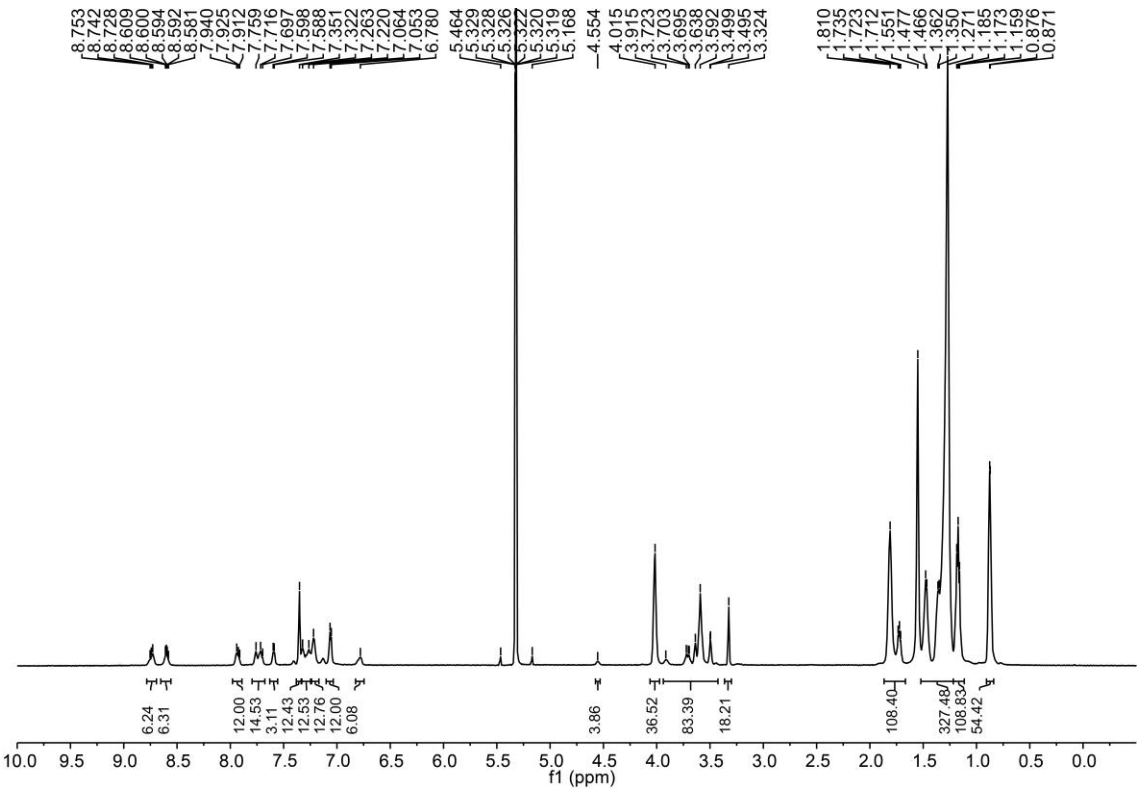

Fig. S53. ^{1}H NMR spectrum (600 MHz, CD_2Cl_2, 298K) recorded for hexagon **2**.

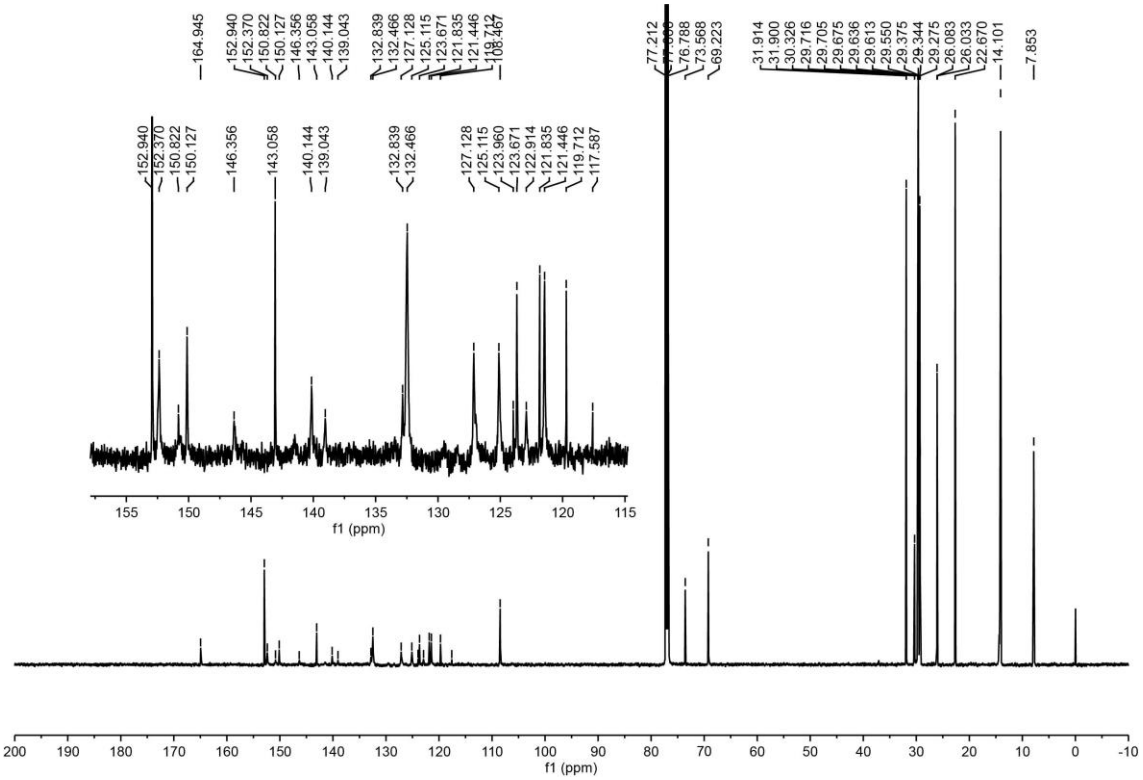

Fig. S54. ^{13}C NMR spectrum (151 MHz, $CDCl_3$, 298 K) recorded for **3c**.

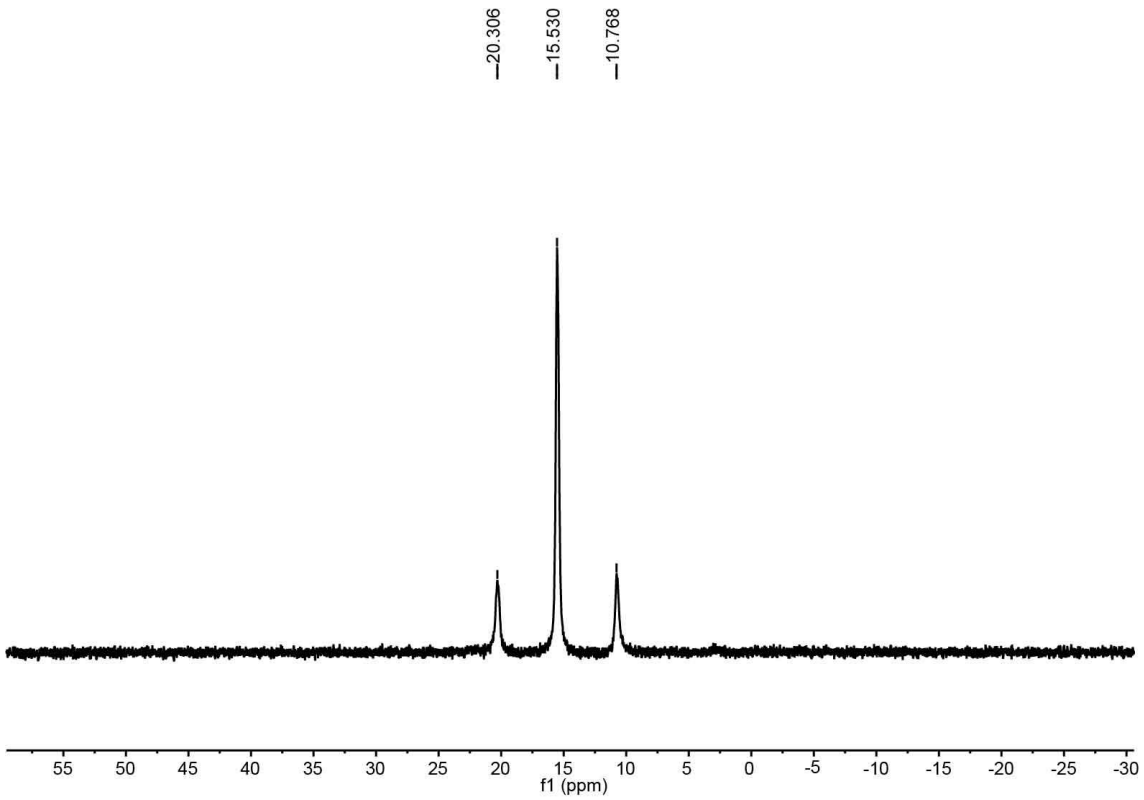

Fig. S55. $^{31}P\{^{1}H\}$ NMR spectrum (243 MHz, CD_2Cl_2, 298 K) recorded for **3c**.

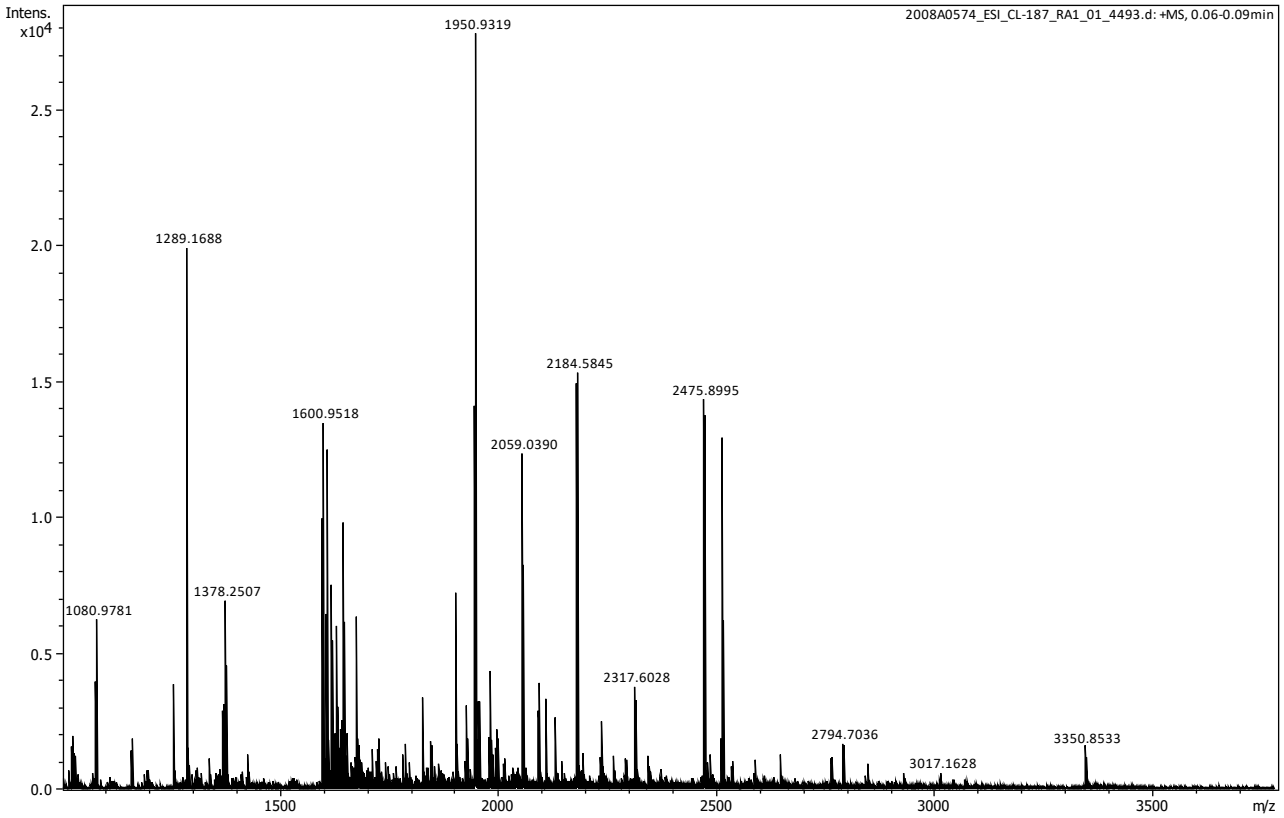

Fig. S56. ESI-TOF-MS spectrum of **3c**

Synthesis of 3d

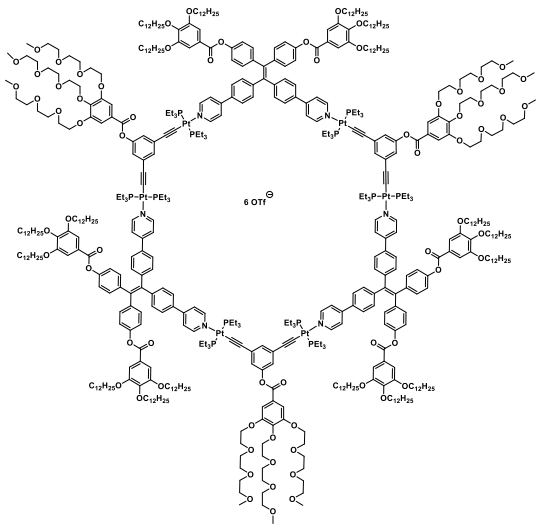

A solution of dipyridyl donor ligand (315.2 mg, 0.166 mmol) in anhydrous dichloromethane (15 mL) was added dropwise to a solution of compound **6** (305.2 mg, 0.166 mmol) in anhydrous dichloromethane (15 mL) under continuous stirring. The reaction mixture was stirred at room temperature for 16 h. The solvent was removed under nitrogen flow to afford hexagon **2**(quantitative yield). ^{1}H NMR (600 MHz, CD_2Cl_2, 298K) δ 8.72 – 8.57 (m, 12H), 7.96 – 7.72 (s, 12H), 7.73 – 7.72 (m, 12H), 7.64 – 7.63 (m, 3H), 7.45 (s, 6H), 7.35 (s, 12H), 7.34 – 7.31 (m, 12H), 7.22 – 7.18 (m, 12H), 7.06 (d, *J* = 8.4 Hz, 12H), 6.93 (s, 6H), 4.27 – 4.23 (m, 18H), 4.02 – 4.0 (m, 36H), 3.88 – 3.79 (m, 18H), 3.70 – 3.66 (m, 36H), 3.51 – 3.48 (m, 18H), 3.33 (s, 18H), 1.86 – 1.67 (m, 108H), 1.52 – 1.22 (m, 324H), 1.22 – 1.12 (m, 108H), 0.91 – 0.82 (m, 54H). ^{13}C NMR (151 MHz, $CDCl_3$, 298K) δ 164.93, 164.81, 152.94, 151.62, 150.13, 143.09, 140.08, 132.43, 127.05, 123.59, 121.42, 119.30, 117.19, 108.94, 108.46, 73.57, 71.66, 71.43, 70.34, 69.44, 69.21, 68.22, 59.82, 59.69, 31.91, 31.89, 30.33, 29.85, 29.72, 29.71, 29.67, 29.63, 29.60, 29.55, 29.37, 29.34, 29.27, 26.08, 26.03, 22.66, 14.09, 7.62. ^{31}P NMR (243 MHz, CD_2Cl_2, 298K) δ 15.80 (s, ^{195}Pt satellites, $^{1}J_{Pt\text{-}P}$ = 2317.24 Hz). ESI-TOF-MS: *m/z* 1713.4868 [**3d** – 6OTf]$^{6+}$, 2085.7761 [**3d** – 5OTf]$^{5+}$.

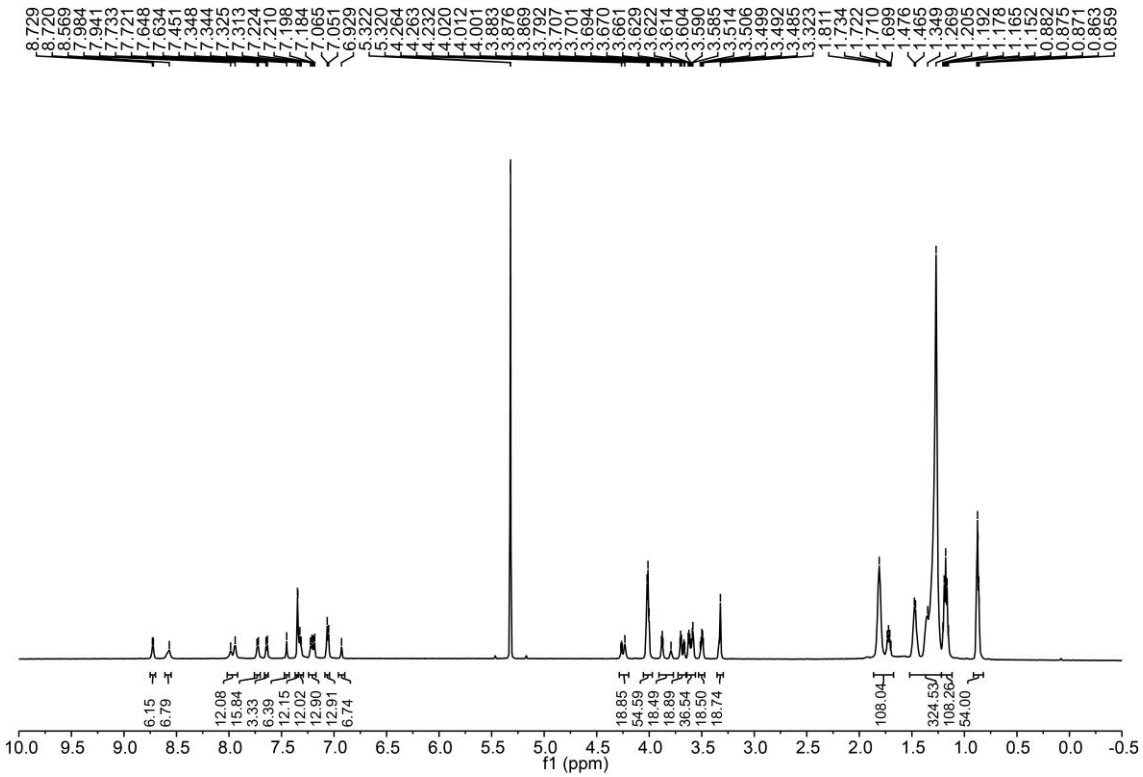

Fig. S57. ^{1}H NMR spectrum (600 MHz, CD_2Cl_2, 298K) recorded for hexagon **3d**.

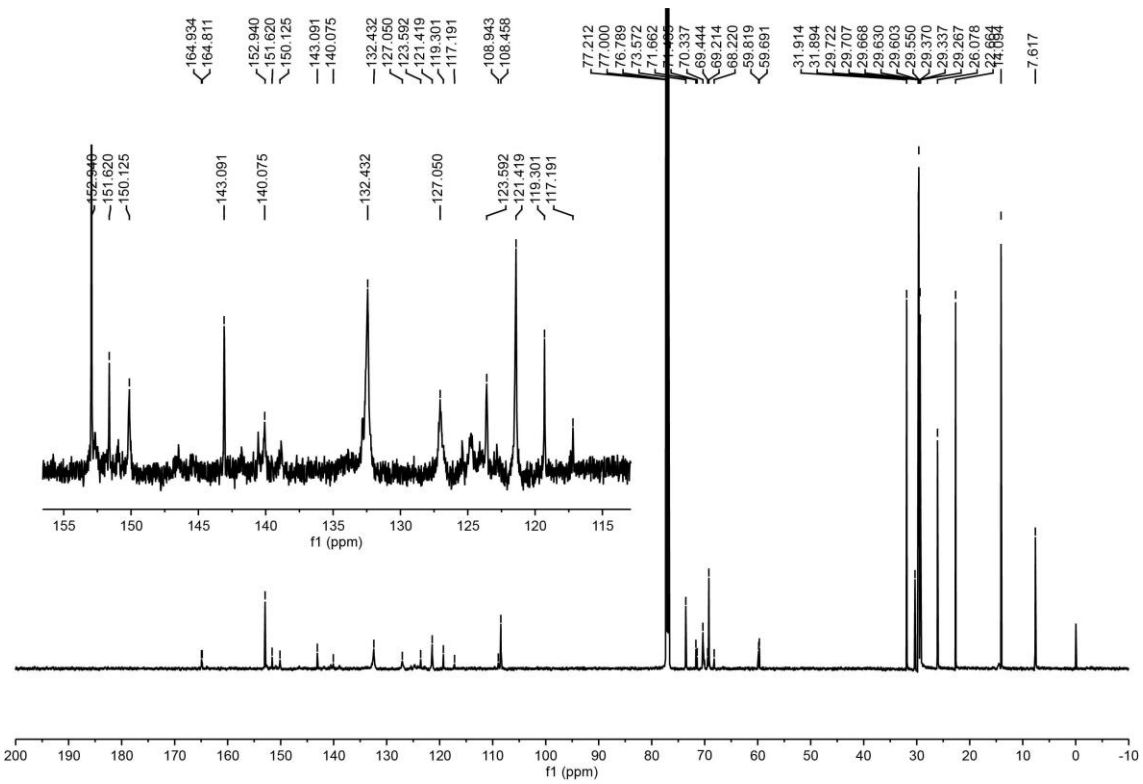

Fig. S58. ^{13}C NMR spectrum (151 MHz, $CDCl_3$, 298 K) recorded for **3d**.

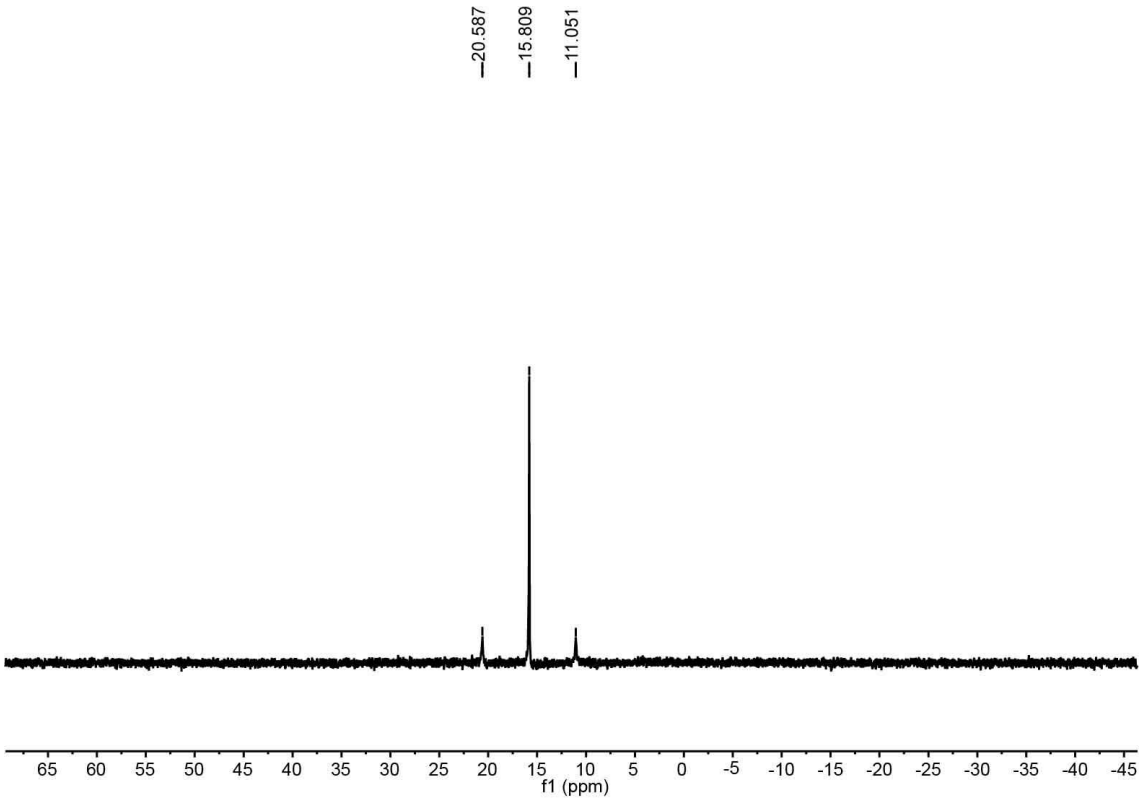

Fig. S59. $^{31}P\{^1H\}$ NMR spectrum (243 MHz, CD_2Cl_2, 298 K) recorded for **3d**.

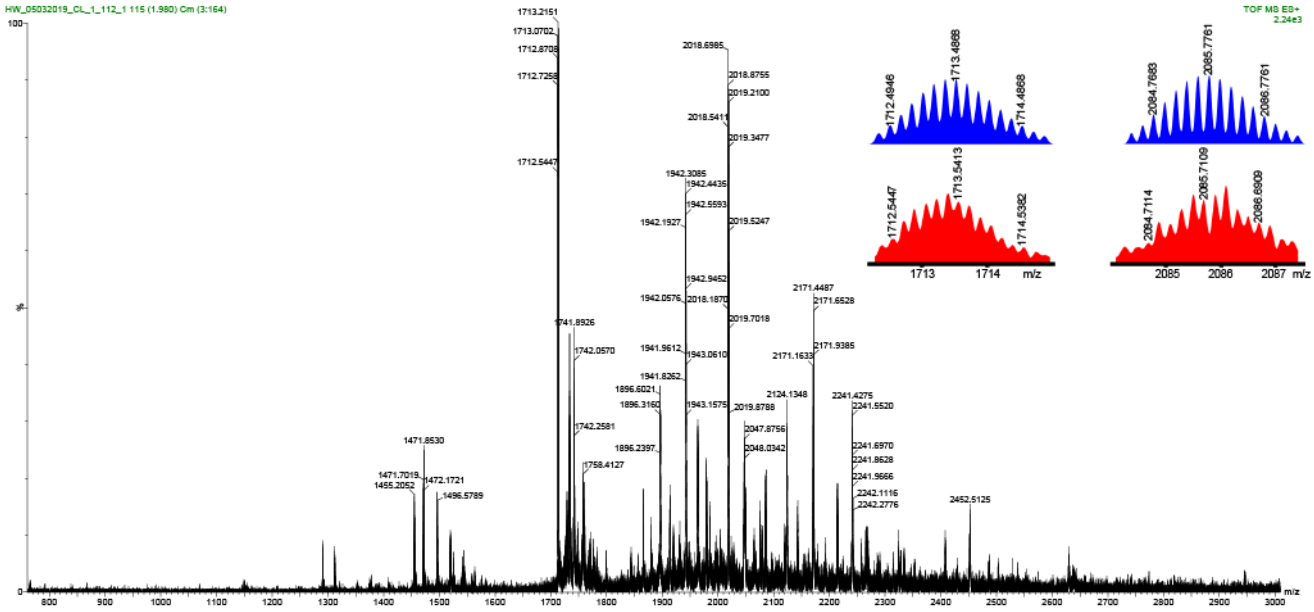

Fig. S60. ESI-TOF-MS spectrum of **3d.**

3. DSC curve

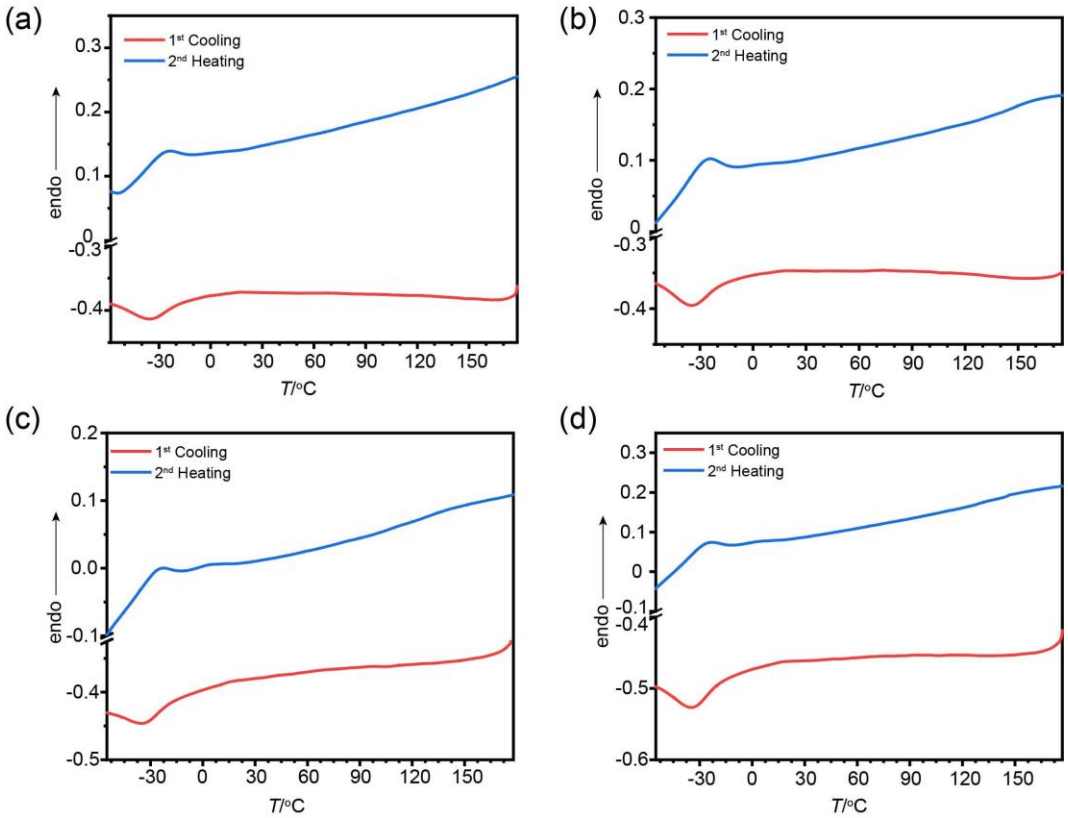

Fig. S61. DSC thermograms of metallacycles (a) **3a,** (b) **3b**, (c) **3c** and (d) **3d**, during the first cooling - second heating cycle. All metallacycles are in mesophase at room temperature. Introducing TEG chains does not significantly alter the DSC curve is due to the close melting point between TEG (-7 ºC) and dodecane (-9.6 ºC). Besides, compounds **3a-3d** tend to form phase of poor order. The coherence, derived from the SAXS signal (2π/FWHM), is smaller than 100 nm, suggesting a relatively short-range periodicity contaning only 5-12 lattices. Such poor order would broaden and weaken peaks in DSC curves, which further enhances the similarity among four compounds.

4. The textures of metalacycles observed between crossed polarizers

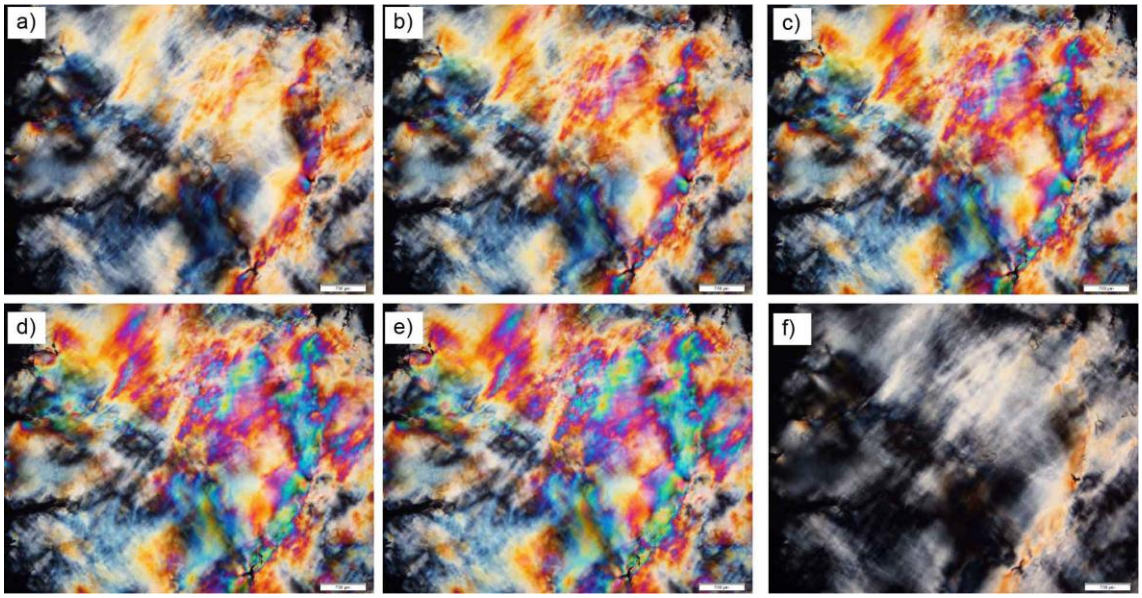

Fig. S62. Optical micrographs of **3a** recorded at 30 ℃ (a), 50 ℃ (b), 70 ℃(c), 90 ℃ (d), 110 ℃ (e), 130 ℃ (f). Introducing TEG chains doesn't alter the nature of columnar phase, which causes no particular changes on POM textures except for birefringence.

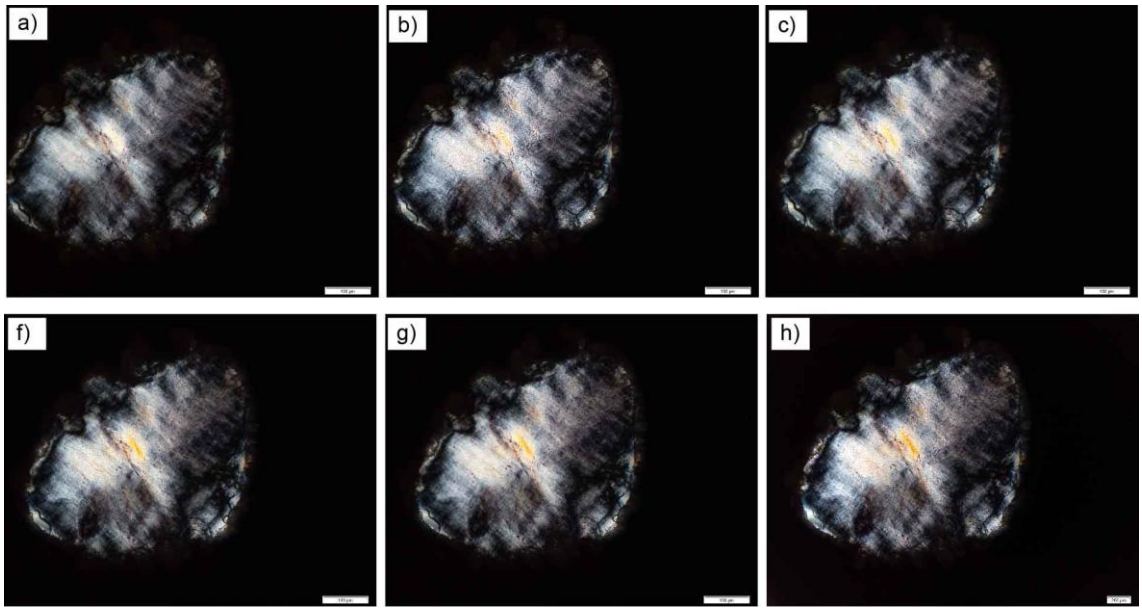

Fig. S63. Optical micrographs of **3b** recorded at 30 ℃ (a), 50 ℃ (b), 70 ℃(c), 90 ℃ (d), 110 ℃ (e), 130 ℃ (f), respectively.

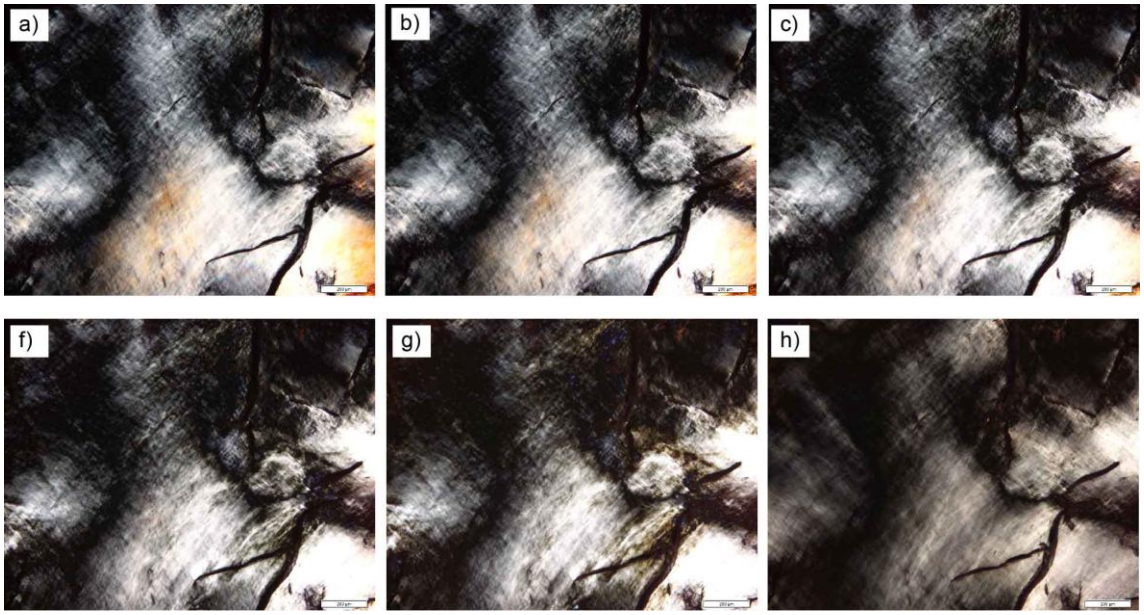

Fig. S64. Optical micrographs of **3c** recorded at 30 ℃ (a), 50 ℃ (b), 70 ℃(c), 90 ℃ (d), 110 ℃ (e), 130 ℃ (f), respectively.

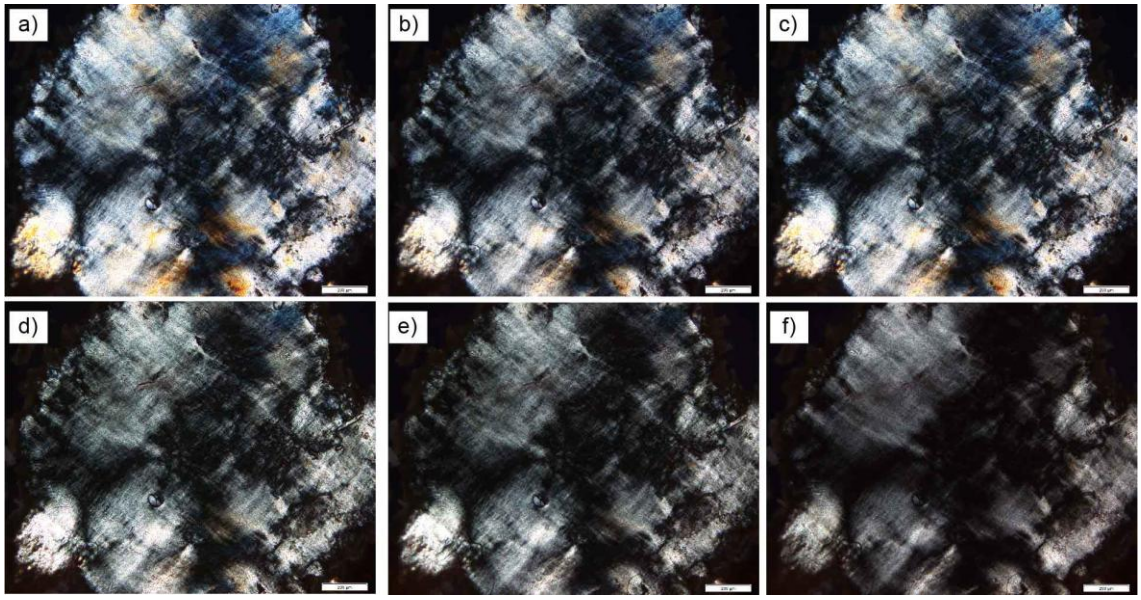

Fig. S65. Optical micrographs of **3d** recorded at 30 ℃ (a), 50 ℃ (b), 70 ℃(c), 90 ℃ (d), 110 ℃ (e), 130 ℃ (f), respectively.

5. SAXS and WAXS results of metallacycles

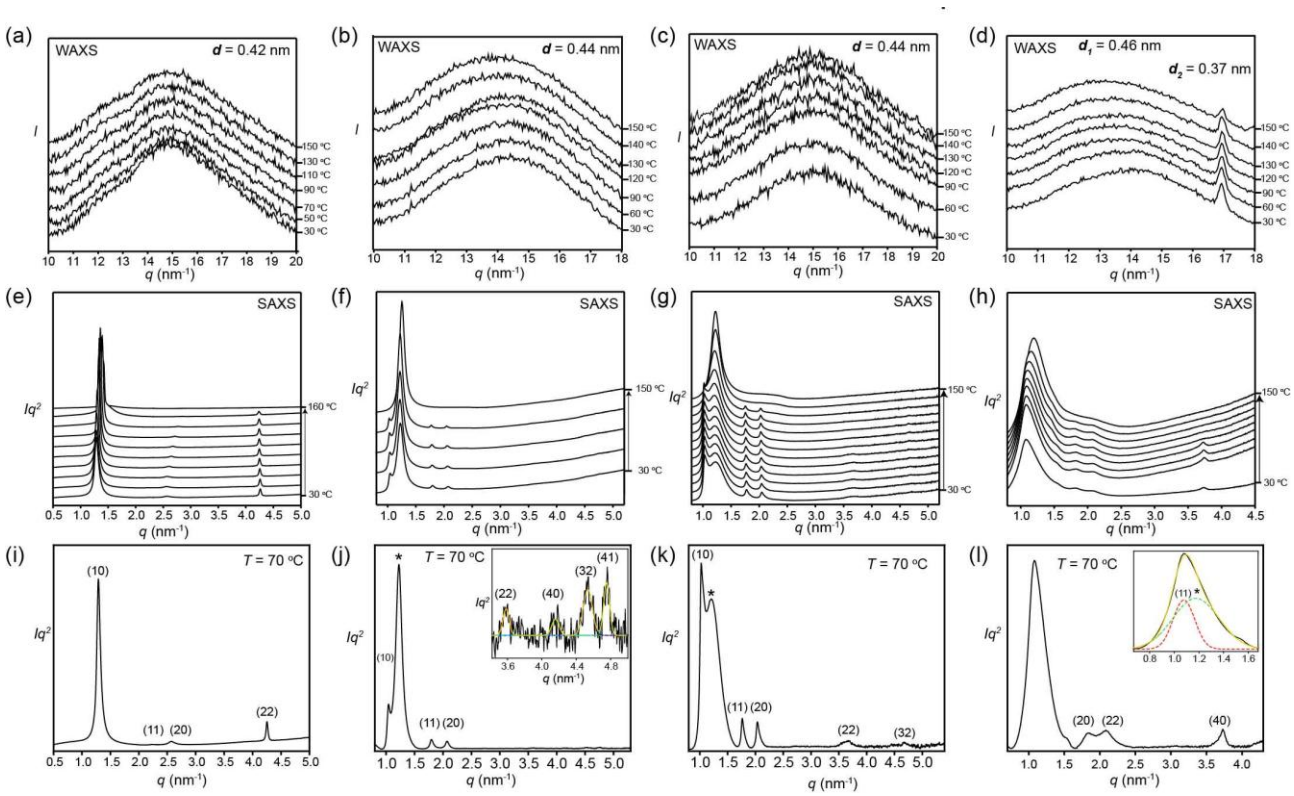

Fig. S66. SAXS and WAXS diffractograms of metallacycles **3a** (a, e), **3b** (b, f), **3c** (c, g), and **3d** (d, h) on heating scan, heating rate used was 10 K min/k. Details of extracting diffraction peaks of SAXS at 70 °C for **3a** (i), **3b** (j), **3c** (k) and **3d** (l).

6. Numerical SAXS data

Table S1. Experimental and calculated *d*-spacings of the observed SAXS reflections of the Col_{hex}/*p*6*mm* phase of **3a** at 70°C. All intensities values are Lorentz and multiplicity corrected.

(*hkl*)	d_{obs}.-spacing (nm)	d_{cal}.-spacing (nm)	*intensity*	*Phase*
(10)	4.86	4.86	100.0	π
(11)	2.81	2.81	0.3	0
(20)	2.44	2.43	2.8	0
a_{hex} = 5.61 nm				

Table S2. Experimental and calculated *d*-spacings of the observed SAXS reflections of the Col_{hex}/ *p*3*m*1 phase of **3b** at 70°C. All intensities values are Lorentz and multiplicity corrected.

(*hk*)	$d_{obs.}$-spacing (nm)	$d_{cal.}$-spacing (nm)	*intensity*	*Phase*
(10)	6.03	6.03	100.0	-0.94 π
(11)	3.49	3.48	17.1	0
(20)	3.03	3.01	14.8	-0.74 π
(22)	1.75	1.74	1.3	/
(40)	1.51	1.51	1.0	/
(32)	1.39	1.38	1.7	/
(41)	1.32	1.32	1.3	/
a_{hex} = 6.96 nm				

Table S3. Experimental and calculated *d*-spacings of the observed SAXS reflections of the Col_{hex}/*p*3*m*1 phase of **3c** at 70°C. All intensities values are Lorentz and multiplicity corrected.

(*hk*)	$d_{obs.}$-spacing (nm)	$d_{cal.}$-spacing (nm)	*intensity*	*Phase*
(10)	6.05	6.05	100.0	-0.94 π
(11)	3.50	3.50	19.3	0
(20)	3.07	3.03	17.7	-0.74 π
(22)	1.75	1.75	7.8	/
(31)	1.68	1.68	2.5	/
(32)	1.40	1.39	1.3	/
(41)	1.34	1.32	2.6	/
a_{hex} = 6.99 nm				

Table S4. Experimental and calculated *d*-spacings of the observed SAXS reflections of the Col_{hex}/*p*3*m*1 phase of **3d** at 70°C. All intensities values are Lorentz and multiplicity corrected. The lattice parameter is determined by high-index peaks and peak (10) is derived from the lattice parameter.

(*hk*)	$d_{obs.}$-spacing (nm)	$d_{cal.}$-spacing (nm)	*intensity*	*Phase*
(10)	6.02	6.02	100.0	-0.94 π
(11)	3.47	3.48	12.4	0
(20)	3.01	3.01	12.4	-0.74 π
(22)	1.74	1.74	5.6	/
(31)	1.67	1.67	5.4	/
(32)	1.36	1.38	1.3	/
(50)	1.19	1.20	8.2	/
(33)		1.16		/
a_{hex} = 6.95 nm				

7. Determination the *p*3*m*1 phase and its phase angles

The assignment of *p*3*m*1 phase is based on not only the phase separation between alkyl/TEG chains and macrocycle shape, but also a full spectrum of macrocycle LC study. The phase separation between TEG and alkyl chains is strong enough to guide the assembly of macrocycles for rhombic macrocycle according to our previous work[S10], where ±120° rotation of macrocycles along columnar axis exhibit quasi-hexagonal order in 2D lattice with weak luminescence (quantum yield <12%). Replacing the rhombic macrocycle by hexagonal one removes such rotation, which promotes the quantum yield significantly in current work (>18%). However, pure alkyl chains cannot restrict the local in-plane rotation due to their dynamic nature in **3a** (Fig 4g). With the aid of TEG chains and strong enough phase separation, the local in-plane rotation is gradually fixed and boosts the quantum yield to 47%. Such fixation naturally breaks the symmetry of *p*6*mm* due to phase separation between TEG and alkyl chains. This leads to the low symmetry *p*3*m*1 phase, similar to the formation of another *p*3*m*1 LC, by polyphiles, too[S11].

Besides, the phase assignment is also supported by the extra broad peak from TEG cluster. The case is found in our previous work[S10] and other liquid crystal phases such as SmA+ phase formed by triphilic

T-shaped molecules[S12]. The TEG chains simultaneously introduces phase separation and in-plane fixation of free rotation in **3a**. Former effect expands the 2D lattice from 4.9 nm to 6.0 nm and latter effect induces the extra broad peak around 5.2 nm. The experimental results suggest the local domains with three-fold symmetry and different orientations (red/blue area in Fig S67) as well as mixing chains boundaries in between (grey area in Fig S67). If the overall symmetry is six-fold, i.e. conventional *p*6*mm*, which means the macrocycles adapt in-plane free-rotation as **3a**, the TEG cluster would be very small and diverse, eliminating the broad peak.

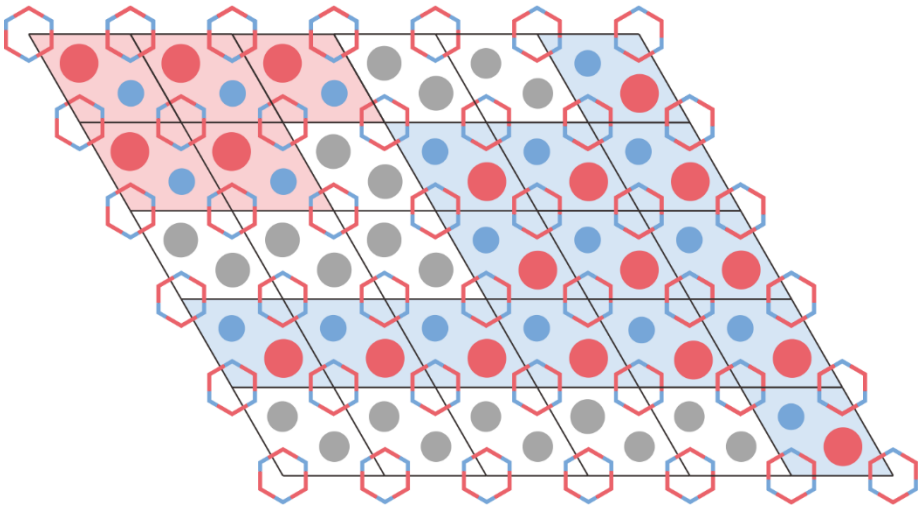

Fig S67. The in-plane rotation of metallacycles and resulted clusters of TEG chains.

To solve the phase problem of *p*3*m*1 phase, a model was constructed to simulate the phase angle based on volume and electron density of different parts in the metallacycle in **Fig. 3c**. All parameters used are measured from the Materials Studio after geometry optimization. The metallacycle is represented by six aromatic rods with averaged electron density of 500/nm^3 (501/nm^3 for **3a**, 500/nm^3 for **3b**, 503/nm^3 for **3c** and 518/nm^3 for **3d**). We note that changing electron density without altering relatively high and low shows negligible influence on phase angle (< 2°). The size of metallacycle edge is 1.8 nm*0.35 nm. The Pt atoms and OTfs are 0.4 nm*0.6 nm with 674/nm^3 electron density, centered at 1/3 position of each edge. For alkyl chains, the electron density is 441/nm^3 and TEG is 509/nm^3. Considering the phase separation between them, both peripheral soft chains are treated as circles with smooth edge. Volume of both chains is estimated by the volume increment. In liquid crystal state, the 18 alkyl chains attached to three TPEs occupy a cylinder whose radius is 2.0 nm and height is 0.45 nm. Similarly, 9 TEGs attached to diplatinum(II) corner requires radius of 1.4 nm. With all these parameters, the Fourier transform result of the model in **Fig. 3c** can be calculated analytically and, as a consequence, the relative intensity and phase angle can be obtained as in **Table S5**.

Table S5. Simulated scattering intensity and phase by model in **Fig. 3c**.

(*hk*)	I_{sim}	Phase/°
(10)	100	-170
(11)	22.5	0
(20)	33.4	-134
(22)	0.02	180
(31)	10.6	52
(32)	5.5	-38
(40)	8.6	-58
(41)	6.6	0
(33)	0.28	180
(50)	1.37	-62
(42)	4.0	-122

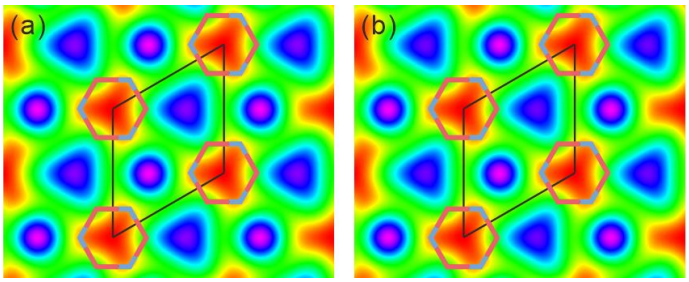

Fig. S68. Reconstructed ED maps of (a) **3b** and (b) **3c**.

The main source of deviation between simulated intensity and experimental result is from the electron density of alkyl chains (purple vs blue triangles) as shown in **Fig. 3e-f**. As explained in the maintext, metallacycles have to adapt local free rotation due to insufficient TEG volume, such rotation would fill alkyl chains into TEG region, leading to the decrease of electron density in alkyl region. With same phase angle combination, the experimental ED maps of **3b** and **3c** in **Fig. S68** are qualitatively same as **3d**.

8. Photophysical studies and additional discussion

1. Absorption and emission spectra

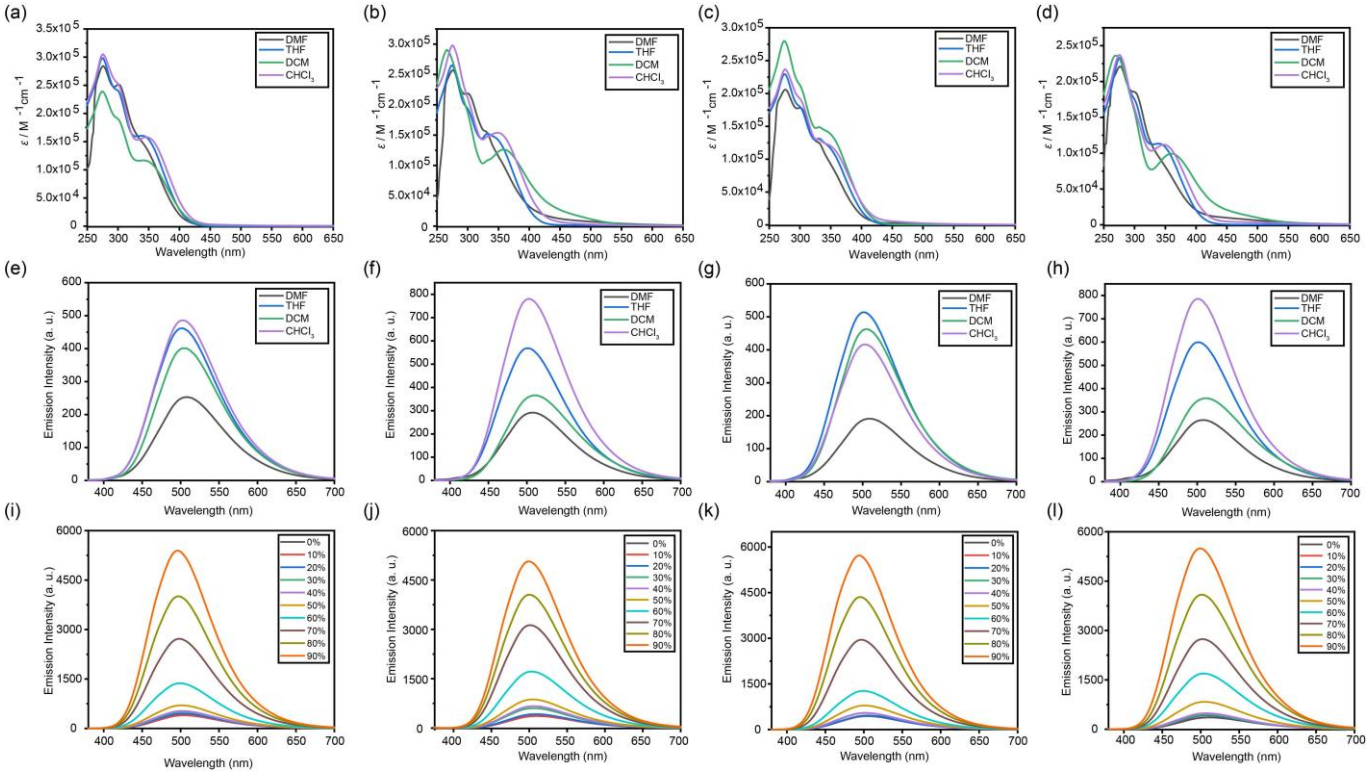

Fig. S69. UV/vis absorption, fluorescence emission spectra of metallacycyes **3a** (a, e), **3b** (b, f), **3c** (c, g) and **3d** (d, h) in different solvents. Emission spectra of **3a** (i), **3b** (j), **3c** (k) and **3d** (l) in dichloromethane/hexane (λ_{ex} = 365 nm, c = 10 μM).

2. Properties summary

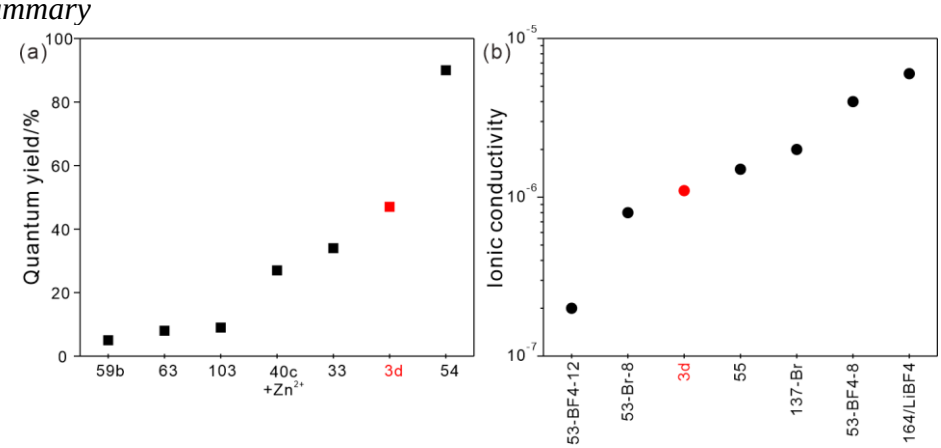

Fig. S70. (a) The quantum yield of luminescent metallomesogens in solid state in ref S6. (b) Ionic conductivity of thermotropic liquid crystal below 50°C in ref S7. **3d** is in red with high emission and good ionic conductivity.

3. Optimized molecular model and space filling calculation

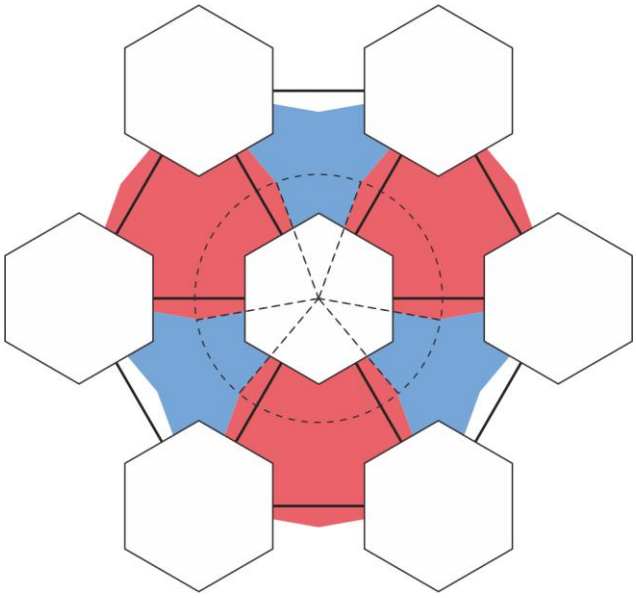

Fig. S71. Scheme of volume requires for alkyl chains (red) and TEG (blue).

To estimate the theoretical best ratio between alkyl and TEG chains, a rough model ignoring the metallacycle size was constructed in **Fig. S71**. Since TPE corner has larger size than diplatinum(II) corner, measured from geometric optimized model, TPE occupies ~80° while diplatinum(II) just occupies 40°, i.e. in 2:1 ratio. The lattice parameter is assumed to be 7 nm and metallacycle side is 1.8 nm. It's easy to calculate the area of red region occupies 52.0%, blue region occupies 28.2% and hollow hexagon occupies 19.8%. Thus, ideally, the volume of TEG is 54.1% of alkyl chains would fill the space properly if the density deviation between them is ignored.

Similar model could also qualitatively explain the swelling of lattice parameter. Judged from **3a**, the area alkyl chain occupied is 18.74 nm^2 in the lattice and hexagon occupies 8.42 nm^2. For **3b-d**, alkyl chains are suppressed into the red region. Based on the area ratio (θ) between the red and blue region, ideal lattice parameter (a) for properly filling can be calculated by the equation 4.

$$a = ((18.74\times(1+\theta)+8.42)\times 2/3^{1/2})^{1/2} \qquad \text{(Eqution S4)}$$

The calculated ideal lattice parameter for equally distributed TEG/alkyl (θ = 100%) is 7.3 nm and for θ = 54.1% is 6.6 nm. The experimental results (a = 6.9 - 7.0 nm) is exactly in the middle of the two cases, indicating that the 6-fold topological feature of metallacycle plays a critical role in stacking. TEG units and alkyl chains are indeed filled in the blue/red sectors, swelling the hexagonal cell.

9. References

S1. *Chem. Commun.* **2016**, *52*, 9009-9012.

S2. *Inorganic Chemistry*, **2021**, *60*, 9387-9393.

S3. *Designed monomers and polymers*, **2006,** *9*, 413-424.

S4. *Dyes and Pigments*, **2018**, 152, 43-48.

S5. *Macromolecules.* **2007**, *40*, 5290-5293.

S6. *Chem. Rev.* **2021**, *121*, 12966-13010.

S7. *Chem. Rev.* **2016**, *116*, 4643-4807.

S8. *J. Am. Chem. Soc*, **2021**, *143*, 399-408.

S9. *J. Am. Chem. Soc.* **2018**, *140*, 5049–5052.

S10. *Angew. Chem. Int. Ed.* **2020**, *132*, 10143-10150.

S11. *Angew. Chem. Int. Ed.* **2008**, *47*, 6080-6083.

S12. *Chem. Commun.* **2018**, *54*, 12306-12309